# Brine management strategies for desalination systems: Decision support system

# Engineering Honours Thesis (ENG470)

By Rhys Farrall

23/01/2022

Supervised by Dr. Philip Schneider

An honours thesis paper submitted to Murdoch University to fulfil the requirements of the degree of Bachelor of Environmental Engineering 2021

## Abstract

This thesis explores and evaluates a decision support system (DSS) for the management of desalination brine. The rapid uptake of desalination technologies to meet freshwater demands has led to producing a significant quantity of brine, which is a highly saline solution. Currently, the most popular brine management method in Western Australia (WA) is disposal by surface water discharge (into the ocean), deep-well injection or evaporation ponds. Brine disposal isn't a long-term sustainable option due to the environmental impacts it can cause, such as salinisation. Brine treatment methods that reduce the liquid volume of brine partially or completely are still under development or aren't currently economically viable.

This thesis uses two multi-criteria analysis techniques. These are interval Analytical Hierarchy Process (AHP) and Technique for Order Preference by Similarity to Ideal Solution (TOPSIS) under hybrid information. The use of interval AHP gives decision-makers a reliable method of assigning appropriate weightings to the chosen criteria, using the relative importance between each criterion. The DSS uses TOPSIS to allow for different information types (crisp numbers, interval numbers, fuzzy triangular numbers representing linguistic terms) within the DSS.

To showcase the DSS, a case study was developed using 4 emerging brine treatment technologies, membrane distillation (MD), forward osmosis (FO), osmotically-assisted reverse osmosis (OARO) and eutectic freeze crystallisation (EFC). The results suggest that the most to least appropriate technology are MD, FO, EFC and OARO. Sensitivity analyses using a Monte Carlo simulation determined the influence of varying different criteria weightings on the TOPSIS process. MD was the most dominant appropriate technology with little confusion between FO, which was consistently ranked 2$^{nd}$. Sensitivity analysis of the entire DDS requires further validation of the interval AHP.

## Acknowledgements

I would firstly like to thank my academic supervisor Dr. Phil Schneider, who has been a wonderful supervisor over the last year. Thank you for the ongoing support and allowing access to your wide wealth of knowledge and guidance. There were some frustrating modelling errors along the way and lack of support from corresponding authors that gave a response in less than 5 minutes but we made it in the end. I'd like to thank my family for always supporting me throughout my university career.

## Contents

## List of figures

## List of tables

List of abbreviations

| | |
|---|---|
| AHP | Analytical hierarchy process |
| CAPEX | Capital Expenditure |
| DS | Draw solution |
| DSS | Decision support system |
| DWI | Deep-well injection |
| ED | Electrodialysis |
| EDR | Electrodialysis reversal |
| EFC | Eutectic Freeze Crystallisation |
| FFE | Falling film evaporator |
| FO | Forward osmosis |
| FS | Feed solution |
| HPRO | High pressure reverse osmosis |
| IBS | Ideal Best Solution |
| IWS | Ideal Worst Solution |
| MCr | Membrane crystallisation |
| MD | Membrane distillation |
| MED | Multi-effect distillation |
| MLD | Minimal Liquid Discharge |
| MSF | Multi-stage flash distillation |
| OARO | Osmotically assisted reverse osmosis |
| OPEX | Operating Expenditure |
| RO | Reverse osmosis |
| SA | Sensitivity Analysis |
| SEC | Specific energy consumption |
| SWD | Surface water discharge |
| TDS | Total dissolved solids |
| TOPSIS | Technique for Order Preference by Similarity to an Ideal Solution |
| WWTP | Wastewater treatment plant |
| ZLD | Zero Liquid Discharge |

# 1 Introduction

Water scarcity is a significant challenge to the sustainable development of human society. Only 3% of the total water present on Earth is freshwater, while the remaining 97% is saline [1]. Of the 3%, only 0.5% is readily available, the remaining freshwater is unavailable, as it is stored in glaciers and snowcaps [2]. The increase in human population from 7.6 billion people in 2018 to 9.4-10.2 billion by 2050, climate change, economic development and rising living standards will result in high per capita water consumption and contribute to water scarcity [3]–[5]. Recent studies on water scarcity have estimated that 40% of the global population in 2014 experiences severe water scarcity, and it is expected to increase to 60% by 2025 [6], [7]. The increasing strain on conventional water resources has triggered a global search for sustainable alternative water resources.

Desalination is a popular alternative water resource, with many countries utilising it to bolster existing conventional freshwater sources to meet growing demand. There is a wide variety of desalination technologies commercially available. They can be separated into membrane-based and thermal-based technologies. Membrane systems such as reverse osmosis (RO) are the most popular desalination technology. With 69% of the estimated 15,906 operational desalination plants in 2018 utilise RO, followed by Multi-Stage Flash (MSF) and Multi-Effect Distillation (MED), which are thermal-based techniques, at 18% and 7%, respectively [6]. All desalination techniques separate undesirable components, such as dissolved solids, from the feed water and create a freshwater stream (permeate) and a by-product stream, known as brine, that consists of the compounds that were removed from the freshwater stream.

Desalination systems close to the sea often discharge the brine back into the ocean, while inland systems employ a wide variety of disposal methods. Concerns regarding the long-term sustainability and environmental impacts of current brine disposal methods have led to the development of two approaches of managing brine. Minimal liquid discharge (MLD) aims to minimise the amount of brine and utilises primarily membrane-based treatment methods. Zero liquid discharge (ZLD) aims to completely eliminate the need for brine disposal and produce a solid by-product in the form of salt. This is achieved through the use of a combination of a membrane-based and thermal-based treatment technologies.

## 1.1 Aims and Objectives

The overall aim of this project is to develop a decision support system (DSS) to aid in the selection of brine management strategies for desalination systems. The main objectives of the project are as follows:

1. Review current brine disposal and treatment methods, outlining the limitations and strengths of each method.
2. Develop a DSS based on a multi-criteria analysis framework and go through a case study through the following steps:
    a. Select a suitable multi-criteria framework for the DSS.
    b. Produce suitable criteria to be used within the framework.
    c. Develop a case study to showcase the DSS.
3. Assess the sensitivity and robustness of the decision support system by conducting a sensitivity analysis.

## 1.2 Thesis Structure and Scope

Section 1 (Introduction) introduces the background for the thesis, with Section 1.1 outlining the aims and objectives. Section 2 (Literature Review) provides a review of the literature relevant to brine management and its properties. Section 2.1 (Desalination Brine and its Environmental Impacts) outlines the properties of brine which cause complications in brine volume reduction and current disposal methods employed globally. Section 2.2 (Brine Treatment Strategies) provides details on the working principles, limitations and strengths of membrane-based technologies (Sections 2.2.1-2.2.5) and thermal-based technologies (Sections 2.2.6-2.2.10).

Section 3 (Methodology) introduces the multi-criteria analysis framework and criteria development. Section 3.1 outlines the development of suitable independent criteria that could be used in the DDS. Sections 3.2 and 3.3 show the mathematical models for the

Interval Analytical Hierarchy Process (AHP) and the Technique for Order Preference by Similarity to Ideal Solution (TOPSIS) used in the development of the DDS. Section 4 goes through a case study, including the selection of appropriate criteria for a specific situation and a DDS demonstration. Section 5 (Results and Discussion) will consist of the results of the case study and outline how a sensitivity analysis was conducted and its findings. Sections 6, 7 and 8 will consist of the conclusion, references and appendix, respectively.

# 2 Literature Review

The literature review will be covering the following topics:

1. Brine characteristics and challenges in producing high total dissolved solid (TDS) brine.
2. Environmental impacts of inland brine disposal.
3. Current inland brine disposal methods.
4. Brine treatment methods for minimal liquid discharge and zero liquid discharge systems, covering:
    a. The working principles behind each technology.
    b. Development status (market readiness).
    c. Limitations and current areas of research.
    d. Energy consumption.

## 2.1 Desalination Brine and its Environmental Impacts

Brine, also known as reject or concentrate, is a highly saline solution that contains the filtered dissolved solids, organic contaminants and pretreatment chemicals (i.e., antiscalant, coagulants and flocculants). Brine is measured by its total dissolved solids (TDS), usually measured as mg/L. Brackish water has a TDS ranging from 1,000 to 15,000 mg/L, brine produced from this source water typically has a TDS between 5,000 to 55,000 mg/L [8], [9]. The quality and quantity of brine can be determined by the desalination technology's recovery rate, feed water quality and pretreatment methods employed [10].

Brine is commonly returned to the environment (without treatment) by surface water discharge, evaporation ponds, sewer discharge, land application and deep-well injection. Brine possesses significant environmental risks, as it's highly saline and has potential contaminants, including pretreatment chemicals, organic compounds and heavy metals. Environmental impacts of brine disposal are reported in three areas the marine environment, groundwater and soil quality.

### 2.1.1 Brine Characteristics

The two important factors to consider for the treatment of brine include the volume of brine to be treated and its initial quality. Recovery rate ($R$) is the percentage of source water ($Q_f$) that is converted to freshwater ($Q_p$) as presented in equation 1.

$$R = \frac{Q_p}{Q_f} 100\% \quad (1)$$

As the recovery rate increases, brine volume decreases and its salinity increases. The volume of brine ($Q_b$)can be determined through the recovery rate (equation 2) or by subtracting the freshwater ($Q_p$) from the source water ($Q_f$), as shown in equation 3.

$$Q_b = Q_f(1 - R) \quad (2)$$

$$Q_b = Q_f - Q_p \quad (3)$$

Brine quality is dependent on the source water quality and the recovery rate of the system. There are complicated methods to determine the quality for specific desalination technologies, however, for the purpose of this review, the simplified calculation will be sufficient (equation 4).

$$TDS_b = TDS_f \frac{1}{1 - R} \quad (4)$$

In equation 4, $TDS_b$ and $TDS_f$ represent the total dissolved solids present in the brine and feed, respectively. The remaining term ($\frac{1}{1-R}$) is the concentration factor (CF), and is shown in equation 5. It is a factor that represents the degree of concentration of the source water compared to brine.

$$CF = \frac{Q_f}{Q_f - Q_p} = \frac{1}{1 - R} \quad (5)$$

For brackish water reverse osmosis (BWRO), the concentration factor is usually between 2.5 to 10, correlating with recovery rates of 65% to 90%, respectively [11].

### 2.1.2 Challenges with Producing High-TDS Brine

Treating source water (seawater and brackish water) to a high standard using desalination results in a high-TDS brine. As the brine concentrates within the desalination system, treatment challenges such as scaling, fouling and corrosion are more likely to occur. Scaling occurs when inorganic salts precipitate and clog working surfaces, such as membranes, pipes, fittings and heat exchangers. Scaling is more prone to occur in membrane-based systems, than in thermal-based systems [12]. Similar to scaling, organic fouling occurs when organic material is lodged and grows on the working surface (membrane or heat exchanger) of the desalination technology [13]. Corrosion is associated with changes to processing conditions (temperature), and water chemistry (pH and salt formation). To minimise the likelihood of fouling, scaling and corrosion, physical and chemical pretreatment can be utilised to adjust feed water conditions [14]. The predominant pretreatment method used in desalination and brine concentration technologies is chemical pretreatment (antiscalant, scaling inhibitors, acids, bases, coagulants) [15]. Pretreatment is explored in-depth by Semblante et al. [16] and Kaplan, et al. [17] and states the importance of this field of research to the realisation of membrane-based zero liquid discharge (ZLD) systems.

### 2.1.3 Environmental Impacts

In recent years, the environmental impacts of brine disposal in published literature have been limited to the marine environment [4], [18]–[22]. The environmental risks of brine disposal of inland systems are explained superficially or not mentioned at all, by those in the desalination community. The focus on the marine environment is most likely a consequence of two factors. The prominence of seawater desalination systems and 79% of desalination plants are within 10km of a coastline, making it a cost-effective disposal method [6]. The main environmental risk of inland brine disposal is salinisation, caused by the increased salt load in the soil and groundwater.

Currently, more than 1,000,000 hectares of agricultural land in Western Australia are affected by natural and anthropogenic salinisation, resulting in economic damage of approximately $519,000,000 per annum to the agricultural sector [23], [24]. The effects of salinity on plant growth are diverse, due to the complex interactions between the biochemical, physiological and morphological processes that take place in the soil [25]. Presence of salt in the soil and groundwater can subject plants to osmotic stress, which contributes to nutrient deficiencies, primarily carbon and nitrogen uptake [26], [27]. This significantly hinders plant growth, due to the requirement of carbon, primarily in the form of $CO_2$ for photosynthesis [28]. The osmotic stress also limits the uptake of water from the soil [29]. Contamination from heavy metals, such as cadmium, lead, copper, zinc and iron, can also adversely affect plant growth, productivity and presents a human health risk [30], [31].

#### 2.1.4 Brine disposal methods

Conventional brine disposal methods include surface water discharge, evaporation ponds, land application, deep-well injection and sewer discharge. None of these disposal methods can be universally applied for a given desalination technology, size or location. Rather the suitability of a given disposal method is determined by the quality, quantity and composition of the brine, geographical location, capital and operating costs and local regulations [4], [32].

##### 2.1.4.1 Surface Water Discharge

Surface water discharge (SWD) consists of disposing brine in the ocean, lakes, rivers or any other water body. SWD is a common disposal method for desalination plants that utilise seawater, due to the close proximity to the ocean in most cases [33], [34]. Outfall structures are common among seawater desalination systems, but implementations on inland systems are limited. Seawater brine outfalls utilise high-pressure diffusers, that discharge brine at high velocity into the receiving body [35]. The diffusers increase the mixing efficiency between the brine and the receiving body, by increasing the area that mixing is taking place, which reduces the direct environmental risks of the point-source brine disposal [36]. A limitation of inland SWD is finding a suitable water body to receive the brine, which conforms with local regulations and doesn't contaminate a freshwater resource. Brine can be mixed with a less contaminated waste stream, such as wastewater treatment plant (WWTP) effluent, to meet regulatory standards. However, the use of waste streams can add additional environmental risks, such as introducing additional nutrients, leading to eutrophication of the receiving water body.

#### 2.1.4.2 Evaporation Ponds

Evaporation ponds are a very mature technology, utilised for centuries to produce sea salt from seawater. Evaporation ponds consist of a shallow basin that is filled with brine, which is evaporated by solar radiation. Evaporation ponds have a simple structure, maintenance is trivial, few mechanical components and can be used to harvest salts and minerals [37], [38]. Other than the production of salts, evaporation ponds can also be used for aquaculture of marine species and algal cultivation that could be converted into feedstock [39]. As a system dependant on solar radiation, arid or semi-arid climates are required, there is also a large land requirement [40], [41]. Pond depth, which is determined by the evaporation rate of the area and the required pond liner also contribute to the feasibility of an evaporation pond [19]. One key issue with evaporation ponds, is if the pond lining is breached, causing the brine to infiltrate into the soil and groundwater.

#### 2.1.4.3 Land Application

Land application disposal consists of irrigating salt-tolerant plants (halophytic) or grasses. Halophytic plants can be characterised by their tolerance to salinity (TDS) higher than 2,000 mg/L, in comparison, most plants can tolerate a salinity of <500 mg/L [4], [42]. The adoption of this technique is currently limited to small quantities of brine [4], [19], [43]. Large scale applications are limited by low crop yield associated with halophytic crops, climatic conditions, seasonal demand, soil degradation and groundwater contamination [44], [45]. The design behind this technique is similar to an artificial wetland and is dictated by which halophytic plant is being utilised, soil type and brine characteristics [46].

#### 2.1.4.4 Deep-well Injection

Deep-well injection (DPI) is a disposal method that consists of injecting brine into a confined aquifer. This method is popular among brackish water systems of all sizes [47]. This method is only appropriate if a confined aquifer can store all brine produced over the desalination technologies expected operating lifespan [40]. The key environmental concern with DPI is the contamination of adjacent freshwater aquifers [48]. This risk can be substantially reduced if hydrogeological surveys are undertaken to verify whether the aquifer is suitable for DPI [49].

#### 2.1.4.5 Sewer Discharge

For the sewer discharge disposal method, brine is directed towards a connected sewage system, to be treated at the downstream wastewater treatment plant (WWTP). Sewer discharge is only suitable for small scale BW systems, as salinity in the wastewater network can negatively influence the WWTP treatment process, if secondary treatment is being conducted. When the salinity of wastewater exceeds a TDS of 20000 mg/L, nitrogen removal by the microbes utilised in the activated sludge process (secondary water treatment process) is severely impacted [50]. The reduction in nutrient removal could indirectly cause the WWTP not to meet water treatment regulations. Therefore, only small quantities of brine can be disposed of into the sewer network.

## 2.2 Brine Treatment Strategies

Increasing uptake of desalination technologies to meet the water requirements for human consumption and industry, has illuminated environmental risks of typical disposal methods (SWD, DPI, evaporation ponds, land application and sewer discharge), causing increasingly stringent regulations to be imposed. This has encouraged research into sustainable brine management strategies. There are two broad approaches currently being investigated which are, Minimal Liquid Discharge (MLD) and Zero Liquid Discharge (ZLD) [4], [10], [21], [51]. MLD aims to reduce the volume of brine produced, while, ZLD processes the brine produced by MLD until the liquid component is removed entirely, and only solids (salts and minerals) remain [52]. The solid waste from ZLD can be disposed of, sold or processed further to produce goods like fertiliser and caustic soda.

MLD and ZLD both start with technologies that concentrate brine. These technologies generally consist of membrane-based technologies. The preference for these technologies as the first stage of brine treatment is due mostly to the capital and operational costs involved with the alternative options, which are primarily thermal-based technologies [53]. However, thermal-based technologies and a small quantity of membrane-based technologies that can produce a solid product, are required in a ZLD framework. Therefore, the brine volume reduction from membrane-based technologies, results in a reduction of the operational capacity required for the technologies used in a ZLD framework.

Membrane-based brine treatment technologies utilised in MLD and ZLD systems are covered in sections 2.2.1-2.2.5, meanwhile, sections 2.2.6-2.2.10 will discuss the thermal-based technologies. The main points of interest for each technology are the working principles, limitations and operating parameters of the relevant technology. A summary of this information is presented in Table 1.

### 2.2.1 Reverse Osmosis and High-Pressure Reverse Osmosis

As previously mentioned, reverse osmosis (RO) is the most commercially successful desalination technology. RO is a pressure driven process, by which hydraulic pressure is applied to the feed water (brine), to force permeate (freshwater) to the other side of a semipermeable membrane. To produce permeate, the applied pressure has to be greater than the osmotic pressure between the brine and permeate.

The osmotic pressure of a saline solution can be estimated using van't Hoff's equation (equation 6), where, Π is the osmotic pressure in Pascals, n represents the moles of solute, V is volume of solvent, R is the gas constant ($8.3145 * 10^3 \frac{Pa*L}{K*mol}$) and $i$ is the species.

$$\Pi = i\frac{n}{V}RT \qquad 6$$

From this equation, the hydraulic pressure required to produce permeate for any TDS can be calculated. Figure 1 shows the minimum hydraulic pressure required for a solution of pure NaCl, which is a good approximation of the TDS of brackish water, seawater and brine, as the main constituents are sodium and chlorine. The units used for osmotic pressure isn't usually Pascals, instead Bar is preferred (1 Bar = 100,000 Pascals).

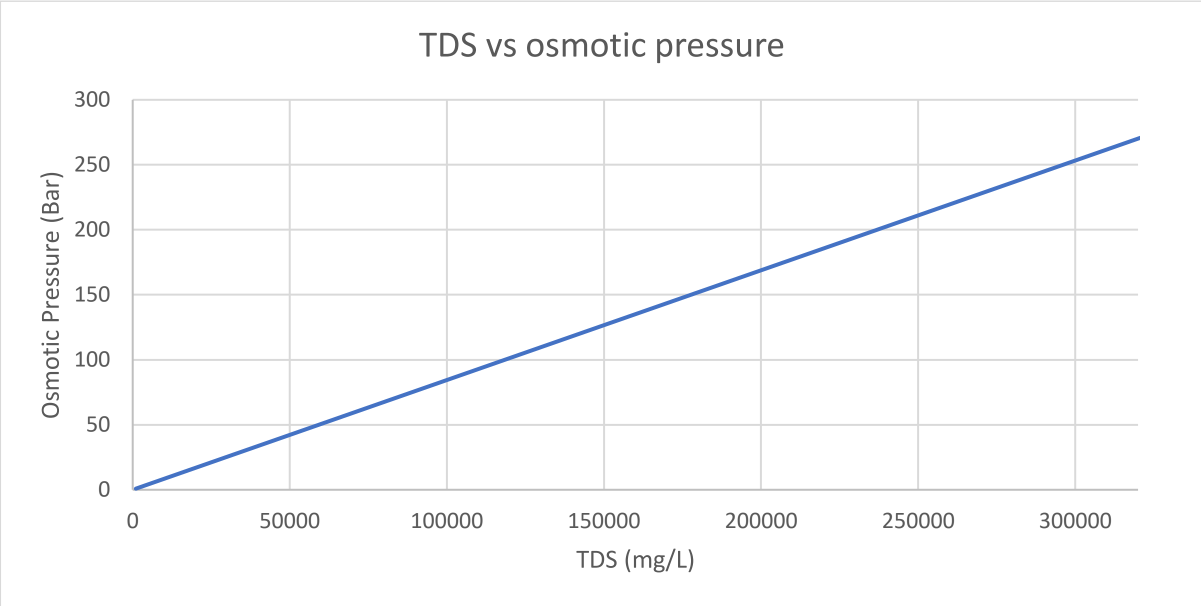


*Figure 1: TDS vs osmotic pressure for a solution with only NaCl.*

RO membranes used in conventional desalination are limited to TDS outlet concentrations up to 70,000 mg/L [54]. However, as the TDS increases, the associated recovery rate can become as low as 10% [55]. Therefore, conventional RO membranes are not suitable for concentrating high-TDS for MLD or ZLD systems.

This limitation triggered the development of membranes that can handle the extreme pressure required for concentrating high-TDS brine. Any RO system operating above a TDS of 70,000 mg/L or 82 Bar, is often referred to as high-pressure RO (HPRO) [53]. Saltworks and Dupont have recently advertised membranes that can operate up to 120 bar, which correlates with an approximate TDS limit of 130,000 mg/L [56], [57]. The specific energy consumption (SEC) is the amount of energy required to produce a specific amount of product (permeate). For HPRO systems the SEC is estimated to be between 3 to 9 kWh/m$^3$. In comparison RO has a SEC between 1.2 to 1.5 kWh/m$^3$[58], [59].

### 2.2.2 Forward Osmosis

Unlike RO, Forward Osmosis (FO) is an osmotically-driven process that uses a draw solution of higher osmotic pressure to draw permeate out of the feed solution using a semipermeable membrane [60], [61]. Figure 2 shows a typical layout of a FO system.

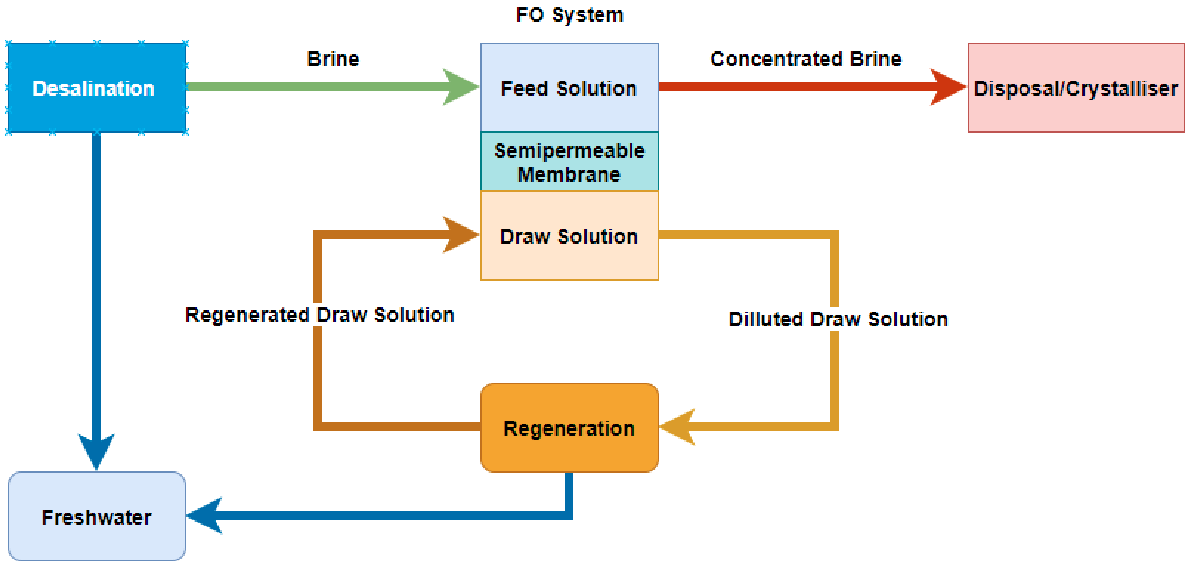


*Figure 2: Simple layout of a Forward Osmosis (FO) system.*

As external pressure isn't required for this process, FO has the potential to be very energy efficient if draw solution recovery, also known as regeneration, isn't used. A recent study found that the SEC of FO without a regeneration process uses between 0.02 to 1.86 kWh/m$^3$ [59]. However, if regeneration systems are implemented with the FO system, typically seen in combined systems like MLD and ZLD, the energy demand increases substantially [62]. The addition of a regeneration system, increases the SEC to between 6.8 to 16.7 kWh/m$^3$ [63]. The SEC for the regeneration system is dependent on the draw solution, separation technique required for that draw solution and the quality of the feed solution. The primary area of research for FO is in the development of viable draw solution for the FO systems [64]. Current draw solutions limit FO to TDS between 150,000 to 220,000 mg/L [65].

### 2.2.3 Osmotically Assisted Reverse Osmosis

Osmotically assisted reverse osmosis (OARO) utilises the working principles behind RO and FO. However, unlike in FO, the draw solution (DS) has a lower osmotic pressure compared to the feed solution (FS). The DS reduces the osmotic pressure difference between the solutions, rather than the driving force behind the process, like it is in FO systems. The reduced osmotic pressure differential between the feed and permeate, decreases the necessary hydraulic pressure required to produce permeate [66]. OARO is typically arranged into several stages, also known as sweeps, shown in Figure 3.

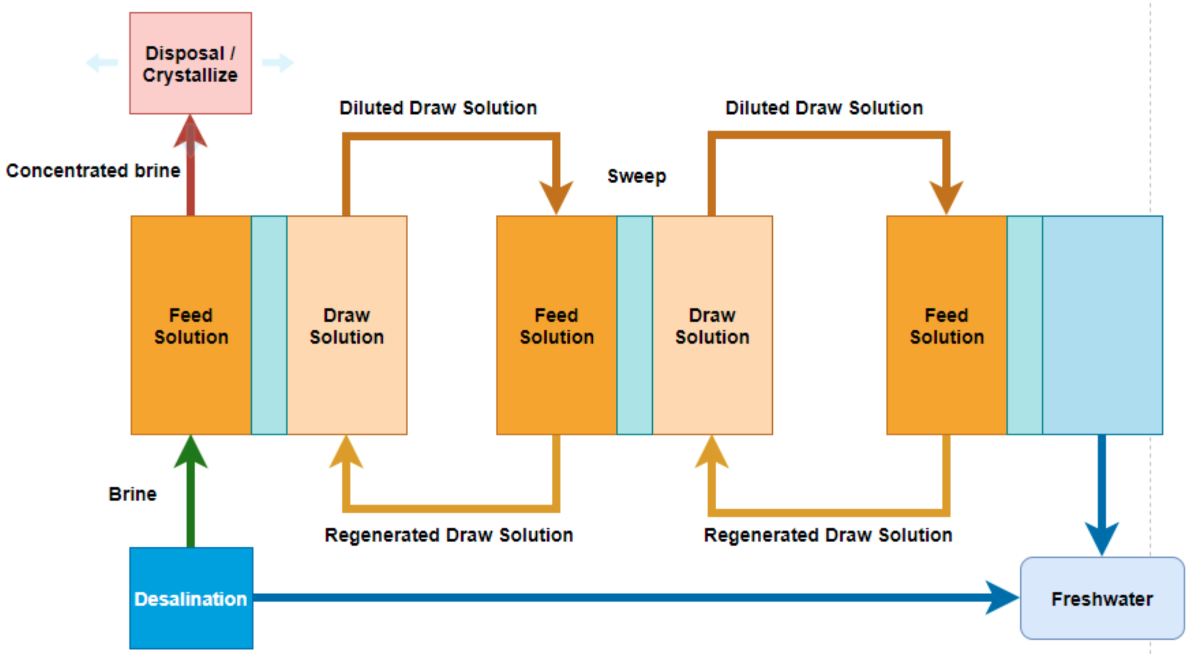


*Figure 3: Schematic for an OARO system.*

This also reduces the limitations imposed by the DS that is currently an issue with FO systems. Therefore, higher TDS feed solutions can be treated using OARO compared to HPRO and FO. OARO currently shares a lot of the disadvantages of FO, such as, availability of viable DS, complex system design (multiple stages) and limitations on the mechanical strength of available membranes [67], [68]. The expected SEC for OARO is between 6 to 19 kWh/$m^3$, dependant on the system design and feed quality [69], [70]. Currently, commercial OARO systems are limited to FS of approximately 160,000 mg/L [71].

### 2.2.4 Membrane Distillation and Membrane Crystallisation

Membrane distillation (MD) is a thermally-driven membrane process. It uses a hydrophobic membrane, that allows water vapour to pass through, but acts like a physical barrier for liquids and solids [72]. When a temperature differential > 5 C° exists between the feed and permeate, water evaporates from the feed and passes through the membrane, and condenses on the other side [73]. The feed temperature in MD is often between 45 and 85 C° [74]. As a thermally driven process, there are no limitations imposed by the osmotic pressure of the feed water, therefore, theoretically there is no limit to the TDS of the feed water [75]. MD systems can often be enhanced by utilising a waste heat streams [76].

There are 4 main configurations for MD, namely, direct contact MD (DCMD), air gap MD (AGMD), vacuum MD (VMD) and sweeping gas MD (SGMD) [77]. The advantages and disadvantages of these configurations are explored in detail by Ahmed et al, who also cover alternative heating techniques commonly associated with MD systems [78]. The most commercially successful configuration is DCMD, however the AGMD and VMD have been used in ZLD systems [79], [80]. Energy consumption in MD literature typically displayed as the specific thermal energy consumption (STEC), which is the amount of energy in the form of heat required to produce a specific amount of product, with the units of kWh/m$^3$. For the 4 configurations mentioned previously, the STEC value fluctuates between 54.5 to 350 kwh/m$^3$, and a SEC between 39 to 67 kWh/m$^3$ [10], [81].

Membrane crystallisation (MCr) is the first technology on this list that can directly produce added value products. In essence, MCr is an extension of the MD process. The environment created during the MD process is well suited to heterogeneous nucleation, which can be carried to a crystallisation tank to grow further [82]. As it is an extension to the MD process it has no theoretical TDS limit and similar SEC.

### 2.2.5 Electrodialysis and Electrodialysis Reversal

Electrodialysis (ED) and electrodialysis reversal (EDR) are processes that utilise electricity to create a driving force. Both techniques use ion exchange membranes that allow for the transport of ions [83]. These membranes can further be categorised into anion exchange membranes (AEM) and cation exchange membranes (CEM), which allow the transport anions or cations, respectively [84]. These membranes are then alternated in a stack, with a cathode and anode at each end to produce an electrical field.

The electrical field draws cations and anions in the direction of the oppositely charges cathode or anode. Although conventional ED and EDR systems are targeted towards low TDS (< 10,000 mg/L) feed sources, there are commercially available conventional ED and EDR systems suited to feed sources with TDS > 70,000 mg/L [85]–[89]. Currently, there is little literature on the maximum feed TDS of conventional ED and EDR systems, however, common assumptions on the limitations range from 150,000 to 200,000 mg/L [10], [86], [90]. The SEC of conventional ED and EDR systems is estimated to be between 7 and 15 kWh/m$^3$ for high TDS fluids [91].

### 2.2.6 Brine Concentrator

Brine concentrator (BR) is a term that covers different configurations of evaporators. There are 3 main configurations namely, falling film evaporator (FFE), horizontal spray and flat-plate evaporator, of which FFE is the most widely used [92]. The working principle behind these evaporators is heavily based on shell and tube heat exchanger design. A thin film of liquid flows over a vertical, horizontal or inclined surface. When the contact surface is exposed to a heat source, usually steam, it causes the liquid to transform into vapour, which is collected at the end of the process, to be condensed in a separate chamber [93].

A drawback of falling film evaporator is that it's very difficult to scale down, as the reduction in surface area negatively affects the evaporation efficiency [94]. Evaporators can also be paired with recompression systems, namely, mechanical vapour recompression (MVR) and thermal vapour recompression (TVR). Recompression systems are usually only coupled with multi-effect (stage) evaporation systems [95]. Recompression systems improve the energy efficiency of evaporation systems, making them more economical [96]. Due to the widespread nature of FFE use in multiple industries, finding a reasonable value for SEC for concentrating brine has proven difficult, and will be omitted.

### 2.2.7 Multi-Stage Flash Distillation and Multi-Effect Distillation

Multi-Stage Flash distillation (MSF) and Multi-Effect Distillation (MED) are the most popular desalination technology after RO and are thermal-based technologies. Both systems are very similar, both use heat to evaporate the feed water in stages and condenses the water vapour to produce freshwater.

One of the few technical and economic analyses of MSF for brine concentration was conducted by Eiff et al. and found that a combined MD-MSF-crystalliser was more economical to operate than a standalone MD system, due to the benefit of the salts produced [97]. One of the reasons why MSF and MED systems aren’t widely used for high-TDS solutions is because the materials used in typical systems don’t have the required resistivity to corrosion [98]. Replacement of contact surfaces with corrosion-resistant materials is currently very expensive.

The SEC for MED is between 5.5 to 21.35 kWh/m$^3$, while MSF is between 10 to 27.25 kWh/m$^3$ [40], [99]–[101]. However, this appears to the SEC to treat brackish water and seawater, rather than concentrated brine. Therefore, the SEC is most likely higher for concentrated brine treatment. As mentioned previously with MD, thermal systems theoretically have extremely high TDS limits, and in the case of MFS and MED, TDS is limited to the corrosive resistance of the contact surfaces.

### 2.2.8 Spray Drying

Spray dryers (SD) are an alternative method to traditional crystallisers. However, SD produces a mixed collection of salts from concentrated brine. Currently, SD has been used sparingly in brine management strategies, however it is used widely in food (e.g., milk powder, instant coffee, baby foods), pharmaceutical (e.g., perfume, probiotics, oil) and chemical (e.g., fuel injectors) industries [102]. Brine is injected into the drying chamber by a single or dual fluid nozzle atomiser to form small droplets. The dispersed brine (droplets) then come into contact with a hot convective medium (usually air, but nitrogen is also utilised in some situations), dehydrating individual droplets and forms a dried product (mixed salts). The mixed salts can be collected through use of a cyclone separator and a bag filter [103]. In most circumstances, SD doesn’t allow for the recovery of additional freshwater. A suitable SEC for this technology couldn’t be found in literature due to 2 factors, limited research on SD that utilise brine and the effects of viscosity on energy performance. Viscous fluids stick to the atomiser, which hinders the dispersion of droplets in the drying chamber and reduces the energy efficiency of the atomiser. However, for saline brines the effect of viscosity would be minor.

### 2.2.9 Eutectic Freeze Crystallisation

Freeze crystallisation is an assortment of different techniques that have been around for centuries, including utilisation by sailors to harvest freshwater during long journeys. There are 4 main types of freeze crystallisation: Direct contact freezing, vacuum freezing, indirect contact freezing and eutectic separation (also known as eutectic freezing). The only freeze crystallisation technology applicable for brine management is eutectic freeze crystallisation (EFC), developed in the 1970s [104]. The state of the solution is determined by the temperature of the solution and the concentration of relevant salts that can be formed. There are 4 main phases, unsaturated solution (all liquid), ice and concentrated (saturated) solution, salt and concentrated solution and ice and salt. The eutectic point is the operational temperature and concentration for EFC, and the point in which salt and ice form simultaneously. Ice is less dense than water, so it floats to the top of the chamber. Meanwhile, the salt formed is denser than water and sinks to the base of the chamber. The ice and salt can then be separated from the solution at the top and bottom of the chamber. Williams et al, explains the history and operation of freeze crystallisation in more depth[105].

The advantages of EFC compared to conventional brine treatment technologies are:

1. It doesn't require pretreatment chemicals.
2. Thermodynamically, the energy required for heat of vaporisation is higher (approximately six times) than heat of fusion. Therefore, freezing technologies theoretically use less energy than evaporative processes [106]. In practice, EFC has demonstrated 60-70% energy reduction compared to traditional evaporative processes [106], [107].
3. Ice formed from an aqueous solution is pure [108].
4. Ice and salt have different densities, which allows for gravitational separation.

5. Corrosive conditions usually seen in evaporative technologies are minimal in EFC, resulting in less stringent construction materials.
6. Specific salts of high purity can be harvested by operating several EFC stages at different temperatures, by taking advantage of the unique crystallisation temperatures of pure salts [109].

Researchers have published a significant range of SEC for EFC from 4-150 kWh/m$^3$. The wide range of values is primarily due to the composition of the solutions used in the EFC [4], [109]. Randall et al, mentioned that most of the research on EFC was conducted with only 1-2 salts present in solution [106]. There is currently a lack of research on EFC for complex solutions, such as desalination brine. However, as mentioned previously, using a staged approach shows potential for complex solutions containing multiple salts. EFC has been used for TDS of 300,000 mg/L (30 wt%) for salty whey (behaves similarly to a pure NaCl-$H_2O$ system). With a lower temperature, the TDS range would increase, at the cost of higher energy consumption [109].

### 2.2.10 Wind-Assisted Intensified Evaporation and Convection-Enhanced Evaporation

Wind-assisted intensified evaporation, also known as wind-aided intensification of vaporisation (WAIV) is a relatively new technology first proposed by Gilron et al, in 2003 [110]. It Consists of a series of vertically mounted evaporation surfaces consisting of woven netting, non-woven geotextiles or tuff (volcanic rock) [111], [112]. Brine is then dispersed onto the evaporation surfaces, generally through perforated pipes with pressurised brine to create a falling film. WAIV generally refers to using natural wind as the only driving force, however, wind availability is a limiting factor [113]. Convection-enhanced evaporation (CEE) uses a similar approach to WAIV, however, the main difference is wind is generated using a fan [113]. Both systems can allow recycling of brine that isn't evaporated and freshwater isn't recovered in either system. WAIV and CEE are often compared to evaporation ponds due to the similar concepts in their design. WAIV and CEE utilise a wetted surface allowed loading of 30-40 m$^2$ per m$^2$ footprint [114]. Energy consumption is only contributed by pumps (in a WAIV system) and fans (in a CEE system). The author expects a maximum SEC of approximately 0.8 kWh/m$^3$.

## 2.3 Summary of brine treatment technologies

A summary of the key parameters the brine treatment technologies covered in Sections 2.2 are provided in Table 1. The primary purpose of this table is to facilitate the addition of more technologies to the DDS at a later date. This thesis will only be covering 4 technologies.

*Table 1: Summary of the brine treatment technologies covered in the Literature Review.*

| Technology | TDS Limitation | Recovery Rate | Advantages | Challenges | Technology Maturity | Specific Energy Consumption (SEC) | Production Cost | References |
|---|---|---|---|---|---|---|---|---|
| **Membrane-based** | | | | | | | Panagopoulos et al., is used for all production costs [4] | |
| **RO** | $70{,}000\ {}^{mg}/_{L}$ | Up to 65-90% | Small energy consumption | Intensive pretreatment requirements | Developed commercially available technology | $1.2 - 1.5\ {}^{kWh}/_{m^3}$ | $\$0.75/_{m^3}$ (US) of freshwater produced | [56]–[59] |
| **HPRO** | $130{,}000\ {}^{mg}/_{L}$ | Up to 50% | Small energy consumption | -Intensive pretreatment requirements<br><br>-Availability of HPRO membranes | Developed commercially available technology | $3 - 9\ {}^{kWh}/_{m^3}$ | $\$0.79/_{m^3}$ (US) of freshwater produced | [56]–[59] |
| **FO** | $150{,}000 - 220{,}000\ {}^{mg}/_{L}$ | Up to 98% | -No feed pressure required<br><br>-Small energy consumption (if regeneration isn't used) | -Availability of suitable draw solutions<br><br>-intensive pretreatment requirements | Developing technology | $0.02 - 1.86\ {}^{kWh}/_{m^3}$ with no regeneration (recovery of freshwater)<br><br>$6.8 - 16.7\ {}^{kWh}/_{m^3}$ with regeneration | $\$0.63/_{m^3}$ (US) of freshwater produced | [59], [63], [65] |

| | | | | | | | | |
|---|---|---|---|---|---|---|---|---|
| | | | -High rejection rate | -Salt precipitation on working surface inhibits flux and recovery | | | | |
| **OARO** | $160,000\ {}^{mg}/_{L}$ | Up to 72% | -No feed pressure required<br><br>-High rejection rate | -Availability of suitable draw solutions<br><br>-intensive pretreatment requirements<br><br>-Salt precipitation on working surface inhibits flux and recovery | Developing technology | $6 - 19\ {}^{kWh}/_{m^3}$ | $\$2.40/_{m^3}$ (US) of freshwater produced | [69]–[71] |
| **MD and MCr** | -Both technologies have no theoretical limit<br><br>MCr produces a mixed salt | Up to 90% (potentially 100%) | -No feed pressure required<br><br>-Can be paired with waste heat streams to increase efficiency | -intensive pretreatment requirements<br><br>-Salt precipitation on working surface inhibits | Developing technology | $39 - 67\ {}^{kWh}/_{m^3}$ | $\$1.17/_{m^3}$ (US) of freshwater produced for MD<br><br>$\$1.24/_{m^3}$ (US) of | [10], [77], [78], [81] |

| | | | | | | | | |
|---|---|---|---|---|---|---|---|---|
| | | | | flux and recovery<br><br>-Membranes have low thermal efficiency | | | freshwater produced for MCr | |
| **ED and EDR** | $150{,}000 - 200{,}000\ {}^{mg}/_{L}$ | Up to 86% | No substantial advantages | -Energy consumption increases with TDS<br><br>-Intensive pretreatment if feed brine has organics present | Developing Technology | $7-15\ {}^{kWh}/_{m^3}$ | ${\$0.85}/_{m^3}$ (US) of freshwater produced | [85]–[91] |
| **Thermal-based** | | | | | | | | |
| **BC** | Reasonable value wasn't found, however, as a thermal system it can be assumed to be $> 200{,}000\ {}^{mg}/_{L}$ | Assumed to be >90%. | Widespread technology present in multiple fields | -Hard to scale-down<br><br>-Energy intensive<br><br>-high capital costs of material to | Developed technology | Wasn't found specifically for high-TDS brine | ${\$1.22}/_{m^3}$ (US) of freshwater produced, however this is most likely for large installations. Expected to | [94], [96] |

| | | | | | | | | |
|---|---|---|---|---|---|---|---|---|
| | | | | prevent corrosion | | | increase in smaller systems | |
| **MFS and MED** | -No theoretical limit<br><br>-Limited by corrosive resistance of the material used | Up to 80-90% | -Widespread technology<br><br>-Can potentially use waste heat | -Energy intensive<br><br>-High capital cost due to corrosive resistant material requirement | Developed technology | $10-27.25\ kWh/_{m^3}$ for MFS<br><br>$5.5-21.35\ kWh/_{m^3}$ for MED | $\$1.40/_{m^3}$ (US) of freshwater produced for MSF<br><br>$\$1.10/_{m^3}$ (US) of freshwater produced for MED<br><br>Most likely costs for larger systems. For smaller scale systems cost is expected to increase substantially | [40], [98]–[101] |

| | | | | | | | | |
|---|---|---|---|---|---|---|---|---|
| **SD** | -No theoretical limit<br><br>Limited mostly by the viscosity of the fluid | No recovery | -Widespread technology<br><br>-produces salts | -Freshwater could be recovered, however it would be expensive | Developed technology | Wasn't found specifically for brine | Wasn't found specifically for brine | [102], [103] |
| **EFC** | No theoretical limit | 100% | -Thermodynamically it requires less energy than evaporative systems<br><br>-No pretreatment required<br><br>-Salt precipitation can be selective, producing high purity salt<br><br>-Lower requirement on corrosive resistant materials for construction | -Capitally expensive<br><br>-Hasn't been used for complex brine solutions | Developing technology | $4-150\ kWh/_{m^3}$ | $\$1.42/_{m^3}$ (US) of freshwater produced | [106]–[109] |
| **WAIV** | No theoretical limit | No recovery | -Simple<br><br>-Higher working surface evaporation | -No obvious disadvantages | Developing technology | Assumed to be around $0.8\ kWh/_{m^3}$ | Doesn't produce freshwater | [110]–[114] |

| | | | | | | | | |
|---|---|---|---|---|---|---|---|---|
| | | | rates than evaporation ponds (less footprint)<br><br>-Mixed salts can be collected | -Higher capital than evaporation ponds | | | | |

# 3 Methodology

It is challenging to select suitable brine management strategies because decision-makers have to consider various aspects, such as capital cost, electrical consumption and production cost. Therefore, the selection process is typically based on a multi-criteria decision analysis (MCDA). An MCDA is a decision support system (DSS), which is an information system that supports a decision-maker to produce consistent and fast responses to a problem [115]. Therefore, a good DSS has the following attributes [116];

1. Capable of representing and analysing information relevant to the goal of the DSS.
2. Flexible and robust
3. Produces a useful output that is relevant to the objective.

Other forms of DSSs include Life Cycle Assessments (LCA), Mathematical Models (MM), Intelligent DSS (IDSS) or combinations of LCA, MM, MCDA and IDSS [117]. The MCDA method has been applied to various fields, for instance, the medical industry [118], environmental management [119], [120], risk management [121], agriculture [122], energy sector [123], etc. Popular MCDA techniques include weighted sum method, weighted product method, Technique for Order Preference by Similarity to Ideal Solutions (TOPSIS), Performance Ranking Organisation Method for Enrichment of Evaluations (PROMETHEE) and Analytical Hierarchy Process (AHP) [123].

There are multiple MCDAs for selecting suitable desalination locations and technologies. For example, Dweiri, Khan and Almulla used Analytical Hierarchal Process (AHP) to rank sustainable desalination plant locations [124]. Ghassemi and Danesh used Fuzzy-AHP and TOPSIS to select desalination technologies for brackish water [125]. Several other authors have utilised versions derived from AHP in conjunction with other MCDA tools, such as TOPSIS or PROMETHEE [125]–[128]. From these studies arise the following concerns:

1. Some techniques struggle with assigning weightings to criteria with regards to ambiguity and uncertainty.

2. Most of these MCDA techniques can’t handle multiple data types (e.g., interval numbers, crisp numbers and fuzzy numbers).

Wang et al, also reviewed similar trends in literature and developed a MCDA model for hybrid information that addresses the concerns mentioned and will be adopted as the framework for this methodology [129]. The multi-criteria framework was developed by combining Interval AHP and the TOPSIS under hybrid information techniques (Figure 4).

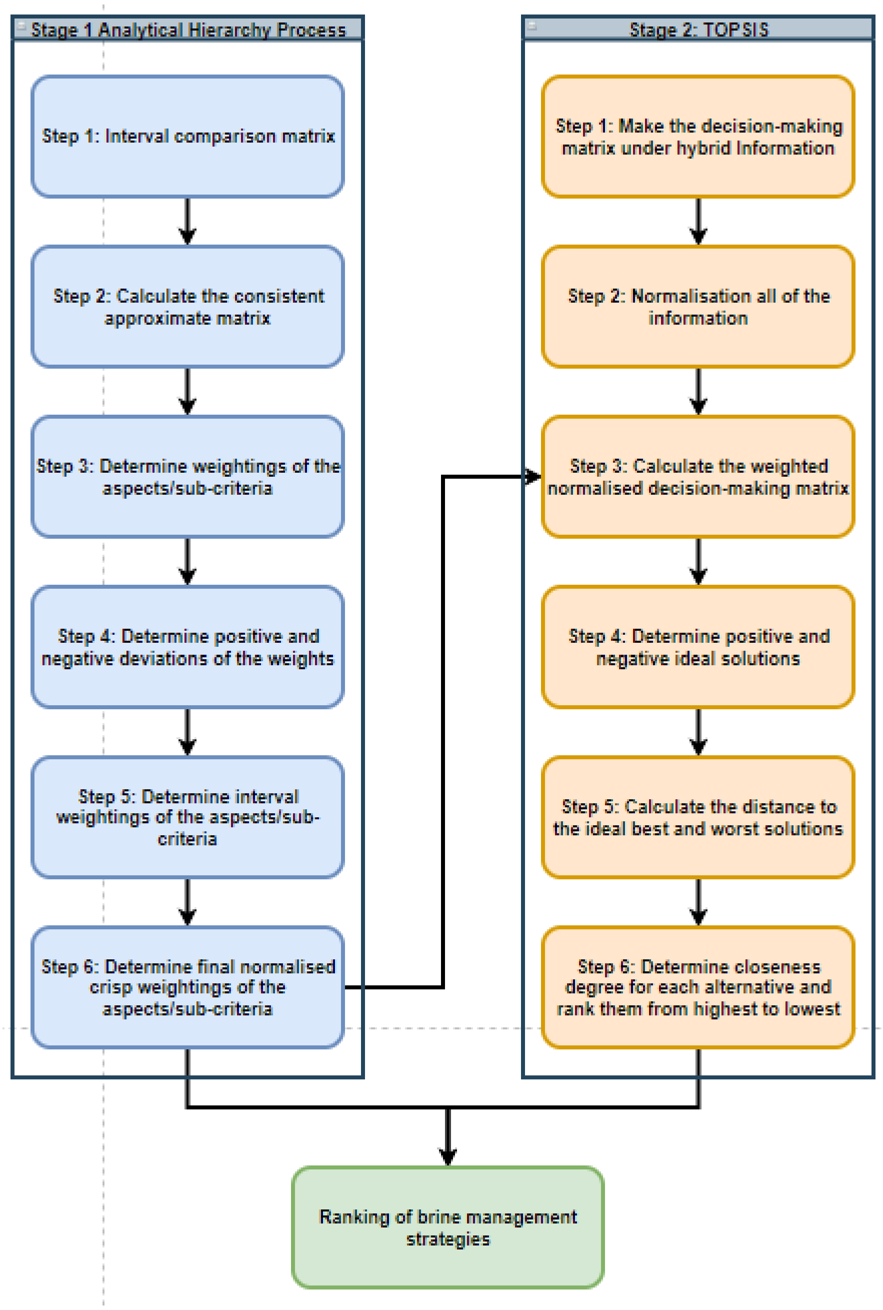


*Figure 4: Framework for MCDA under hybrid information.*

The framework is divided into 2 stages, with each phase addressing one of the previously mentioned concerns. Employing Interval AHP to cover the 1st concern, calculating the weights of criteria and TOPSIS under hybrid information to mitigate the 2nd concern, ranking technologies using multiple types of data. The calculations shown in Sections 3.2 and 3.3 were utilised in excel to create the decision support system, no existing software packages for interval AHP or TZOPSIS were used. The main benefit of conducting the thesis this way is developing a deeper understanding of how the model is operating. IF a software package was used it is a “black box” approach where there is no control of whats happening inside the model.

## 3.1 Criteria Development

The first step of any MCDA technique is determining what criteria apply to the current task or problem. MCDA techniques often employ a hierarchy structure with overarching aspects or global variables encompassing criteria tied to a theme. For example, the 3 pillars of sustainability i.e., economic, environmental and social, which are present in most MCDAs [130]. However, sometimes projects can evolve, requiring additional aspects to be considered. In addition to the economic, environmental and social considerations, technical considerations surrounding the technology are required to evaluate brine management strategies. The technical aspect plays an important role in selecting an appropriate brine management strategy and is independent of the other 3 aspects (economic, social and environmental (Figure 5).

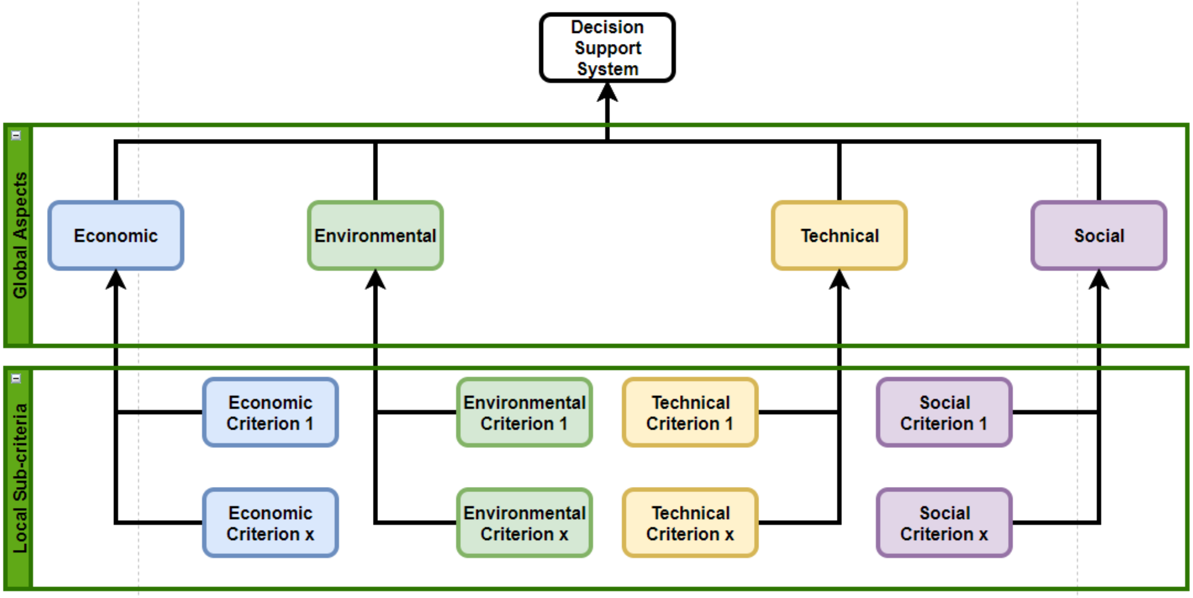


*Figure 5: Decision Support System criteria tree diagram.*

The 4 aspects encompass all considerations that contribute to the overall evaluation of brine management strategies. Sub-criteria for each aspect were designed and evaluated using the following principles [131]:

1. All sub-criteria are related to the definition of the aspect.
2. All criteria are independent.
3. The criteria can be depicted quantitatively or qualitatively.

Principles 2 and 3 are particularly important. If 2 criteria aren't independent, then the commonality of both sub-criteria has been assigned 2 weightings. The results of DDS with dependant criteria could deceive the decision-maker by assigning a higher weighting to criterion unintentionally. DSSs must consider the objective facts (hard/quantitative information) and subjective opinions (soft/qualitative information) that contribute to the problem or selection process.

The selection of aspects and sub-criteria for individual projects within the area of brine management strategies will change for each project. Therefore, developing a master list of criteria that encapsulates most of the likely criteria decision-makers would consider is a reasonable approach (Figure 6). Decision-makers can select and make additional aspects and sub-criteria, assuming the 3 principles listed previously are upheld.

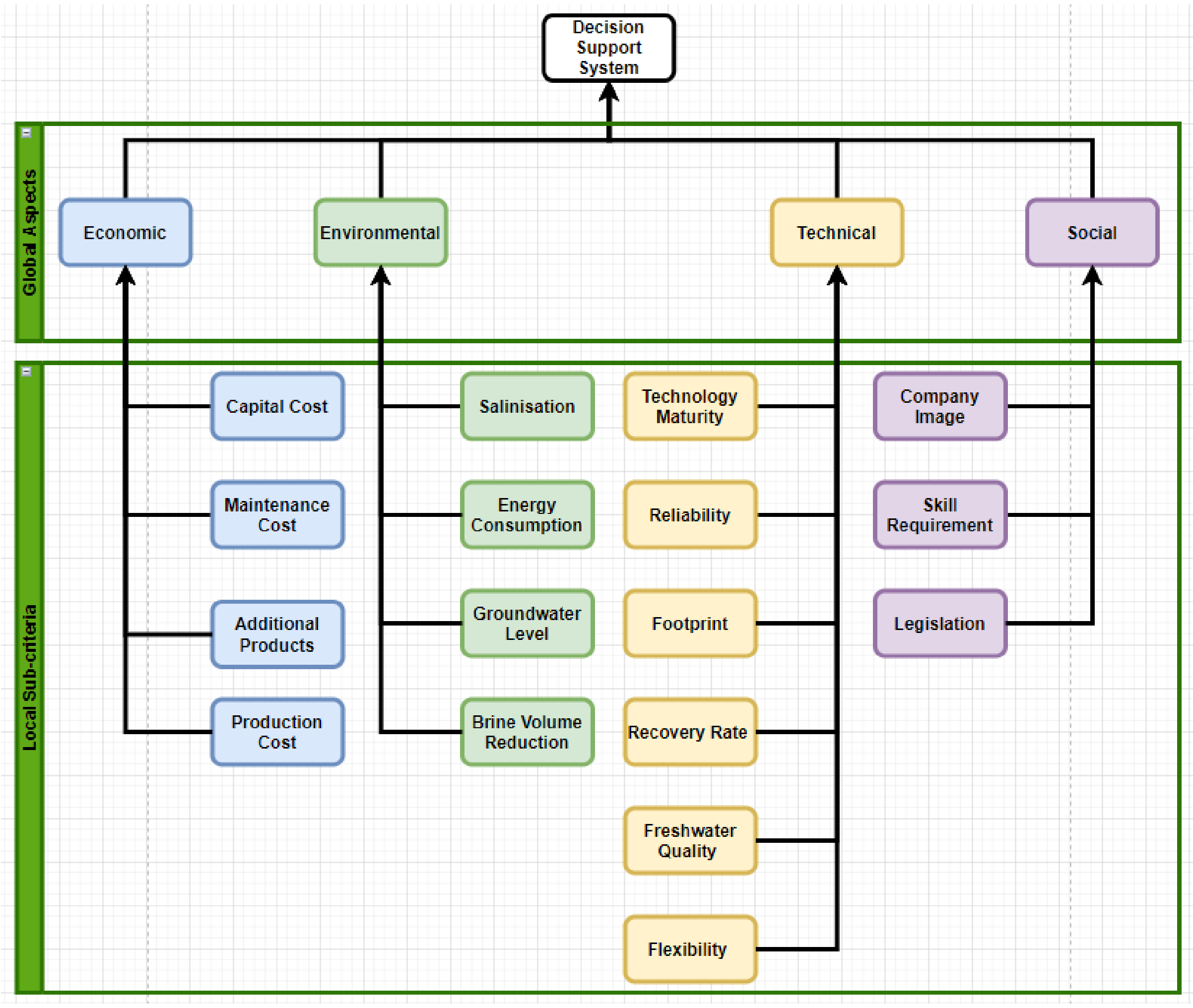


*Figure 6: Master list of criteria used for a brine management DDS.*

The economic aspect contains the sub-criteria components of capital and maintenance costs and producing added-value products. However, the production cost of freshwater is an important economic criterion for technologies with long operational lifetimes (20+ years). The environmental aspect considers the potential impacts of salinisation, energy consumption, groundwater level and brine volume reduction. Energy consumption is a sub-criterion to the environmental aspect due to the intrinsic link between energy usage and carbon footprint. Groundwater level encapsulates potential limitations on the quantity of feed water available for desalination compared to the amount of freshwater required. Salinisation is an indication of the risk and impact of salinisation in the surrounding area if something goes wrong i.e., the lining of an evaporation pond breaks. This is an important criterion if comparing brine disposal methods to treatment methods such as MLD and ZLD.

For example, the impact of a contamination site on agricultural land would be larger than a urban built-up area, such as, a rural town.

The sub-criteria for the technical aspect contain the considerations directly related to the technology covering areas, such as technology maturity, reliability, footprint (size), the recovery rate of freshwater, fresh water quality and flexibility. Technology maturity and reliability are implying the degree of the market readiness of the technology, and in some circumstances can be combined into a singular criterion (market readiness). Footprint accounts for stakeholders or decision-makers finding machinery or built-up processing environments (i.e., evaporation ponds) utilising large areas unfavourably. Recovery of freshwater takes into consideration that not all brine treatment methods recover usable freshwater. There is some crossover between brine volume reduction under the environmental aspect and freshwater recovery. The decision-maker should only be applying one of these sub-criteria (brine volume reduction or recovery rate) to any MCDA. Based on whether the decision-makers considerations primarily fall under environmental concerns (brine minimisation) or technical constraints (recovery rate)? Under most circumstances, freshwater quality is unlikely to play a considerable role in the multi-criteria analysis as all of the technologies that produce additional freshwater covered in the literature review produces drinking quality water. Flexibility accounts for a technology's ability to meet the brine volume produced effectively. This is mostly applicable for small ($1 - 100\ {}^{L}/_{hr}$) to medium ($100 - 500\ {}^{l}/_{hr}$) scale systems. The author believes some technologies will experience efficiency loss or require additional infrastructure to accommodate particular technologies i.e., stop-start systems where brine volume is too low for a continuous system.

The social considerations are more straightforward in comparison to the other 3 aspects. Company image relates to the concept of social license to operate. It refers to the approval of local communities and stakeholders that the organisation has behaved in a socially and environmentally responsible way [132]. The skill required to operate the technology is also an important factor when dealing with remote locations. Finally, the considerations of current and future legislation on the suitability of a particular technology.

## 3.2 Interval Analytic Hierarchy Process (AHP)

The Interval Analytic Hierarchy Process can be divided into 6 steps, shown previously in Figure 4 as stage 1 [129]. All of the necessary calculations were derived from Wang and other's work[129]. The first step is establishing the interval comparison matrix (equation 7). The matrix is designed with a total of n criteria or aspects being evaluated and compared, noted as $\{C_1, C_2 \cdots, C_n\}$. Then assigning interval numbers rating the importance between each pair of criteria and aspects. Interval numbers are represented by $a_{ij}^{\pm}$ (equation 8) ($i = 1, 2, \cdots, n; j = 1, 2, \cdots, n$), where $a_{ij}^{-}$ and $a_{ij}^{+}$ represent the lower and upper bound of $a_{ij}^{\pm}$, respectively. Then using Saaty's nine-scale importance system to guide the assignment of appropriate values to the upper and lower bounds of $a_{ij}^{\pm}$, which are used in the traditional AHP method (Table 2).

| *AHP Step* | Calculation/Matrix | *Eq. Number* |
|---|---|---|
| *1* | $$\begin{array}{|c|c|c|c|c|} \hline & C_1 & C_2 & \cdots & C_n \\ \hline C_1 & 1 & a_{12}^{\pm} & \cdots & a_{1n}^{\pm} \\ \hline C_2 & a_{21}^{\pm} & 1 & \cdots & a_{2n}^{\pm} \\ \hline \vdots & \vdots & \vdots & \ddots & \vdots \\ \hline C_n & a_{n1}^{\pm} & a_{n2}^{\pm} & \cdots & 1 \\ \hline \end{array}$$ | *7* |
| *1* | $a_{ij}^{\pm} = [\, a_{ij}^{-} \;\; a_{ij}^{+}]$ | *8* |

The use of interval numbers in the interval comparison matrix reduces the ambiguity of the decision-makers judgement. For example, if a decision-maker expresses their opinion as "strongly less important" to "moderately less important" then the values of 3 and 5 can be used based on Saaty's scale, as the lower and upper bounds of $a_{ij}^{\pm}$, represented as [3 5]. Using crisp numbers, the decision-maker would be forced to choose a singular expression from Saaty's scale. After comparing each pair of criteria/aspect, the interval comparison matrix can be constructed.

*Table 2: Saaty's nine-scale for relative importance* [133].

| Definition | Explanation | Scale |
|---|---|---|
| **Equal importance** | $C_i$ is equally important comparing with $C_j$ | 1 |
| **Extremely less important** | $C_i$ is extremely less important comparing with $C_j$ | 2 |
| **Strongly less important** | $C_i$ is strongly less important comparing with $C_j$ | 3 |
| **Less important** | $C_i$ is less important comparing with $C_j$ | 4 |
| **Moderately less important** | $C_i$is moderately less important comparing with $C_j$ | 5 |
| **Moderately important** | $C_i$is moderately important comparing with $C_j$ | 6 |
| **Strong importance** | $C_i$is strongly important comparing with $C_j$ | 7 |
| **Very strong Importance** | $C_i$is very strongly important comparing with $C_j$ | 8 |
| **Extreme importance** | $C_i$is extremely important comparing with $C_j$ | 9 |

Progressing further, the consistent approximate matrix (equation 9) can be derived from the interval comparison matrix. Each element of the consistent approximate matrix is denoted by $m_{ij}$ $(i = 1, 2, \cdots, n)$: $(j = 1, 2, \cdots, n)$, calculated through equation 10. Where $m_{ij}$ symbolises the relative priority of the $i$-th criterion to the $j$-th criterion. Lower values indicating more favourable outcomes.

| AHP Step | Calculation/Matrix | Eq. Number |
|---|---|---|
| 2 | $$\begin{array}{|c|c|c|c|c|} \hline & C_1 & C_2 & \cdots & C_n \\ \hline C_1 & 1 & m_{12} & \cdots & m_{1n} \\ \hline C_2 & m_{21} & 1 & \cdots & m_{2n} \\ \hline \vdots & \vdots & \vdots & \ddots & \vdots \\ \hline C_n & m_{n1} & m_{n2} & \cdots & 1 \\ \hline \end{array}$$ | 9 |
| 2 | $$m_{ij} = \left(\prod_{k=1}^{n} \frac{a_{ik}^{-} a_{ik}^{+}}{a_{jk}^{-} a_{jk}^{+}}\right)^{1/2n}$$ | 10 |

The 3rd and 4th step of the Interval AHP process is the determination of the crisp weightings and its positive and negative deviations. The crisp weights ($w_i^*$) are determined by equation 11, using values from the consistent approximate matrix. Then calculating the positive and negative deviations of the crisp weightings ($w_i^*$). Using elements from the interval comparison and consistent approximate matrices to calculate the deviation matrices, following equations 12 and 13 for positive and negative deviation matrices respectively. The positive ($\Delta w_i^+$) and negative ($\Delta w_i^-$) deviations of the crisp weightings of the $i$-th criterion are calculated using the positive and negative deviation matrices alongside elements from the consistent approximate matric, in equations 14 and 15 for positive and negative deviations, respectively.

| *AHP Step* | *Calculation/Matrix* | *Eq. Number* |
|---|---|---|
| *3* | $w_j^* = \frac{1}{\sum_{i=1}^{m} m_{ij}}$ | *11* |
| *4* | $\begin{array}{cccccc} & C_1 & C_2 & \cdots & C_n \\ C_1 & 1 & a_{12}^{+} - m_{12} & \cdots & a_{1n}^{+} - m_{1n} \\ C_2 & a_{21}^{+} - m_{21} & 1 & \cdots & a_{2n}^{+} - m_{2n} \\ \vdots & \vdots & \vdots & \ddots & \vdots \\ C_n & a_{n1}^{+} - m_{n1} & a_{n2}^{+} - m_{n2} & \cdots & 1 \end{array}$ | *12* |
| *4* | $\begin{array}{cccccc} & C_1 & C_2 & \cdots & C_n \\ C_1 & 1 & m_{12} - a_{12}^{-} & \cdots & m_{1n} - a_{1n}^{-} \\ C_2 & m_{21} - a_{21}^{-} & 1 & \cdots & m_{2n} - a_{2n}^{-} \\ \vdots & \vdots & \vdots & \ddots & \vdots \\ C_n & m_{n1} - a_{n1}^{-} & m_{n2} - a_{n2}^{-} & \cdots & 1 \end{array}$ | *13* |
| *4* | $\Delta w_i^{+} = \sqrt{\frac{\sum_{j=1}^{n}({a_{ij}}^{+} - m_{ij})^2}{\left(\sum_{j=1}^{n} m_{ij}\right)^4}}$ | *14* |
| *4* | $\Delta w_i^{-} = \sqrt{\frac{\sum_{j=1}^{n}(m_{ij} - a_{ij}^{-})^2}{\left(\sum_{j=1}^{n} m_{ij}\right)^4}}$ | *15* |

As indicated in Wang et al's paper the 5th and 6th step consist of applying the positive and negative deviations to the crisp weighting and determining the final weightings [129]. By applying the positive and negative weight to the crisp weighting creates an interval weight ($\Delta w_i^{\pm}$) for the $i$-th criterion or aspect, as shown in equation 16. The upper and lower bounds of $\Delta w_i^{\pm}$ are represented by $w^{+}$ and $w^{-}$, respectively, with the subscript $i, g$ and $i, l$ representing the $i$-th aspect (economic, technological, environmental, social) and $i$-th local sub-criteria, respectively. The weightings of the aspects are then applied to each sub-criterion related to it, creating a set of global interval weightings ($GW_i^{\pm}$) for all criteria, through equation 17. The midpoint ($MP_i$) of each global interval weight is then calculated and converted to a normalised crisp weight ($w_i$), through equations 18 and 19, respectively.

| *AHP Step* | Calculation/Matrix | *Eq. Number* |
|---|---|---|
| *5* | $\Delta \mathrm{w}_{\mathrm{i}}^{\pm} = [\mathrm{w}_{\mathrm{i}}^{*} - \Delta \mathrm{w}_{\mathrm{i}}^{-}, \mathrm{w}_{\mathrm{i}}^{*} + \Delta \mathrm{w}_{\mathrm{i}}^{+}] = [\mathrm{w}_{\mathrm{i,l}}^{-}, \mathrm{w}_{\mathrm{i,l}}^{+}] = [\mathrm{w}_{\mathrm{i,g}}^{-}, \mathrm{w}_{\mathrm{i,g}}^{+}]$ | *16* |
| *5* | $GW_i^{\pm} = [w_{i,l}^{-} * w_{i,g}^{-}, w_{i,l}^{+} * w_{i,g}^{+}]$ | *17* |
| *6* | $MP_i = \frac{GW_i^{\pm}}{2}$ | *18* |
| *6* | $w_i = \frac{MP_i}{\sum_{i=1}^{n}(MP_i)}$ | *19* |

## 3.3 Technique for Order Preference by Similarity to an Ideal Solution under Hybrid Information (TOPSIS)

Technique for Order Preference by Similarity to an Ideal Solution under Hybrid Information (TOPSIS) can support a decision-making matrix composed of different types of data to rank brine management strategies or technologies. The main types of data that will be utilised in this document are crisp numbers (whole numbers), interval numbers (range of values) and triangular fuzzy numbers. The TOPSIS under Hybrid Information process can be summarised in the following six steps. All of the equations for TOPSIS shown in this section are derived from Wang et al's work [129].

The first step in the TOPSIS is similar to AHP and consists of producing a decision-making matrix. Consisting of crisp numbers, interval numbers and fuzzy numbers, as presented in equation 20.

| *TOPSIS step* | *Calculation/Matrix* | | | | | *Eq. Number* |
|---|---|---|---|---|---|---|
| | | $A_1$ | $A_2$ | $\cdots$ | $A_M$ | |
| | $C_1$ | $x_{11}$ | $x_{12}$ | $\cdots$ | $x_{1M}$ | |
| | $\vdots$ | $\vdots$ | $\vdots$ | $\ddots$ | $\vdots$ | |
| | $C_K$ | $x_{K1}$ | $x_{K2}$ | $\cdots$ | $x_{KM}$ | |
| | $C_{K+1}$ | $y^{\pm}_{(K+1)1}$ | $y^{\pm}_{(K+1)2}$ | $\cdots$ | $y^{\pm}_{(K+1)M}$ | |
| *1* | $\vdots$ | $\vdots$ | $\vdots$ | $\ddots$ | $\vdots$ | *20* |
| | $C_{K+L}$ | $y^{\pm}_{(K+L)1}$ | $y^{\pm}_{(K+L)2}$ | $\cdots$ | $y^{\pm}_{(K+L)M}$ | |
| | $C_{K+L+1}$ | $z^{\pm}_{(K+L+1)1}$ | $z^{\pm}_{(K+L+1)2}$ | $\cdots$ | $z^{\pm}_{(K+L+1)M}$ | |
| | $\vdots$ | $\vdots$ | $\vdots$ | $\ddots$ | $\vdots$ | |
| | $C_{K+L+T}$ | $z^{\pm}_{(K+L+T)1}$ | $z^{\pm}_{(K+L+T)2}$ | $\cdots$ | $z^{\pm}_{(K+L+T)M}$ | |

$A_j(j = 1, 2, \cdots, M)$ represents the $j$-th brine management strategy/technology. $C_i(i = 1,2, \cdots, K)$, $C_i(i = K + 1, K + 2, \cdots, K + L)$ and $C_i(i = K + L + 1, K + L + 2, \cdots, K + L + T)$ represents the criteria that can be described by crisp numbers, interval numbers and fuzzy numbers, respectively. Different data-types in the decision-making matrix use the notation of $x_{ij}(i = 1,2, \cdots, K)$, $y^{\pm}_{ij} = [y^{-}_{ij}\ ,\quad y^{+}_{ij}](i = K + 1, K + 2, \cdots, K + L)$ and $z'_{ij} = [z^{l}_{ij}\ ,\quad z^{m}_{ij}\ ,\quad z^{h}_{ij}](i = K + L + 1, K + L + 2, \cdots, K + L + T)$ for crisp numbers, interval numbers and fuzzy numbers, respectively. The superscripts – and + denote the lower and upper bounds of an interval number. While the superscripts $l, m$ and $h$ are representing the low, medium and high values of the fuzzy numbers. To distinguish matrices and individual elements within a matrix, the author will use square brackets to denote a matrix and commas to denote separate elements and equations relating to separate elements.

Crisp numbers are used when the relevant data of a criterion is determined to be hard evaluation criteria i.e., objective facts. Interval numbers are used when the data can't be presented as crisp number and may vary depending on a variety of circumstances i.e., energy consumption. Fuzzy numbers are used to rate criteria that can't be numerically represented, but can be rated relative to other alternatives using linguistic terms i.e., extremely bad, bad, good, extremely good. Seven linguistic terms are used corresponding to 7 triangular fuzzy number sets, comparing the relative performances of each technology to a particular criterion (Table 3).

*Table 3: Linguistic terms and the corresponding fuzzy numbers.*

| Linguistic Term | Abbreviation | Corresponding Fuzzy number |
|---|---|---|
| Extremely Bad | EB | $[0 \quad 0 \quad 0.1]$ |
| Very Bad | VB | $[0.1 \quad 0.2 \quad 0.3]$ |
| Bad | B | $[0.2 \quad 0.3 \quad 0.4]$ |
| Moderate | M | $[0.4 \quad 0.5 \quad 0.6]$ |
| Good | G | $[0.6 \quad 0.7 \quad 0.8]$ |
| Very Good | VG | $[0.8 \quad 0.9 \quad 1]$ |
| Extremely Good | EG | $[0.9 \quad 1 \quad 1]$ |

The next step is to normalise all of the data-types to eliminate the impacts of the units corresponding to each criterion with the ranking process. The data entered into the decision-making matrix will fall into one of two categories. The 1$^{st}$ category is known as a benefit-type criteria (BC), where higher values for a particular criterion is more beneficial to a technology. The 2$^{nd}$ category is the opposite of the benefit-type criteria, known as a cost-type criteria (CC), where data with the smallest values are preferred. Crisp numbers, interval numbers and fuzzy numbers can be normalised using equations 21, 22 and 23, respectively.

| TOPSIS step | Calculation/Matrix | Eq. Number |
|---|---|---|
| 2 | $Nx_{ij} = \begin{cases} \dfrac{x_{ij} - \min\limits_{j}^{M}\{x_{ij}\}}{\max\limits_{j}^{M}\{x_{ij}\} - \min\limits_{j}^{M}\{x_{ij}\}} \; (j = 1,2 \cdots, M: j \epsilon BC \\ \dfrac{\max\limits_{j}^{M}\{x_{ij}\} - x_{ij}}{\max\limits_{j}^{M}\{x_{ij}\} - \min\limits_{j}^{M}\{x_{ij}\}} \; (j = 1,2 \cdots, M: j \epsilon CC \end{cases}$ | 21 |
| 2 | $Ny_{ij}^{\pm} = \begin{cases} \dfrac{y_{ij}^{-} - \min\limits_{j}^{M}\{y_{ij}^{-}\}}{\max\limits_{j}^{M}\{y_{ij}^{+}\} - \min\limits_{j}^{M}\{y_{ij}^{-}\}}, \dfrac{y_{ij}^{+} - \min\limits_{j}^{M}\{y_{ij}^{-}\}}{\max\limits_{j}^{M}\{y_{ij}^{+}\} - \min\limits_{j}^{M}\{y_{ij}^{-}\}} \\ (j = 1,2 \cdots, M: j \epsilon BC \\ \dfrac{\max\limits_{j}^{M}\{y_{ij}^{+}\} - y_{ij}^{+}}{\max\limits_{j}^{M}\{y_{ij}^{+}\} - \min\limits_{j}^{M}\{y_{ij}^{-}\}}, \dfrac{\max\limits_{j}^{M}\{y_{ij}^{+}\} - y_{ij}^{-}}{\max\limits_{j}^{M}\{y_{ij}^{+}\} - \min\limits_{j}^{M}\{y_{ij}^{-}\}} \\ (j = 1,2 \cdots, M: j \epsilon CC \end{cases}$ | 22 |
| 2 | $Nz_{ij}' = \begin{cases} \dfrac{z_{ij}^{l} - \min\limits_{j}^{M}\{z_{ij}^{l}\}}{\max\limits_{j}^{M}\{z_{ij}^{h}\} - \min\limits_{j}^{M}\{z_{ij}^{l}\}}, \dfrac{z_{ij}^{m} - \min\limits_{j}^{M}\{z_{ij}^{l}\}}{\max\limits_{j}^{M}\{z_{ij}^{h}\} - \min\limits_{j}^{M}\{z_{ij}^{l}\}}, \dfrac{z_{ij}^{h} - \min\limits_{j}^{M}\{z_{ij}^{l}\}}{\max\limits_{j}^{M}\{z_{ij}^{h}\} - \min\limits_{j}^{M}\{z_{ij}^{l}\}} \\ (j = 1,2 \cdots, M: j \epsilon BC \\ \dfrac{\max\limits_{j}^{M}\{z_{ij}^{h}\} - z_{ij}^{h}}{\max\limits_{j}^{M}\{z_{ij}^{h}\} - \min\limits_{j}^{M}\{z_{ij}^{l}\}}, \dfrac{\max\limits_{j}^{M}\{z_{ij}^{h}\} - z_{ij}^{m}}{\max\limits_{j}^{M}\{z_{ij}^{h}\} - \min\limits_{j}^{M}\{z_{ij}^{l}\}}, \dfrac{\max\limits_{j}^{M}\{z_{ij}^{h}\} - z_{ij}^{l}}{\max\limits_{j}^{M}\{z_{ij}^{h}\} - \min\limits_{j}^{M}\{z_{ij}^{l}\}} \\ (j = 1,2 \cdots, M: j \epsilon CC \end{cases}$ | 23 |

Where the normalised data of crisp numbers, interval numbers and fuzzy numbers are denoted by $\mathrm{Nx_{ij}}$ $(j = 1,2,\cdots,K)$, $\mathrm{Ny_{ij}^{\pm}} = [Ny_{ij}^{-}\ ,\quad Ny_{ij}^{+}](i = K+1, K+2,\cdots,K+L)$ and $\mathrm{Nz_{ij}'} = [Nz_{ij}^{l}\ ,\quad Nz_{ij}^{m}\ ,\quad Nz_{ij}^{h}](i = K+L+1, K+L+2,\cdots,K+L+T)$, respectively. Each normalised value has the same form as the original input data-type. Therefore, crisp numbers are presented as individual values, interval numbers are represented in a 1 by 2 matrix and fuzzy numbers are presented in a 1 by 3 matrix. The normalised data can then be transferred to a normalised hybrid information matrix (equation 24).

| *TOPSIS step* | *Calculation/Matrix* | *Eq. Number* |
|---|---|---|
| *2* | (matrix below) | *24* |

| | $A_1$ | $A_2$ | $\cdots$ | $A_M$ |
|---|---|---|---|---|
| $C_1$ | $Nx_{11}$ | $Nx_{12}$ | $\cdots$ | $Nx_{1M}$ |
| $\vdots$ | $\vdots$ | $\vdots$ | $\ddots$ | $\vdots$ |
| $C_K$ | $Nx_{K1}$ | $Nx_{K2}$ | $\cdots$ | $Nx_{KM}$ |
| $C_{K+1}$ | $Ny_{(K+1)1}^{\pm}$ | $Ny_{(K+1)2}^{\pm}$ | $\cdots$ | $Ny_{(K+1)M}^{\pm}$ |
| $\vdots$ | $\vdots$ | $\vdots$ | $\ddots$ | $\vdots$ |
| $C_{K+L}$ | $Ny_{(K+L)1}^{\pm}$ | $Ny_{(K+L)2}^{\pm}$ | $\cdots$ | $Ny_{(K+L)M}^{\pm}$ |
| $C_{K+L+1}$ | $Nz_{(K+L+1)1}^{\pm}$ | $Nz_{(K+L+1)2}^{\pm}$ | $\cdots$ | $Nz_{(K+L+1)M}^{\pm}$ |
| $\vdots$ | $\vdots$ | $\vdots$ | $\ddots$ | $\vdots$ |
| $C_{K+L+T}$ | $Nz_{(K+L+T)1}^{\pm}$ | $Nz_{(K+L+T)2}^{\pm}$ | $\cdots$ | $Nz_{(K+L+T)M}^{\pm}$ |

The next step is to determine the weighted normalised hybrid information matrix ($WND$), where $WND_{ij}$ represents the normalised data for the $i$-th criterion to the $j$-th technology (equation 25). This is where the normalised crisp weightings calculated at the end of the Interval AHP (equation 19) combines with the TOPSIS process, as seen in Figure 4.

| TOPSIS step | Calculation/Matrix | Eq. Number |
|---|---|---|
| 3 | $WND_{ij} = w_i ND_{ij} = \begin{cases} \begin{cases} w_i N x_{ij} \\ (i = 1, 2, \cdots, K) \\ w_i N y_{ij}^{\pm} \\ (i = K+1, K+2, \cdots, K+L) \\ w_i N z'_{ij} \\ (i = K+L+1, K+L+2, \cdots, K+L+T) \end{cases} \\ \begin{cases} w_i N x_{ij} \\ (i = 1, 2, \cdots, K) \\ \left[ w_i N y_{ij}^{-}, w_i N y_{ij}^{+} \right] \\ (i = K+1, K+2, \cdots, K+L) \\ \left( w_i N z_{ij}^{l}, w_i N z_{ij}^{m}, w_i N z_{ij}^{h} \right) \\ (i = K+L+1, K+L+2, \cdots, K+L+T) \end{cases} \end{cases}$ | 25 |

The next step is to determine the highest and lowest values of the data set of a specific criterion. These values are known as the positive and negative ideal solutions. Positive and negative ideal solutions will be denoted as $v^+$ and $v^-$ respectively. The positive and negative ideal solutions are presented in the same format of the data input i.e., crisp numbers will produce a crisp ideal solution and interval numbers will produce an interval ideal solution. Calculating the positive and negative ideal solutions for each element of $WND$ are attainable through equations 27 and 29, respectively. The positive and negative ideal solutions can then be shown as a matrix through equations 26 and 28, for positive and negative ideal solutions respectively.

| *TOPSIS step* | *Calculation/Matrix* | *Eq. Number* |
|---|---|---|
| *4* | $V^{+}=[v_1^{+},\cdots,v_K^{+}\quad v_{K+1}^{+},\cdots,v_{K+L}^{+}\quad v_{K+L+1}^{+},\cdots,v_{K+L+T}^{+}]$ | *26* |
| *4* | $v_i^{+}=\begin{cases}\max\limits_{j=1}^{M} w_iNx_{ij} \\ (i=1,2,\cdots,K) \\ \left[\max\limits_{j=1}^{M} w_iNy_{ij}^{-},\max\limits_{j=1}^{M} w_iNy_{ij}^{+}\right] \\ (i=K+1,K+2,\cdots,K+L) \\ \left(\max\limits_{j=1}^{M} w_iNz_{ij}^{l},\max\limits_{j=1}^{M} w_iNz_{ij}^{m},\max\limits_{j=1}^{M} w_iNz_{ij}^{h}\right) \\ (i=K+L+1,K+L+2,\cdots,K+L+T)\end{cases}$ | *27* |
| *4* | $V^{-}=[v_1^{-},\cdots,v_K^{-}\quad v_{K+1}^{-},\cdots,v_{K+L}^{-}\quad v_{K+L+1}^{-},\cdots,v_{K+L+T}^{-}]$ | *28* |
| *4* | $v_i^{-}=\begin{cases}\min\limits_{j=1}^{M} w_iNx_{ij} \\ (i=1,2,\cdots,K) \\ \left[\min\limits_{j=1}^{M} w_iNy_{ij}^{-},\min\limits_{j=1}^{M} w_iNy_{ij}^{+}\right] \\ (i=K+1,K+2,\cdots,K+L) \\ \left(\min\limits_{j=1}^{M} w_iNz_{ij}^{l},\min\limits_{j=1}^{M} w_iNz_{ij}^{m},\min\limits_{j=1}^{M} w_iNz_{ij}^{h}\right) \\ (i=K+L+1,K+L+2,\cdots,K+L+T)\end{cases}$ | *29* |

From the positive ideal solutions, the distance to the positive ideal best solutions can be calculated (equations 30-33). The distance to the positive ideal best solution for technology $A_j$ is denoted by $d(A_j, V^{+})$ (equation 30). Calculating the positive distance to the ideal solution for crisp, interval and fuzzy numbers for each criterion is done through equations 31-33. The positive distance between the weighted normalised data ($w_iNx_{ij}$ (crisp numbers), $w_iNy_{ij}^{\pm}$(interval numbers) and $w_iNz_{ij}'$ (fuzzy numbers)) and the ideal positive solution ($v_i^{+}$) for the related criterion is denoted by $d(w_iNx_{ij}, v_i^{+})$, $d(w_iNy_{ij}^{\pm}, v_i^{+})$ and $d(w_iNz_{ij}', v_i^{+})$ for crisp, interval and fuzzy numbers. A similar process is also conducted to determine the negative distance to the ideal worst solution ($d(A_j, V^{-})$), through equations

34-37. The negative distance to the ideal negative solution ($v_i^-$) are denoted by $d(w_i N x_{ij}, v_i^-)$, $d(w_i N y_{ij}^{\pm}, v_i^-)$ and $d(w_i N z'_{ij}, v_i^-)$ for crisp, interval and fuzzy numbers, respectively. A good mental visualisation of the positive and negative distance is imagining a string with a known point somewhere along the string. One end of the string represents the best outcome, meanwhile the other is the worst outcome. The positive distance is the distance between the known point and the best outcome. The negative distance is the distance between the known point and the worst outcome.

| *TOPSIS step* | *Calculation/Matrix* | *Eq. Number* |
|---|---|---|
| *5* | $d(A_j, V^+) = \sqrt{\sum_{i=1}^{K}\left[d(w_i N x_{ij}, v_i^+)\right]^2 + \sum_{i=K+1}^{K+L}\left[d(w_i N y_{ij}^{\pm}, v_i^+)\right]^2 + \sum_{i=K+L+1}^{K+L+T}\left[d(w_i N z'_{ij}, v_i^+)\right]^2}$ | *30* |
| *5* | $d(w_i N x_{ij}, v_i^+) = w_i N x_{ij} - v_i^+$ | *31* |
| *5* | $d(w_i N y_{ij}^{\pm}, v_i^+) = \sqrt{\frac{\left(w_i N y_{ij}^{-} - \max_{j=1}^{M} w_i N y_{ij}^{-}\right)^2 + \left(w_i N y_{ij}^{+} - \max_{j=1}^{M} w_i N y_{ij}^{+}\right)^2}{2}}$ | *32* |
| *5* | $d(w_i N z'_{ij}, v_i^+) = \sqrt{\frac{\left(w_i N z_{ij}^{l} - \max_{j=1}^{M} w_i N z_{ij}^{l}\right)^2 + \left(w_i N z_{ij}^{m} - \max_{j=1}^{M} w_i N z_{ij}^{m}\right)^2 + \left(w_i N z_{ij}^{h} - \max_{j=1}^{M} w_i N z_{ij}^{h}\right)^2}{3}}$ | *33* |

| | | |
|---|---|---|
| 5 | $d\left(A_j, V^-\right) = \sqrt{\sum_{i=1}^{K}\left[d\left(w_i N x_{ij}, v_i^-\right)\right]^2 + \sum_{i=K+1}^{K+L}\left[d\left(w_i N y_{ij}^{\pm}, v_i^-\right)\right]^2 + \sum_{i=K+L+1}^{K+L+T}\left[d\left(w_i N z_{ij}', v_i^-\right)\right]^2}$ | 34 |
| 5 | $d\left(w_i N x_{ij}, v_i^-\right) = w_i N x_{ij} - v_i^-$ | 35 |
| 5 | $d\left(w_i N y_{ij}^{\pm}, v_i^-\right) = \sqrt{\frac{\left(w_i N y_{ij}^{-} - \min_{j=1}^{M} w_i N y_{ij}^{-}\right)^2 + \left(w_i N y_{ij}^{+} - \min_{j=1}^{M} w_i N y_{ij}^{+}\right)^2}{2}}$ | 36 |
| 5 | $d\left(w_i N z_{ij}', v_i^-\right) = \sqrt{\frac{\left(w_i N z_{ij}^{l} - \min_{j=1}^{M} w_i N z_{ij}^{l}\right)^2 + \left(w_i N z_{ij}^{m} - \min_{j=1}^{M} w_i N z_{ij}^{m}\right)^2 + \left(w_i N z_{ij}^{h} - \min_{j=1}^{M} w_i N z_{ij}^{h}\right)^2}{3}}$ | 37 |

Finally, the closeness degree ($CD_i$) can be calculated through equation 38 to determine which technology is the closest to the ideal solution. The closeness degree for each technology is then ranked from highest to smallest, with the highest value representing the most superior (preferred) technology.

| *TOPSIS step* | *Calculation/Matrix* | *Eq. Number* |
|---|---|---|
| 6 | $CD_i = \frac{d\left(A_j, V^-\right)}{d\left(A_j, V^-\right) + d\left(A_j, V^+\right)}$ | 38 |

Unlike the AHP process that requires an iteration of the first 5 steps for aspects and the sets of sub-criteria i.e., 1+ however many aspects there are. The TOPSIS process is complete after only 1 iteration.

# 4 Case Study

A case study was developed to showcase the DDS using 4 brine management technologies, namely, membrane distillation (MD), forward osmosis (FO) with regeneration (ability to recover freshwater), osmotically-assisted reverse osmosis (OARO) and eutectic freeze crystallisation (EFC). Minimal liquid discharge (MLD) is the current mindset for most decision-makers in the brine management domain. Therefore, 3 out of the 4 technologies selected are primarily used for MLD. Meanwhile, EFC is included as a representation of the current status of thermal technologies aiming for zero liquid discharge (ZLD). The selection of technologies was also partially made based on the authors understanding of each technology to ensure assigned values to subjective variables, i.e., variables with linguistic terms, were reasonable. This section is separated into 2 components, namely criteria selection and model demonstration. Criteria selection goes through the selection of criteria. The model demonstration section goes through the AHP and TOPSIS process outlined in sections 3.2 and 3.3 using relevant input data from literature and the authors understanding of each technology.

## 4.1 Criteria Selection

Capital cost and production cost were selected as a measurement of economic performance. Both criteria utilised crisp numbers. Capital costs have assumptions based on the author's knowledge. This is primarily an artefact of the current state of most of the brine treatment technologies. It is challenging to find Capital Expenditure (CAPEX) and Operating Expenditure (OPEX) in literature for technologies that aren't technologically mature (lab-scale or pilot-scale). This is also the justification for not including maintenance costs as an economic indicator.

The author is utilising the energy consumption and total dissolved solids (TDS) limit of each technology as the performance indicators for the environmental aspect. As previously mentioned, energy consumption has a direct relationship to the carbon footprint of the technology. The TDS limit of the technology is used as a crude indirect representation of the recovery rate and brine volume reduction of the technology. The relationship between TDS limit and volume was outlined in Section 2.1.1 Brine Characteristics. The data types for energy consumption and TDS of the brine are interval numbers and crisp numbers, respectively. In some situations, energy consumption has been identified as a crisp number in the literature. However, transforming crisp numbers into an interval number is straightforward, i.e., $8\ {kWh}/{m^3}$ transforms into [$8\ {kWh}/{m^3},\quad 8\ {kWh}/{m^3}$]. All of the necessary data for capital cost, production cost, energy consumption and TDS of the brine was collected through various sources, summarised in Table 1.

The technical aspect involves applying 4 sub-criteria, technology maturity, technology reliability, footprint and flexibility. By including technology maturity and reliability as sub-criteria to the technical aspect, using it to gauge the market readiness of each technology. Footprint and flexibility are used to indicate how large the system is and how well it adapts to different feed volumes. The footprint (area) of each technology given an interval number representing the author's best guess of the size of the technology. Currently, in the literature the size of each technology is rarely mentioned. Under ideal conditions the footprint of the system would be identified as a crisp number. The model will be using linguistic terms for technology maturity, technology reliability and flexibility. The social aspect is made up of the following components, skill requirement and company image. Both sub-criteria are assigned linguistic terms, as they can't be represented numerically. A summary of the selected sub-criteria is shown in Figure 7.

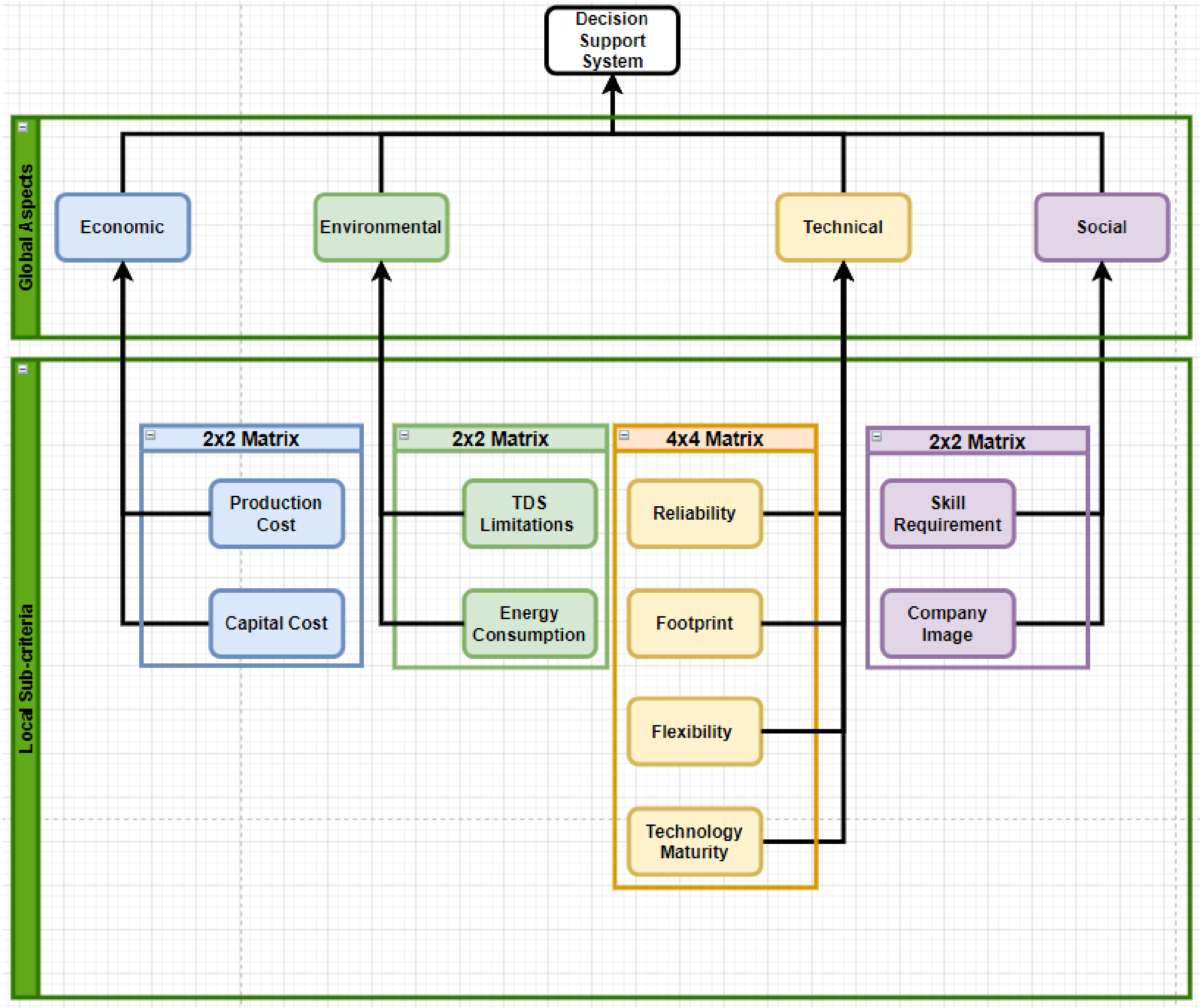


*Figure 7:Case study- DDS criteria and aspect tree.*

## 4.2 Model Demonstration

Firstly, using the interval AHP method to determine the weightings of all the aspects and related sub-criteria. The first step is to populate the interval comparison matrix for the aspects and the sub-criteria. Ideally, the interval comparison matrices are populated by multiple decision-makers. However, for this case study, the interval comparison matrices were populated by the author. The interval AHP process for the technical sub-criteria was also not populated, because the author's attempt to verify the model with the paper it was adapted from, failed, and the reason why is unclear. Attempts to communicate with the corresponding authors of the paper the methodology is adapted from also fell through. In order to navigate around this issue, the author assigned local interval weightings (step 5 of

AHP) directly for the technical sub-criteria. Further repercussions of this workaround will be discussed in the discussion section and through a sensitivity analysis. The populated interval comparison matrix for the 4 aspects (economic, environmental, technical and social) is presented in Table 4. The cells that overlap aspects or sub-criteria of the same type are always allocated the value $[1 \quad 1]$ as their importance to itself is always equal (1 is equal importance going back to Saaty's nine-scale in Table 2).

*Table 4: Populated interval comparison matrix for the economic, environmental, technical and social aspects.*

| | ECONOMIC | ENVIRONMENTAL | TECHNICAL | SOCIAL |
|---|---|---|---|---|
| **ECONOMIC** | $[1 \quad 1]$ | $[1/2 \quad 1]$ | $[1/3 \quad 1]$ | $[1/4 \quad 1/3]$ |
| **ENVIRONMENTAL** | $[1 \quad 2]$ | $[1 \quad 1]$ | $[1/5 \quad \frac{1}{4}]$ | $[1/4 \quad 1/3]$ |
| **TECHNICAL** | $[1 \quad 3]$ | $[4 \quad 5]$ | $[1 \quad 1]$ | $[1/2 \quad 1]$ |
| **SOCIAL** | $[3 \quad 4]$ | $[3 \quad 4]$ | $[1 \quad 2]$ | $[1 \quad 1]$ |

The values chosen by the decision-makers for the interval comparison matrix are used to populate the consistent approximate matrix by using following equations 9 and 10. For example, calculating the value of the cell in the 1st row and 2nd column of the consistence approximate matrix is shown in equation 39. For future reference, the subscript 12 refers to the cell in the 1st row and 2nd column. Populating the remaining cells results in a complete consistent approximate matrix (

Table 5).

$$m_{12} = \left(\frac{1 * 1 * \frac{1}{2} * 1 * \frac{1}{3} * 1 * \frac{1}{4} * \frac{1}{3}}{1 * 1 * 1 * 2 * 1 * 3 * 3 * 4}\right)^{\frac{1}{2*4}} = 0.3432 \quad (39)$$

*Table 5: Consistent approximate matrix for the AHP Process.*

| | Economic | Environmental | Technical | Social |
|---|---|---|---|---|
| **Economic** | 1 | 0.3432 | 1.1906 | 0.8963 |
| **Environmental** | 0.3014 | 1 | 1.1157 | 0.8399 |
| **Technical** | 0.8399 | 0.8963 | 1 | 2.3409 |
| **Social** | 1.1157 | 1.1906 | 4.1300 | 1 |

The next step of the AHP process (step 3), determines the weights of the aspects or sub-criteria according to equation 11. Examples of calculating the weights for the economic, environmental, technical and social aspects are shown in equations 40-43.

$$\omega_{economic} = \frac{1}{1 + 0.3014 + 0.8399 + 1.1157} = 0.3070 \quad (40)$$

$$\omega_{Environmental} = \frac{1}{0.3432 + 1 + 0.8963 + 1.1906} = 0.2915 \quad (41)$$

$$\omega_{Technical} = \frac{1}{1.1906 + 1.1157 + 1 + 4.1300} = 0.1345 \quad (42)$$

$$\omega_{Social} = \frac{1}{0.8963 + 0.8399 + 2.2409 + 1} = 0.1970 \quad (43)$$

We now calculate the positive and negative deviations of the weights. Firstly, the deviation matrices need to be constructed. According to equation 12, the positive deviation matrix can by populated by following the example shown in equation 44 for each cell of the positive deviation matrix. Populating the positive deviation matrix results in Table 6. The negative deviation matrix can be populated according to equation 13. An example of the calculation in each cell of the negative deviation matrix and the fully populated matrix is shown in equation 45 and Table 7.

$$\omega_{12}^{+} = a_{12}^{+} - m_{12} = 1 - 0.3432 = 0.6568 \qquad 44$$

*Table 6: AHP Process – Populated positive deviation matrix.*

| | Economic | Environmental | Technical | Social |
|---|---|---|---|---|
| **Economic** | $0$ | $0.6568$ | $-0.1906$ | $-0.5630$ |
| **Environmental** | $1.6986$ | $0$ | $-0.8657$ | $-0.5099$ |
| **Technical** | $2.1631$ | $4.1037$ | $0$ | $-1.3409$ |
| **Social** | $2{,}8843$ | $2.8094$ | $-2.1300$ | $0$ |

$$\omega_{12}^{-} = m_{12} - a_{12}^{-} = 0.3432 - 0.5 = -0.1568 \qquad 45$$

*Table 7: AHP Process – Populated negative deviation matrix.*

| | Economic | Environmental | Technical | Social |
|---|---|---|---|---|
| **Economic** | $0$ | $-0.1568$ | $0.8576$ | $0.6463$ |
| **Environmental** | $-0.6989$ | $0$ | $0.9157$ | $0.5899$ |
| **Technical** | $-0.1601$ | $-3.1037$ | $0$ | $1.8409$ |
| **Social** | $-1.8846$ | $-1.8397$ | $3.1300$ | $0$ |

The next step uses the positive and negative deviation matrices to determine the positive and negative deviations of each aspect or sub-criteria. An example of calculating the positive and negative deviations of the economic aspect using the respective matrices is shown in equations 46 and 47.

$$\Delta w_{economic}^{+} = \sqrt{\frac{\sum_{j=1}^{n}(a_{ij}{}^{+} - m_{ij})^2}{\left(\sum_{j=1}^{n} m_{ij}\right)^4}}$$

46

$$= \sqrt{\frac{0^2 + 0.6568^2 + -0.1906^2 + -0.5630^2}{(0 + 0.6548 - 0.1906 - 0.5630)^4}} = 0.0753$$

$$\Delta w_{economic}^{-} = \sqrt{\frac{\sum_{j=1}^{n}\left(m_{ij} - a_{ij}^{-}\right)^2}{\left(\sum_{j=1}^{n} m_{ij}\right)^4}}$$

47

$$= \sqrt{\frac{0^2 - 0{,}1568^2 + 0.8576^2 + 0.6463^2}{(0 - 0.1568 + 0.8576 + 0.6463)^4}} = 0.0922$$

Applying the positive and negative deviations to the aspect weightings calculated in equations 40-43 creates the interval weights of each aspect by following equation 16. The results of this calculation are summarised in Table 8.

*Table 8: AHP Process - Deviations and interval weights of the economic, environmental, technical and social aspects.*

| | *Economic* | *Environmental* | *Technical* | *Social* |
|---|---|---|---|---|
| *Positive deviation* | 0.0753 | 0.1860 | 0.1873 | 0.0824 |
| *Negative deviation* | 0.0922 | 0.1220 | 0.1401 | 0.0740 |
| *Interval weights* | $[0.2148 \quad 0.3823]$ | $[0.1696 \quad 0.4776]$ | $[-0.0056 \quad 0.3218]$ | $[0.1230 \quad 0.2793]$ |

Calculating the local interval weights of the sub-criteria under the economic, environmental, technical and social aspects is conducted similarly to how the aspect interval weights are calculated. The main notable difference between calculating the interval weights is the size of the matrices, which is tied to the number of sub-criteria, i.e., if there are 2 sub-criteria under the social aspect then the relevant matrix size is a 2x2 matrix. The size of the sub-criteria matrices was previously indicated in Figure 7. The local interval weightings for the sub-criteria then need to be converted into global interval weights by following equation 17. Moving forward in the AHP process, the next step is calculating the midpoints of each global interval weight as seen in equation 18. The final step of the AHP process involves calculating the crisp weightings for each sub-criteria following equation 19. An example of the process of converting local interval weightings of the sub-criteria into crisp weightings is demonstrated through equations 48-50 for the capital cost sub-criteria. A summary of the entire process for all sub-criteria is shown in Table 9.

$$GW_i^{\pm} = \left[w_{i,l}^{-} * w_{i,g}^{-}, w_{i,l}^{+} * w_{i,g}^{+}\right]$$
$$= [0.5147 * 0.2148 \quad 0.6863 * 0.3823] = [0.1106 \quad 0.2624] \qquad 48$$

$$MP_{capital\ cost} = \frac{0.1106 + 0.2624}{2} = 0.1865 \qquad 49$$

$$\omega_{capital\ cost} = \frac{MP_i}{\sum_{i=1}^{n}(MP_i)} = \frac{0.1865}{1.1192} = 0.1666 \qquad 50$$

*Table 9: TOPSIS Process - Conversion of local sub-criteria weightings into crisp weightings.*

| Conversion from local weightings to crisp weightings | | | | | | | | | |
|---|---|---|---|---|---|---|---|---|---|
| Aspects | Aspect weightings | | Sub-criteria | Local Interval weights | | Global interval weightings | | Mid-Point | Crisp weightings |
| | Lower bound | Upper bound | | Lower bound | Upper bound | Lower bound | Upper bound | | |
| Economic | 0.2148 | 0.3823 | Capital cost | 0.5147 | 0.6863 | 0.1106 | 0.2624 | 0.1865 | 0.1666 |
| | | | Production cost | 0.3431 | 0.5147 | 0.0737 | 0.1968 | 0.1352 | 0.1208 |
| Environmental | 0.1696 | 0.4776 | TDS Limitation | 0.2679 | 0.5359 | 0.0454 | 0.2559 | 0.1507 | 0.1346 |
| | | | Energy consumption | 0.5359 | 0.8038 | 0.0909 | 0.3839 | 0.2374 | 0.2121 |
| Tech | -0.0056 | 0.3218 | Footprint | 0.3500 | 0.4000 | -0.0020 | 0.1287 | 0.0634 | 0.0566 |
| | | | Technology maturity | 0.0900 | 0.1400 | -0.0005 | 0.0451 | 0.0223 | 0.0199 |
| | | | Technology Reliability | 0.2500 | 0.3500 | -0.0014 | 0.1126 | 0.0556 | 0.0497 |
| | | | Flexibility | 0.2000 | 0.3000 | -0.0011 | 0.0965 | 0.0477 | 0.0426 |
| Social | 0.1230 | 0.2793 | Company image | 0.3431 | 0.5147 | 0.0422 | 0.1438 | 0.0930 | 0.0831 |
| | | | Skill req | 0.5147 | 0.6863 | 0.0633 | 0.1917 | 0.1275 | 0.1139 |

Moving forward to the start of the TOPSIS process requires creating a multi-data decision-making matrix comprised of all the hard and soft information that relates to each sub-criteria (Table 10). For the capital cost, due to the poor market readiness of the 4 technologies being assessed, values have been assigned based on the author's knowledge and correspondence with Dr Vishnu Ravisankar, a desalination expert at Murdoch University [134]. There is fairly high confidence with the placement of MD and FO as the cheapest and second-cheapest options. However, the placements of OARO and EFC could switch based on the system sizing. The TDS limitation for technologies indicated as "no theoretical limit" in Table 1, were assigned a value of $360{,}000\ {}^{mg}/_{L}$, which corresponds with the saturation point of pure NaCl in water at $25\ °C$ [135]. Assumptions were also made on the footprint of each technology, based on the author's knowledge and previous work experience in the desalination industry. The linguistic terms in Table 10 can be converted to fuzzy triangular numbers by following the corresponding number sets shown in Table 3. A decision-making matrix with only crisp, interval and fuzzy numbers is shown in Table 11. In both Table 10 and Table 11, cells have been highlighted in gold to indicate where an assumption for a hard information data-type has been applied.

*Table 10: TOPSIS Process - Hybrid information decision-making matrix for hard and soft information types.*

| Sub-criteria | Units | MD | | FO with regeneration | | OARO | | EFC | |
|---|---|---|---|---|---|---|---|---|---|
| Capital Cost | $ | 10,000 | | 12,000 | | 13,500 | | 14,000 | |
| Production Cost | $\$/m^3$ | 1.17 | | 0.63 | | 2.4 | | 1.42 | |
| TDS Limitation | TDS (mg/L) | 360,000 | 360,000 | 150,000 | 220,000 | 160,000 | 160,000 | 360,000 | 360,000 |
| Energy consumption | $kWh/m^3$ | 39 | 67 | 6.8 | 16.7 | 6 | 19 | 4 | 150 |
| Footprint | $m^2$ | 6 | 10 | 8 | 12 | 8 | 10 | 6 | 10 |
| Technology maturity | linguistic | M | | B | | B | | G | |
| Technology Reliability | linguistic | G | | M | | M | | VB | |
| Flexibility | linguistic | G | | B | | M | | G | |
| Company Image | linguistic | M | | G | | G | | B | |
| Skill req | linguistic | M | | G | | M | | M | |

*Table 11: TOPSIS Process - Hybrid information decision-making matrix for hard and soft information types with fuzzy numbers.*

| Sub-criteria | Units | MD | | | FO with regeneration | | | OARO | | | EFC | | |
|---|---|---|---|---|---|---|---|---|---|---|---|---|---|
| Capital Cost | $ | 10,000 | | | 12,000 | | | 13,500 | | | 14,000 | | |
| Production Cost | $\$/_{m^3}$ | 1.17 | | | 0.63 | | | 2.4 | | | 1.42 | | |
| TDS Limitation | TDS limit | 360,000 | 360,000 | | 150,000 | 220,000 | | 160,000 | 160,000 | | 360,000 | 360,000 | |
| Energy consumption | $kWh/_{m^3}$ | 39 | 67 | | 6.8 | 16.7 | | 6 | 19 | | 4 | 150 | |
| Footprint | m2 | 6 | 10 | | 8 | 12 | | 8 | 10 | | 6 | 10 | |
| Technology maturity | fuzzy numbers | 0.4 | 0.5 | 0.6 | 0.2 | 0.3 | 0.4 | 0.2 | 0.3 | 0.4 | 0.6 | 0.7 | 0.8 |
| Technology Reliability | fuzzy numbers | 0.6 | 0.7 | 0.8 | 0.4 | 0.5 | 0.6 | 0.4 | 0.5 | 0.6 | 0.1 | 0.2 | 0.3 |
| Flexibility | fuzzy numbers | 0.6 | 0.7 | 0.8 | 0.2 | 0.3 | 0.4 | 0.4 | 0.5 | 0.6 | 0.6 | 0.7 | 0.8 |
| Company Image | fuzzy numbers | 0.4 | 0.5 | 0.6 | 0.6 | 0.7 | 0.8 | 0.6 | 0.7 | 0.8 | 0.2 | 0.3 | 0.4 |
| Skill req | fuzzy numbers | 0.4 | 0.5 | 0.6 | 0.6 | 0.7 | 0.8 | 0.4 | 0.5 | 0.6 | 0.4 | 0.5 | 0.6 |

From Table 11, the normalisation process for the data inputs can begin (step 2 of TOPSIS). Capital cost and production cost are the only crisp data types in the decision-making matrix. The normalisation process for crisp numbers is done by following equation 21 and selecting whether the data-type is a benefit-type (highest value is the preferred option) or cost-type (lowest value is the preferred option). Both capital cost and production cost are classified as cost-type criteria. The process to normalise crisp data of the cost-type is demonstrated for production costs (PC) of MD, FO with regeneration, OARO and EFC through equations 51-54.

$$NPC_{MD} = \frac{2.4 - 1.17}{2.4 - 0.63} = 0.6949 \tag{51}$$

$$NPC_{FO} = \frac{2.4 - 0.63}{2.4 - 0.63} = 1 \tag{52}$$

$$NPC_{OARO} = \frac{2.4 - 2.4}{2.4 - 0.63} = 0 \tag{53}$$

$$NPC_{EFC} = \frac{2.4 - 1.42}{2.4 - 0.63} = 0.5537 \tag{54}$$

The interval data types must be considered next, namely, TDS limitation, energy consumption and footprint. TDS limitation is a benefit-type, while energy consumption and footprint are cost-type criteria. A demonstration of the normalisation process for TDS limitation (TDSL) and energy consumption (EC) is shown in equations 55-58 and 59-62, to showcase the difference between benefit-type and cost-type criteria, respectively.

$$NTDSL_{MD} = \frac{360{,}000 - 150{,}000}{360{,}000 - 150{,}000}, \frac{360{,}000 - 150{,}000}{360{,}000 - 150{,}000} = [1 \quad 1] \tag{55}$$

$$NTDSL_{FO} = \frac{150{,}000 - 150{,}000}{360{,}000 - 150{,}000}, \frac{220{,}000 - 150{,}000}{360{,}000 - 150{,}000} = [0 \quad 0.3333] \tag{56}$$

$$NTDSL_{FO} = \frac{160{,}000 - 150{,}000}{360{,}000 - 150{,}000}, \frac{160{,}000 - 150{,}000}{360{,}000 - 150{,}000} = [0.0476 \quad 0.0476] \tag{57}$$

$$NTDSL_{EFC} = \frac{360{,}000 - 150{,}000}{360{,}000 - 150{,}000}, \frac{360{,}000 - 150{,}000}{360{,}000 - 150{,}000} = [1 \quad 1] \tag{58}$$

$$NEC_{MD} = \frac{150 - 67}{150 - 4}, \frac{150 - 39}{150 - 4} = [0.5685 \quad 0.7603] \tag{59}$$

$$NEC_{FO} = \frac{150 - 16.7}{150 - 4}, \frac{150 - 6.8}{150 - 4} = [0.9130 \quad 0.9808] \tag{60}$$

$$NEC_{OARO} = \frac{150 - 6}{150 - 4}, \frac{150 - 19}{150 - 4} = [0.8973 \quad 0.9863] \tag{61}$$

$$NEC_{OARO} = \frac{150 - 150}{150 - 4}, \frac{150 - 4}{150 - 4} = [0 \quad 1] \tag{62}$$

The remaining criteria (technology maturity, reliability, flexibility, company image and skill requirement) are classified by fuzzy triangular numbers. How the fuzzy numbers were set up using Saaty's nine-scale forces a benefit-type normalisation approach to fuzzy numbers. It ties into the perceptual understanding of the linguistic terms like "Good" and "Very Bad (VB)" and general social understanding that a higher ranking or score is equivalent to a better outcome (most prominent in the educational domain). Equations 63-66 below use Technology Maturity (TM) to demonstrate the normalisation process for fuzzy triangular numbers. All of the normalised data for all of the remaining criteria are presented in the Appendix (Table 20).

$$NTM_{MD} = \frac{0.4-0.2}{0.8-0.2}, \frac{0.5-0.2}{0.8-0.2}, \frac{0.6-0.2}{0.8-0.2} = [0.3333 \quad 0.5 \quad 0.6667] \tag{63}$$

$$NTM_{FO} = \frac{0.2-0.2}{0.8-0.2}, \frac{0.3-0.2}{0.8-0.2}, \frac{0.4-0.2}{0.8-0.2} = [0 \quad 0.1667 \quad 0.3333] \tag{64}$$

$$NTM_{OARO} = \frac{0.2-0.2}{0.8-0.2}, \frac{0.3-0.2}{0.8-0.2}, \frac{0.4-0.2}{0.8-0.2} = [0 \quad 0.1667 \quad 0.3333] \tag{65}$$

$$NTM_{EFC} = \frac{0.6-0.2}{0.8-0.2}, \frac{0.7-0.2}{0.8-0.2}, \frac{0.8-0.2}{0.8-0.2} = [0.6667 \quad 0.8333 \quad 1] \tag{66}$$

The next step is to calculate the weighted normalised data by multiplying the normalised data with the relevant crisp weightings calculated through AHP following Eq 25. These calculations is shown using production cost, energy consumption and technology maturity through equations 67-70 for crisp numbers, equations 71-74 for interval numbers and equations 75-78 for triangular fuzzy numbers. The remaining weighted normalised data is presented in the Appendix (Table 21).

$$WNPC_{MD} = 0.6949 * 0.1208 = 0.0840 \tag{67}$$

$$WNPC_{FO} = 1 * 0.1208 = 0.1208 \tag{68}$$

$$WNPC_{OARO} = 0 * 0.1208 = 0 \tag{69}$$

$$WNPC_{EFC} = 0.5537 * 0.1208 = 0.0669 \tag{70}$$

$$\begin{aligned} WNEC_{MD} &= [0.5685 * 0.2121 \quad 0.7603 * 0.2121] \\ &= [0.1206 \quad 0.1612] \end{aligned} \tag{71}$$

$$\begin{aligned} WNEC_{FO} &= [0.9130 * 0.2121 \quad 0.9808 * 0.2121] \\ &= [0.1936 \quad 0.2080] \end{aligned} \tag{72}$$

$$\begin{aligned} WNEC_{OARO} &= [0.8973 * 0.2121 \quad 0.9863 * 0.2121] \\ &= [0.1903 \quad 0.2092] \end{aligned} \tag{73}$$

$$WNEC_{MD} = [0 * 0.2121 \quad 1 * 0.2121] = [0 \quad 0.2121] \tag{74}$$

$$\begin{aligned} WNTM_{MD} &= [0.3333 * 0.0199 \quad 0.5 * 0.0199 \quad 0.6667 * 0.0199] \\ &= [0.0066 \quad 0.0099 \quad 0.0133] \end{aligned} \tag{75}$$

$$\begin{aligned} WNTM_{FO} &= [0 * 0.0199 \quad 0.1667 * 0.0199 \quad 0.3333 * 0.0199] \\ &= [0 \quad 0.0033 \quad 0.0066] \end{aligned} \tag{76}$$

$$\begin{aligned} WNTM_{OARO} &= [0 * 0.0199 \quad 0.1667 * 0.0199 \quad 0.3333 * 0.0199] \\ &= [0 \quad 0.0033 \quad 0.0066] \end{aligned} \tag{77}$$

$$\begin{aligned} WNTM_{EFC} &= [0.6667 * 0.0199 \quad 0.8333 * 0.0199 \quad 1 * 0.0199] \\ &= [0.0133 \quad 0.0166 \quad 0.0199] \end{aligned} \tag{78}$$

Following equations 26-29, the ideal best and worst solutions for each criterion can be identified. Using the results from weighted normalised production cost (WNPC) (equations 67-70) as an example, the ideal solution is FO as it has the highest value (0.1208). Meanwhile, the ideal worst solution is OARO as it has the lowest value (0). A summary of the ideal best and worst solutions for each criterion is shown in Table 12.

*Table 12: Ideal best and worst solutions for each criterion of the case study.*

| Criteria | Ideal Best Solution | Ideal Worst Solution |
|---|---|---|
| Capital cost | 0.1666 | 0 |
| Production cost | 0.1208 | 0 |
| TDS limitation | 0.1346 0.1346 | 0 0.0064 |
| Energy consumption | 0.1936 0.2121 | 0 0.1612 |
| Footprint | 0.0189 0.0566 | 0 0.0377 |
| Technology maturity | 0.0133 0.0166 0.0199 | 0 0.0033 0.0066 |
| Technology reliability | 0.0355 0.0426 0.0497 | 0 0.0071 0.0142 |
| Flexibility | 0.0284 0.0355 0.0426 | 0 0.0071 0.0142 |
| Company Image | 0.0554 0.0692 0.0831 | 0 0.0138 0.277 |
| Skill requirement | 0.0570 0.0854 0.1139 | 0 0.285 0570 |

Now that the ideal best and worst solutions for each criterion have been identified, the distance between the weighted normalised data and ideal best and worst solutions can be determined by following equations 31-33 and 35-37 for ideal best and worst solutions respectively (Table 13). From the distance to the ideal best and worst solutions for each criterion, the distance to the ideal best and worst technology can be calculated by following equations 30 and 34 for the best and worst ideal solutions, respectively. Finally, from the distance to the ideal best and worst solutions for each technology, the closeness degree to the best solution can be calculated and ranked from highest (most ideal) to lowest (least ideal) (Table 13).

*Table 13: The closeness degrees for the 4 selected brine management technologies for the case study.*

| | MD | FO | OARO | EFC |
|---|---|---|---|---|
| Distance to ideal best solution | 0.0958 | 0.1469 | 0.2373 | 0.2387 |
| Distance to ideal worst solution | 0.2502 | 0.2211 | 0.1537 | 0.1562 |
| Closeness Degree | 0.7206 | 0.6008 | 0.3931 | 0.3955 |
| Ranking | 1 | 2 | 4 | 3 |

The ranking of the brine management technologies from best to worst is membrane distillation (MD), forward osmosis with regeneration (FO), eutectic freeze crystallisation (EFC and osmotically assisted reverse osmosis (OARO).

## 4.3 Sensitivity Analysis

A sensitivity analysis (SA) is an essential process for any model that could experience uncertainty. Sensitivity analyses are methods used to study the influence of the inputs on the uncertainty of the output variables of a model [136]. One of the techniques often used in sensitivity analyses in fields such as medicine, mathematics, physics and engineering, is a Monte Carlo Simulation (MCS) [137]–[141]. The MCS has a wide variety of different variants. However, the basic premise stays the same. It is an iterative process consisting of alternating the input variables based on an input distribution (e.g., uniform, triangular, normal) into the model and recording the model's output. From the recorded results, statistical information and interpretations can be applied to understand further how the model responds to different input variables. The sensitivity analysis for the model developed in this document followed the schematic seen in Figure 8.

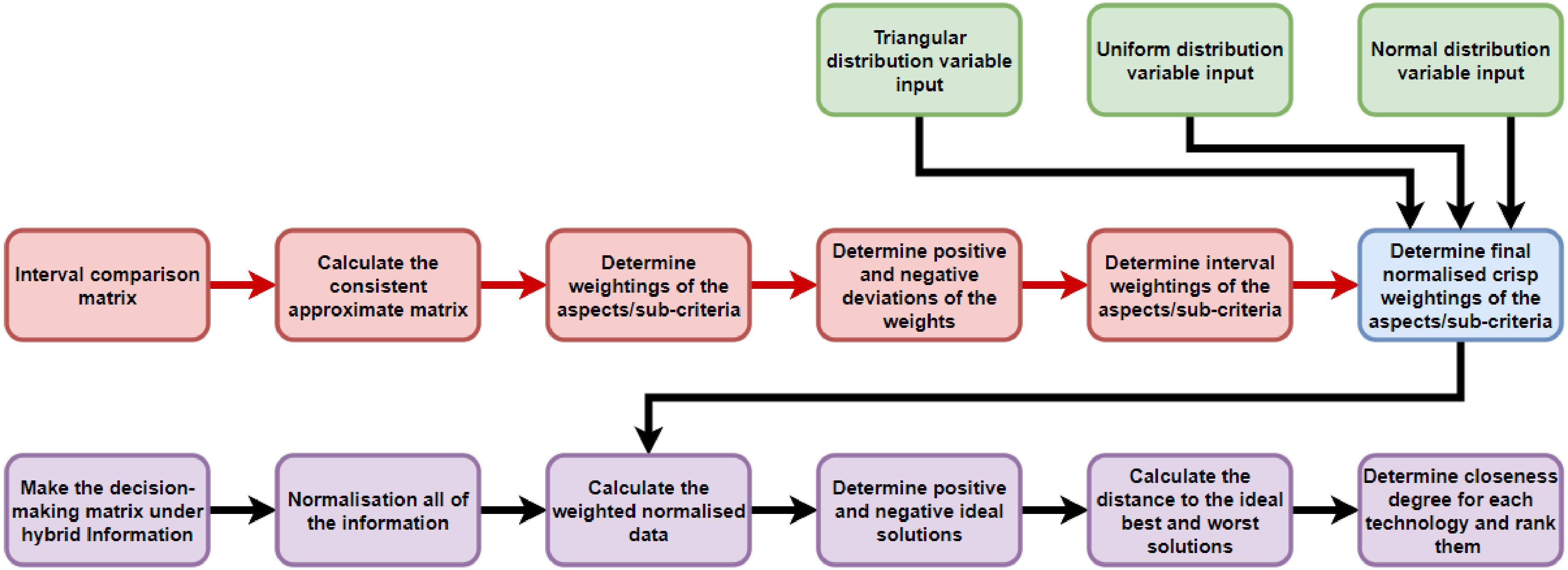


*Figure 8: Monte Carlo Simulation schematic*

The red cells and arrows indicate the steps of the interval analytical hierarchy process (AHP) that have been bypassed, owing to the validation issue mentioned in Section 4.2. There is also the lack of a consistency ratio measurement in the interval AHP seen in the original version of AHP developed by Saaty [133]. The consistency ratio is an important measurement for determining whether the decision maker's comparison matrices are acceptable or needs revision [142]. The cells in green showcase the three different types of distributions, namely triangular, uniform and normal distributions that the SA will employ to assign weightings. There are two methods of variable weighting assignment used in this SA. The first is directly altering the final crisp weightings for every sub-criterion (Method 1). The analysis of this output would then be used to indicate the total variability of each technology. The second is to apply the variable input to 1 aspect (economic, environmental, technical or social) at a time and keeping the remaining weightings for sub-criteria associated with other aspects the same as the case study (Method 2). This approach benefits from isolating aspects to determine which aspects have the most influence on the outputs [143]. This analysis will use only one distribution type at a time.

The SA was developed in excel with the assistance of a macro. The macro copies the closeness degree (last step of TOPSIS, equation 38) for each technology for every set of random weightings to the number of specified iterations (Figure 9). For this SA, there will be 10,000 iterations for each simulation.

```
Sub Montecarlo()
   For Iteration = 1 To Cells(20, 27)
       Cells(29 + Iteration, 26) = Cells(77, 2)
       Cells(29 + Iteration, 27) = Cells(77, 3)
       Cells(29 + Iteration, 28) = Cells(77, 4)
       Cells(29 + Iteration, 29) = Cells(77, 5)
       Cells(29 + Iteration, 25) = Iteration
   Next Iteration
End Sub
```

*Figure 9: Sensitivity analysis macro code.*

Some distribution types have dedicated functions in excel, such as NORM.INV or NORM.DIST for normal distribution. Other distributions use a random number generator in excel using the RAND () function, which produces a uniformly distributed random number between 0 to

1. Extending the range of the RAND () function to the limits of the input variables gives a uniform distribution across the specified range (equation 79). For SA method 1, the global interval weighting for each criterion limits the total range of the uniform random number generator. The upper and lower bounds are shown in Table 9. For the 2nd SA method, the aspect weightings will range from 0 to 0.6. This range accounts for the entire aspect weighting range seen in the model demonstration and applies an estimated upper limit of aspect weightings of 0.6 and a lower limit of 0. This is in comparison to the current aspect weightings for the case study, with an upper limit of 0.48 and a lower limit of 0 (Table 8).

$$\begin{aligned} Uniform\ distribution\ random\ number \\ = (Upper\ bound - Lower\ bound) * RAND(\,) \\ + Lower\ bound \end{aligned} \tag{79}$$

A triangular distribution is a continuous probability distribution that results in a triangular-shaped distribution pattern with a bias towards the most likely (peak) value. In order to simulate a triangular distribution variable input, the distance between the peak value and the lowest value, peak value and the maximum value and the total range need to be known (equations 80-82).

$$Lower\ range = peak\ value - minimum\ value \tag{80}$$

$$Higher\ range = maximum\ value - peak\ value \tag{81}$$

$$Total\ range = maximum\ value - minimum\ value \tag{82}$$

For this MCS, triangular distributions will only be applied to the 1st SA method. The maximum and minimum values are the global interval criteria weightings, and the peak value is the midpoint for that specific criterion weighting (shown in Table 9). Knowing the lower range, higher range and total range, the next step is calculating the triangular random number by following the logic shown in equation 83.

$$IF\ RAND(\,) < \left(\frac{Lower\ range}{Total\ range}\right)\ then$$

$$Random\ Triangular\ number = Minimum + \sqrt{(RAND(\,) * Lower\ range * Total\ range)} \quad 83$$

$$Else\ Random\ Triangular\ number = Maximum - \sqrt{(1 - RAND(\,) * Higher\ range * Total\ range)}$$

Furthermore, a normal distribution, also known as a Gaussian distribution, is a symmetric distribution about the mean value and appears as a bell curve. A normal distribution in excel can be done by using the inbuilt function NORM.INV. However, assumptions need to be made for the mean value ($\mu$) and the standard deviation ($\sigma$). These assumptions were estimated using the 68 95 99.7 empirical rule. Which states that $\mu \pm 1\sigma$ accounts for 68% of the area under the curve, 95% of the values under the curve fall within $\mu \pm 2\sigma$ and $\mu \pm 3\sigma$ represents almost all of the values under the bell curve [144]. For SA method 1, $\mu$ is defined as the midpoint of the global interval weighing and the total range from the midpoint to the lower or upper bound is assumed to be the full range of values ($\sim 3\sigma$) for each criterion. Therefore $\sigma$ can be calculated following equation 84. An example is shown in equation 85 using the capital cost global interval weight information present in Table 9.

$$\sigma = \frac{(midpoint - lower\ bound) * 0.95}{2} \quad 84$$

$$\sigma = \frac{(0.186 - 0.111) * 0.95}{2} = 0.036 \quad 85$$

For the normal distribution of the aspect weightings, Table 14 shows the $\mu$ and $\sigma$ values chosen for each aspect. The author has made the assumption that the economic and environmental aspects would likely see a larger range of potential values than the technical or social aspects. This decision was primarily driven by the general relevance of the criterion under each aspect, i.e., capital cost and energy consumption are likely to have a considerably higher range of weightings than technical criteria (technological maturity, reliability, footprint and flexibility).

*Table 14: Mean value and standard deviations used for aspect weightings in sensitivity analysis.*

| Aspect | Mean value assumption ($\mu$) | Standard Deviation ($\sigma$) |
|---|---|---|
| Economic | 0.3 | 0.14 |
| Environmental | 0.32 | 0.15 |
| Technical | 0.2 | 0.1 |
| Social | 0.2 | 0.1 |

For each set of random global crisp weightings produced for SA method 1, the values need to be normalised to total 1 by following equation 19. There are three main features of the SA outputs that were analysed:

1. The proportion of the time a technology obtains a specific rank.
2. Secondly, the coefficient of variation (equation 86), also known as the relative standard deviation.
3. The maximum, minimum and mean values.

$$Coefficient\ of\ Variation = \frac{\sigma}{\mu} \tag{86}$$

The proportion of the time a particular technology is given the same rank indicates how strong or potentially biased a technology is overall. The coefficient of variation is a measurement of the dispersion or frequency of a given dataset [145]. It is used to measure the reliability or risk, with smaller values implying more reliable (consistent) results. The maximum, minimum and mean values might give insight into what's occurring within the model and why specific outcomes were observed.

# 5 Results and Discussion

This section provides the results and discussion on the two Sensitivity Analysis (SA) methods previously mentioned in Section 4.3. Section 5.1 covers the first method, which varies all global criteria simultaneously. Meanwhile, Section 5.2 will be covering the second method, which involves varying each aspect weighting individually. The discussion will primarily focus on any confusion (competition of 2 or more technologies with the same rank) within the technology rankings. One of the main metrics used in this discussion is the ideal best solution (IBS) and ideal worst solution (IWS) criteria (Table 12). The identified IBS and IWS in the case study for a given criterion will remain the same. Because there have been no alterations to the hybrid information decision-making matrix (Table 10) for either SA method. The raw data produced by the MSC are synthesised into histogram frequency distribution graphs in Appendix 8.2.1 for the first SA method.  The second SA method results are shown in Appendix 8.2.2, 8.2.3, 8.2.4 and 8.2.5 for economic, environmental, technical and social, respectively.

## 5.1 Varying Global Criteria Weightings

For SA method 1, three input distribution types were employed, namely triangular, uniform and normal. Across all three distribution types, membrane distillation (MD) was the most predominant technology. MD is ranked first 98%, 93% and 96% of the time for triangular (Figure 10), uniform (Figure 11) and normal (Figure 12) input distributions, respectively. The main explanation for the dominance of MD as the consistently higher ranked technology is because it doesn't represent any IWS criteria. Whereas forward osmosis (FO), osmotically assisted reverse osmosis (OARO) and eutectic freeze crystallisation (EFC) represent 4, 3 and 5 of the IWS criteria, respectively.

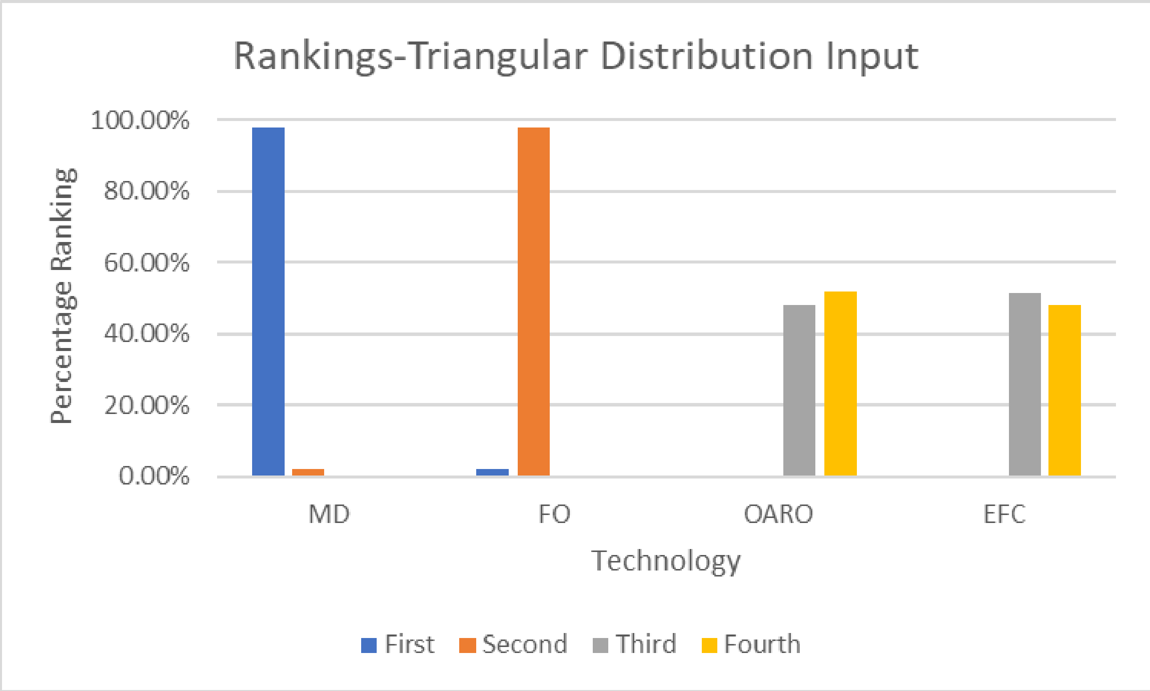


*Figure 10: Ranking breakdown for global varying inputs based on triangular distribution.*

FO is consistently ranked 2$^{nd}$ with a frequency of 98%, 90.5% and 96% for triangular, uniform and normal distribution. However, there is some confusion between MD and FO for 1$^{st}$ and 2$^{nd}$ place, ranging from 2% to 7%. This confusion represents the small window in which the very few criteria where FO triumphs over MD (production cost, energy consumption, company image and skill requirement) outweighs the weightings of the other 6 criteria, which MD benefits more from than FO.

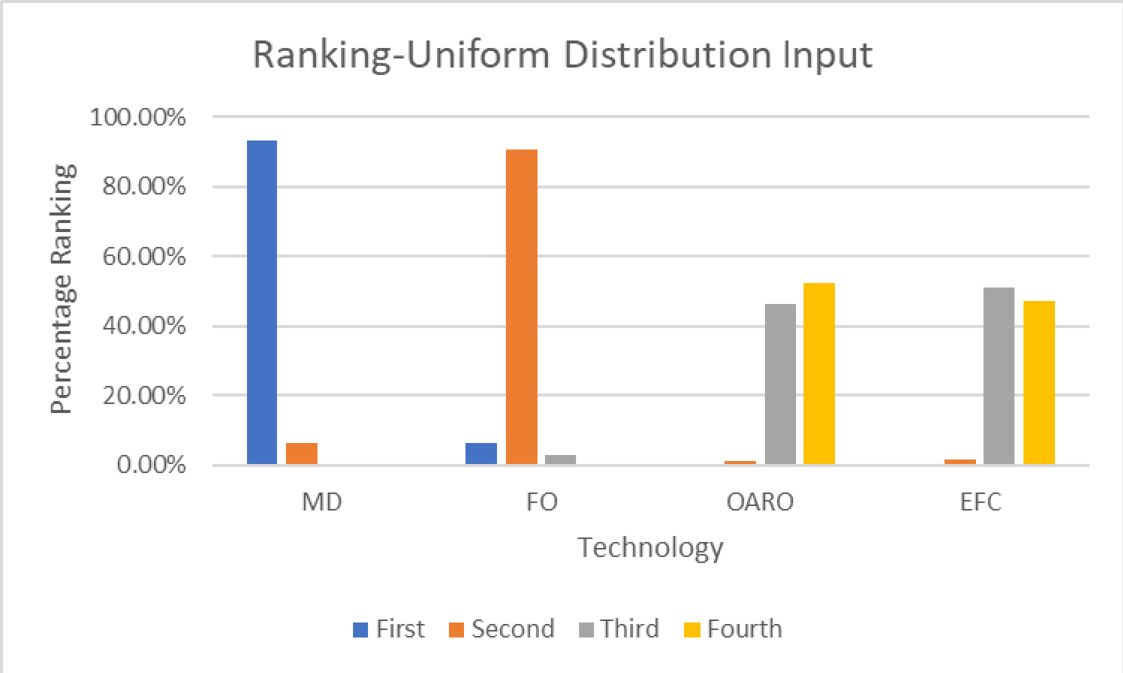


*Figure 11: Ranking breakdown for global varying inputs based on uniform distribution.*

There is also confusion for 3rd and 4th place between OARO and EFC. EFC tends to be ranked 3rd more often than OARO. This is likely due to the larger representation of IBS criteria among the EFC weighted normalised data compared to OARO, which only represents 1 IBS criterion. Making up for the fact that EFC represents 5 of the IWS criteria.

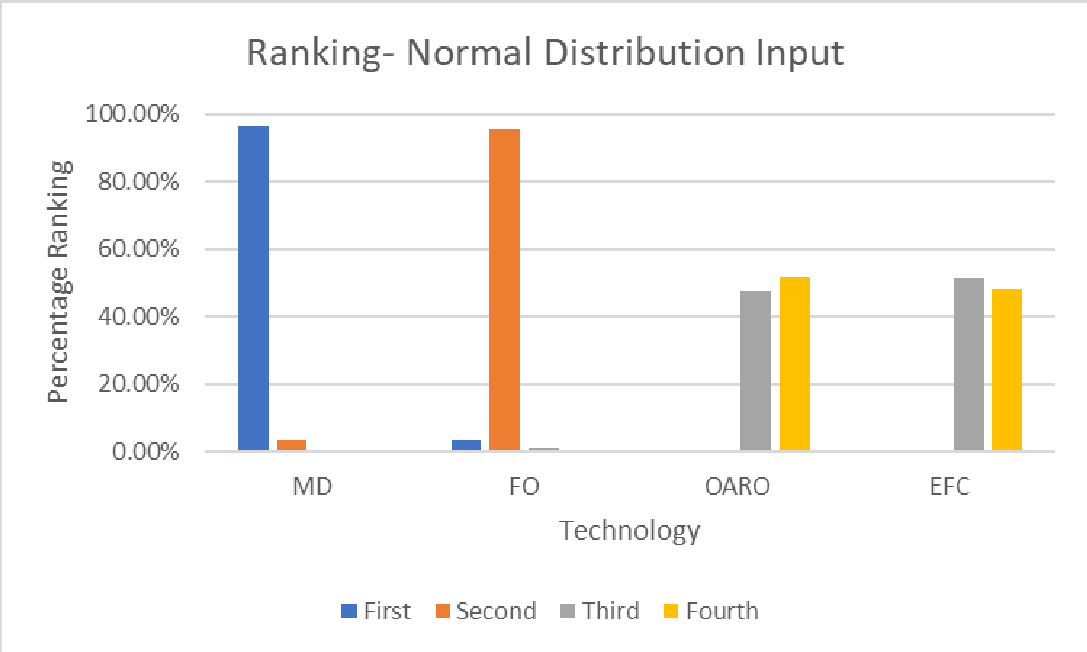


*Figure 12:Ranking breakdown for global varying inputs based on normal distribution.*

The coefficient of variation (risk) follows a similar trend to the ranking order. MD had the lowest risk, and highest mean, minimum and maximum closeness degree values out of the 4 case study technologies for every type of distribution simulated (Table 14). FO follows MD as the 2$^{nd}$ lowest risk factor and 2$^{nd}$ highest mean, minimum and maximum closeness degree values. There is a fair amount of overlap in the maximum and minimum boundaries of MD and FO. Combining this with the previously mentioned ranking frequency indicates that MD and FO share most of the criteria contributing to higher closeness degree values. Otherwise, there would be a much larger proportion of FO systems ranking first. Further proves that production cost, energy consumption, company image and skill requirement are the predominant criteria contributing to the confusion between MD and FO rankings.

*Table 15: Coefficient of variation, mean, minimum and maximum closeness degree values for the Monte Carlo simulation varying global interval input values.*

| Distribution Input Type | Technology | Coefficient of Variation | Mean Closeness Degree | Maximum | Minimum |
|---|---|---|---|---|---|
| Triangular | MD | 4.16% | 0.721 | 0.821 | 0.617 |
| | FO | 8.17% | 0.601 | 0.753 | 0.434 |
| | OARO | 14.01% | 0.391 | 0.561 | 0.216 |
| | EFC | 13.64% | 0.394 | 0.582 | 0.231 |
| Uniform | MD | 5.75% | 0.721 | 0.860 | 0.588 |
| | FO | 11.04% | 0.601 | 0.801 | 0.407 |
| | OARO | 20.08% | 0.386 | 0.635 | 0.186 |
| | EFC | 18.87% | 0.393 | 0.608 | 0.200 |
| Normal | MD | 4.74% | 0.721 | 0.844 | 0.591 |
| | FO | 9.17% | 0.601 | 0.804 | 0.402 |
| | OARO | 16.33% | 0.389 | 0.592 | 0.138 |
| | EFC | 15.46% | 0.395 | 0.629 | 0.189 |

OARO and EFC share a similar mean closeness degree, contributing to the confusion between these two technologies. The maximum and minimum values for OARO and EFC also results in significant overlap between the two technologies. The confusion is most likely resulting from a trait both of these technologies have, if it isn't the IBS for that particular category, then it is most likely to be the IWS or very close to being the IWS.

## 5.2 Varying Individual Aspect Weightings

The following 4 sub-sections will discuss the effects of individually varying the Economic Aspect, Environmental Aspect, Technical Aspect and Social Aspect weightings. It is important to mention that the remaining fixed aspects and criteria weightings were kept identical to the values seen in the case study (Table 9) up until the global interval midpoints. This is because the final crisp weights used in the TOPSIS process still need to sum to 1 by following equation 19. Meaning that the ratio of criteria weightings under each fixed aspect will remain the same. However, the final crisp weighting for fixed criteria will increase with a lower varying aspect weighting and decrease with an increase to the varying aspect weighting.

### 5.2.1 Economic Aspect

Starting with the rankings of the outputs, there is a very small (0.13%) ranking confusion between MD and FO for the normal distribution results (Figure 13). There is, however, no confusion between MD and FO within the simulation results for uniform distribution simulation (Figure 14). Observations of the IBS and IWS (Table 9), along with the weighted normalised hybrid information (see Appendix Table 21), gives no clear indications to the cause of this discrepancy. Further observations on this discrepancy will be using the statistical outputs of the simulation results further into this section.

The confusion between OARO and EFC remains at a similar level to the confusion seen in Section 5.1. There are two reasons for the confusion. Firstly, the economic aspect weighting is directly causing the confusion. Secondly, the weightings for the fixed criteria weightings influence the rankings. Observing the normalised data for the capital and production costs (criteria that are affected by changes to economic weighting), EFC has an overall higher weight assignment than OARO in the weighted normalised hybrid information table (see Appendix for Table 21). Meaning EFC benefits greatly from a higher economic weighting and thus would make itself distinct from OARO. This implies that the fixed criteria is influencing the ranking of OARO more so than EFC.

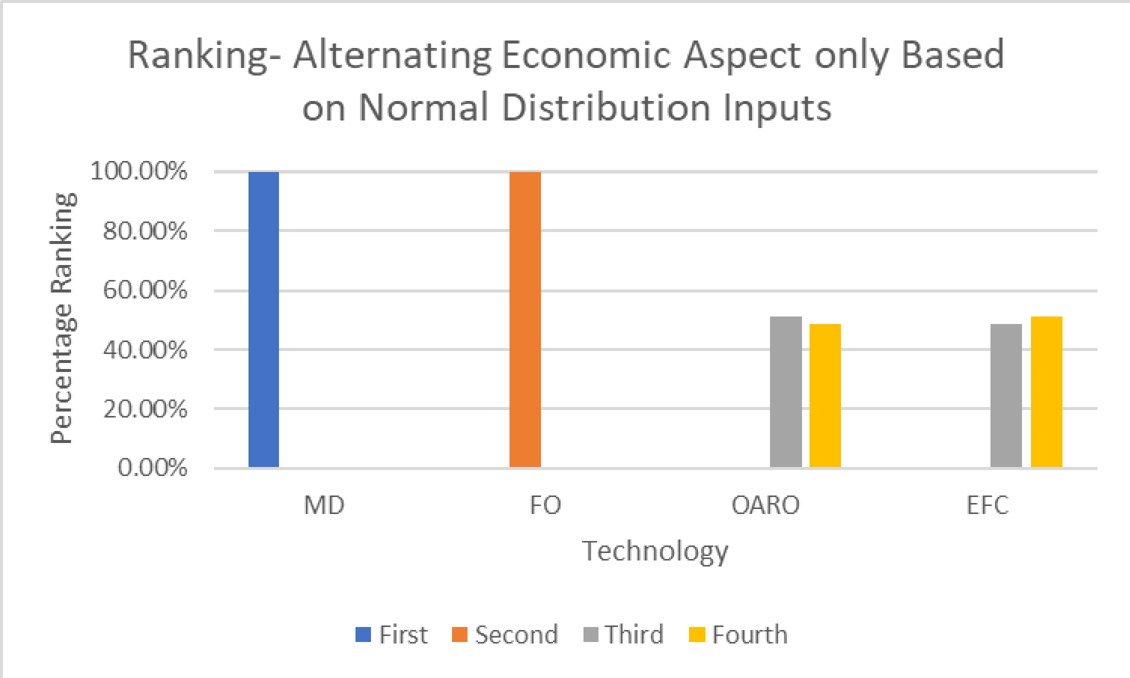


*Figure 13: Technology rankings of the Monte Carlo simulation outputs using alternating economic weightings based on a normal distribution.*

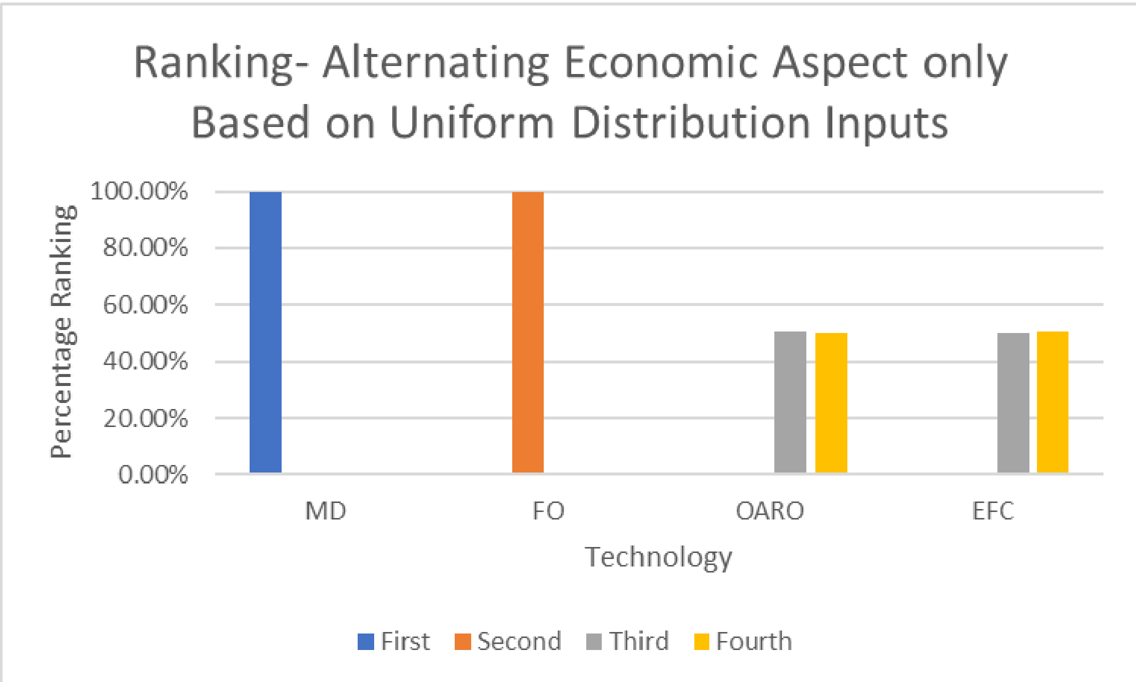


*Figure 14: Technology rankings of the Monte Carlo simulation outputs using alternating economic weightings based on a uniform distribution.*

Interpretations of the statistical information (Table 16) reach similar conclusions to the discussion on technology rankings. The maximum and minimum values of MD and FO don't overlap. However, there is an exception. The minimum closeness degree of 0.435 for MD with varying input based on normal distribution is extremely low and appears to be an outlier. There is speculation that the cause is a negative weighting assignment to the economic aspect. Due to the method used to incorporate the random number generator to the TOPSIS model, the methods used to regulate negative weighting assignments were bypassed. This is causing a reversal of the weighting importance, i.e. a cost-type criterion is acting like a benefit-type criterion for the capital and production cost criteria. The minimum closeness degree of 0.651 for MD in the uniform distribution results reinforces this theory, which was restricted to input aspect weightings between 0 and 0.6. Observations of the output distribution graphs that show the frequency of results also show that by following the 68 95 99.7 empirical rule, the most likely minimum value is approximately 0.63 (see Appendix 8.2.2). Which is higher than the maximum value of FO for the normal distribution outputs.

*Table 16: Statistical outputs of the Monte Carlo simulation when varying only the economic aspect.*

| Distribution Input Type | Technology | Coefficient of Variation | Mean Closeness Degree | Maximum | Minimum |
|---|---|---|---|---|---|
| Normal | MD | 4.75% | 0.715 | 0.796 | 0.435 |
| | FO | 1.85% | 0.598 | 0.625 | 0.531 |
| | OARO | 14.84% | 0.403 | 0.598 | 0.243 |
| | EFC | 8.58% | 0.400 | 0.519 | 0.311 |
| Uniform | MD | 5.84% | 0.714 | 0.777 | 0.651 |
| | FO | 2.23% | 0.598 | 0.618 | 0.577 |
| | OARO | 18.22% | 0.403 | 0.516 | 0.287 |
| | EFC | 10.58% | 0.401 | 0.465 | 0.336 |

### 5.2.2 Environmental Aspect

For the environmental aspect, the trend of MD and FO in 1st and 2nd place is continuing. There is no confusion between the rankings for either distribution type. Confusion between OARO and EFC is slightly less than seen with the economic aspect. Modifying the environmental aspect favours OARO more than EFC but only slightly. This indicates that the criteria associated with the economic and environmental aspects aren't heavily influencing the closeness degree. Or they are negating the influence of the economic aspect on the technical aspect due to similar total weightings between the 2 technologies. As seen in the slight but opposite rankings of OARO and EFC in the results of the economic simulation (Figure 13 and Figure 14) and the environmental simulation (Figure 15 and Figure 16). With this thought in mind and looking back at the rankings seen in Section 5.1 which was indicating that there is a slight advantage of EFC being ranked 3$^{rd}$ over EFC . The remaining 2 aspects are likely to have relatively equal but opposite priority rankings for OARO and EFC.

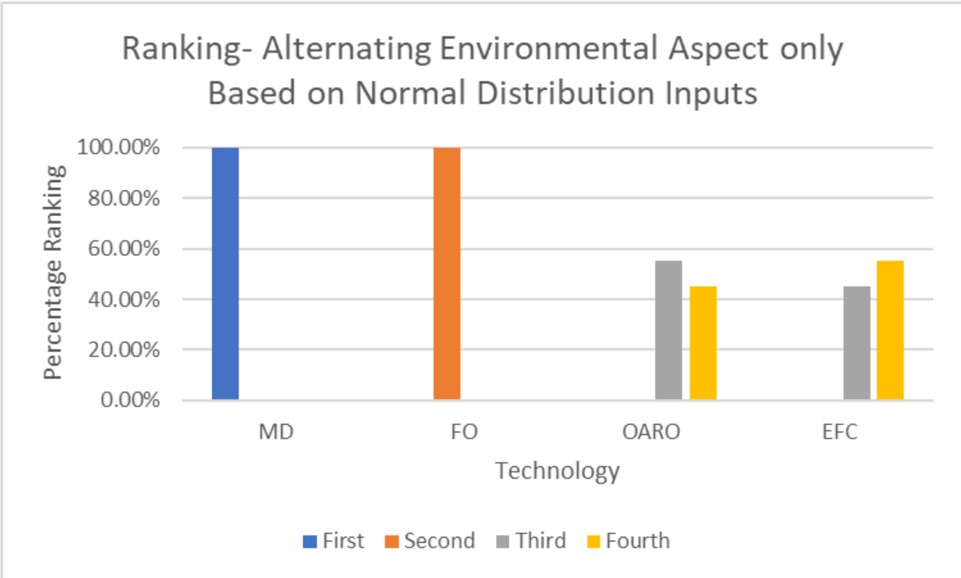


*Figure 15: Technology rankings for Monte Carlo simulation varying the environmental aspect weighting based on a normal distribution.*

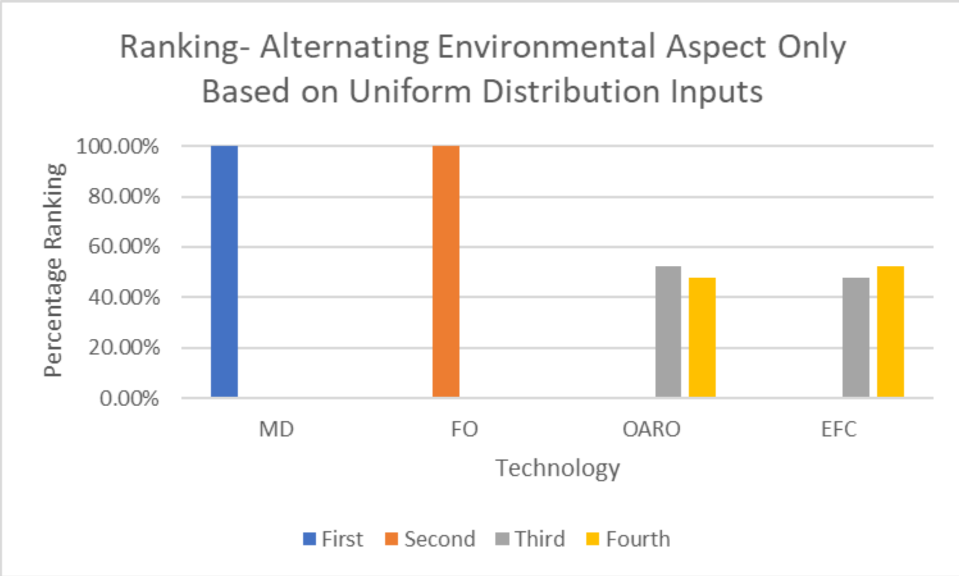


*Figure 16: Technology rankings for Monte Carlo simulation varying the environmental aspect weighting based on a uniform distribution.*

The coefficient of variation is low for MD when using both distribution types (Table 17). This implies that the environmental aspect has very little influence on the closeness degree of MD. This is unusual as MD obtains a high proportion of the environmental criteria weights in the weighted normalised hybrid information matrix (Table 21).

*Table 17: Statistical outputs of the Monte Carlo simulation when varying only the environmental aspect.*

| Distribution Input Type | Technology | Coefficient of Variation | Mean Closeness Degree | Maximum | Minimum |
|---|---|---|---|---|---|
| Normal | MD | 0.55% | 0.719 | 0.726 | 0.709 |
| | FO | 2.61% | 0.614 | 0.646 | 0.581 |
| | OARO | 15.53% | 0.376 | 0.496 | 0.248 |
| | EFC | 11.55% | 0.371 | 0.462 | 0.281 |
| Uniform | MD | 0.62% | 0.720 | 0.726 | 0.713 |
| | FO | 2.99% | 0.617 | 0.646 | 0.590 |
| | OARO | 18.88% | 0.364 | 0.460 | 0.248 |
| | EFC | 13.85% | 0.363 | 0.433 | 0.281 |

### 5.2.3 Technical Aspect

Within the technical aspect, there was no confusion between the rankings of MD and FO for 1st and 2nd. Varying the technical aspect has substantially reduced the confusion between OARO and EFC, as seen in Figure 17 and Figure 18. With EFC gaining a more stable position as the 3rd best technology. This is logical, as EFC represents 3 out of the 4 technical criteria as an IBS. In comparison to OARO, that doesn't represent any IBSs in the technical aspect.

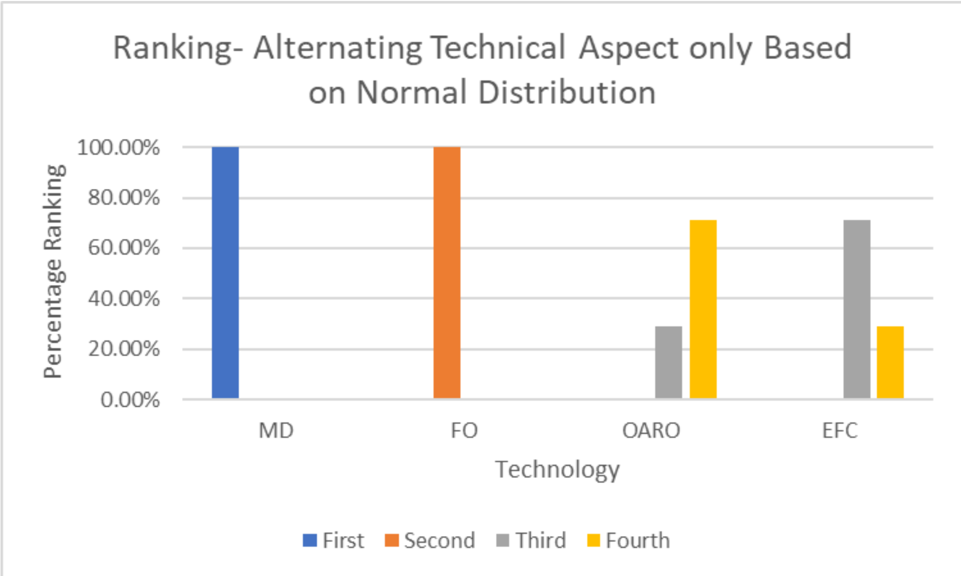


*Figure 17: Technology rankings for Monte Carlo simulation varying the technical aspect weighting based on a normal distribution.*

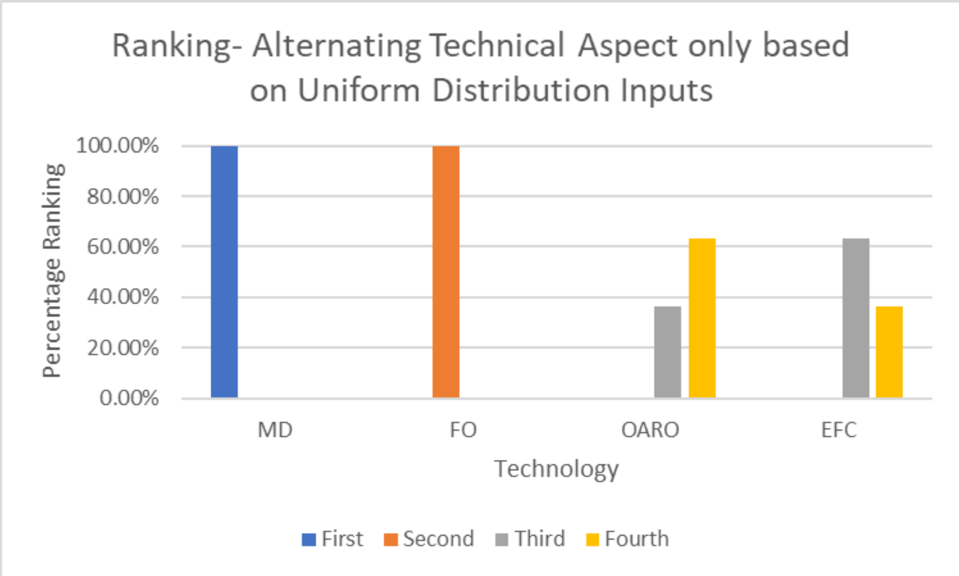


*Figure 18: Technology rankings for Monte Carlo simulation varying the technical aspect weighting based on a uniform distribution.*

FO's mean closeness degree value is closer to the maximum value, unlike the other 3 technologies, which have means closer to the minimum value (Table 18). This difference is likely due to FO representing the 3 out of the 4 IWS criteria under the technical aspect. There is still a significant overlap in the simulation closeness degree values of OARO and EFC. Yet EFC has a much higher chance of ranking 3rd than OARO. This implies that the technical aspect is an influential aspect with regards to the ranking of OARO and EFC. However, it has little influence on the ranking of MD and FO.

*Table 18: Statistical outputs of the Monte Carlo simulation when varying only the technical aspect.*

| Distribution Input Type | Technology | Coefficient of Variation | Mean Closeness Degree | Maximum | Minimum |
|---|---|---|---|---|---|
| Normal | MD | 0.58% | 0.723 | 0.748 | 0.717 |
| | FO | 1.44% | 0.598 | 0.609 | 0.545 |
| | OARO | 0.79% | 0.394 | 0.422 | 0.390 |
| | EFC | 1.15% | 0.397 | 0.423 | 0.391 |
| Uniform | MD | 1.30% | 0.729 | 0.748 | 0.717 |
| | FO | 3.25% | 0.586 | 0.609 | 0.548 |
| | OARO | 1.83% | 0.399 | 0.414 | 0.390 |
| | EFC | 2.47% | 0.404 | 0.424 | 0.391 |

### 5.2.4 Social Aspect

Varying the social aspect is causing a minor confusion (0.13%) between MD and FO for the normal distribution (Figure 19). However, the confusion between MD and FO in uniform distribution MCS results is substantially higher (22.17%) (Figure 20). The ranking results for OARO and EFC are also drastically different depending on the distribution type used. With the normal distribution, the favoured technology is EFC, with it ranking 3rd 60.79% of the time. However, the uniform distribution favours OARO and comes in 3rd 74.72% of the time.

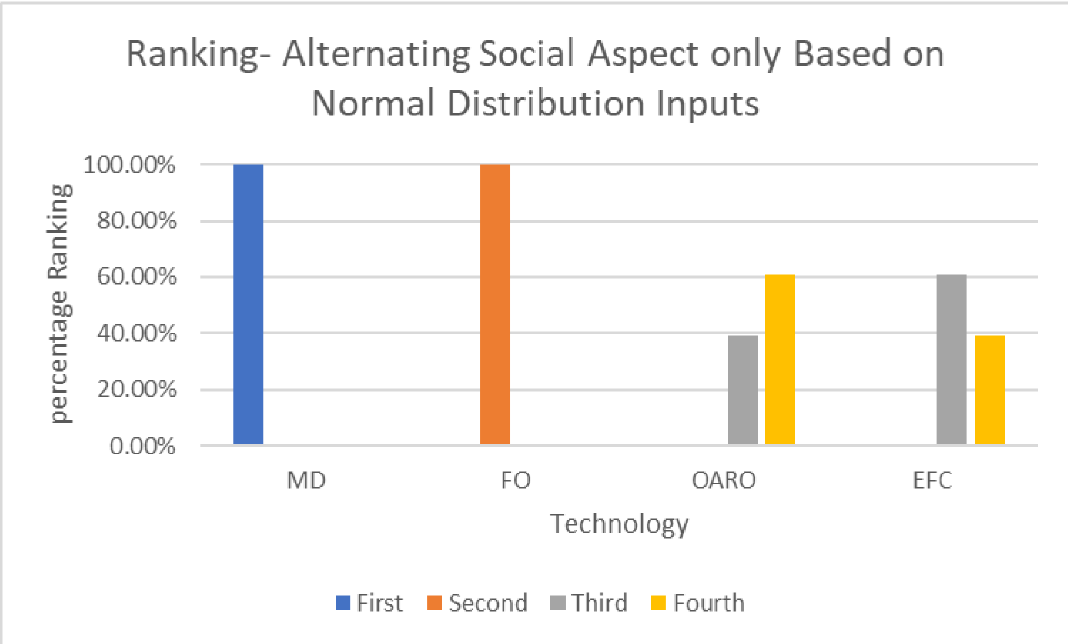


*Figure 19: Technology rankings for Monte Carlo simulation varying the social aspect weighting based on a normal distribution.*

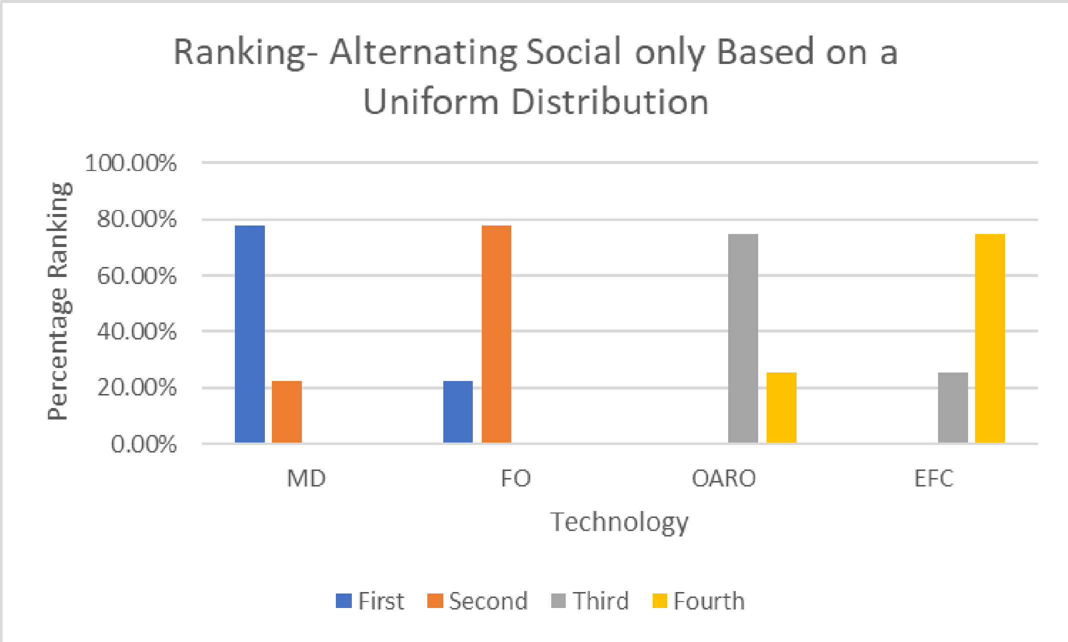


*Figure 20: Technology rankings for Monte Carlo simulation varying the social aspect weighting based on a uniform distribution.*

Starting with the normal distribution results, the shape of the input distribution limits the confusion between MD and FO. Remembering that normal distribution has a bias towards the mean value, which was set to 0.2. It is causing most of the randomly generated social aspect weightings to be between 0 and 0.4. This means that in the lower range of social aspect weighting values, the overwhelming advantage that MD has across the fixed criteria (criteria from the economic, environmental and technical aspects) makes up for MD's slightly worse social aspect weighting compared to FO. The frequency in which the normal distribution inputs breach the higher social aspect weightings necessary for FO to rank higher than MD is rare. OARO and EFC share a similar phenomenon, as the lower social aspect weights allow EFC to benefit from its overwhelming advantage in the technical aspect, which was previously mentioned in Section 5.2.3.

Moving onto the uniform distribution results, the increased range of possible social aspect weightings increase from approximately 0.4 to 0.6. The higher range of values heavily favours FO and OARO against their primary competitors MD and EFC. Within the social aspect, FO represents the IBS for both of the social criteria. Meanwhile, EFC represents both of the IWSs for both of the social aspect criteria. Therefore, higher importance on the social aspect positively influences FO but negative influences EFC.

The statistical information in Table 19 shows that the increase in the available range of social aspect weightings increases the risk. The maximum closeness degree values for MD, OARO and EFC remain constant across both distribution methods. The change from normal to uniform distribution reduces the mean values of MD and EFC but increases for FO and OARO, which follows the expected pattern previously discussed.

*Table 19: Statistical outputs of the Monte Carlo simulation when varying only the social aspect.*

| Distribution Input Type | Technology | Coefficient of Variation | Mean Closeness Degree | Maximum | Minimum |
|---|---|---|---|---|---|
| Normal | MD | 4.78% | 0.722 | 0.772 | 0.581 |
| | FO | 2.20% | 0.601 | 0.669 | 0.584 |
| | OARO | 1.76% | 0.393 | 0.428 | 0.384 |
| | EFC | 2.90% | 0.395 | 0.410 | 0.328 |
| Uniform | MD | 9.36% | 0.683 | 0.772 | 0.574 |
| | FO | 4.55% | 0.619 | 0.674 | 0.584 |
| | OARO | 3.46% | 0.402 | 0.428 | 0.384 |
| | EFC | 6.48% | 0.380 | 0.410 | 0.331 |

# 6 Conclusion

In this work, the development and sensitivity assessment of a decision support system (DSS) for desalination brine management was undertaken. Built upon a combination of two multi-criteria analysis techniques, interval Analytical Hierarchy Process (AHP) and the Technique for Order Preference by Similarity to the Ideal Solution (TOPSIS). There are a wide variety of factors that influence how appropriate a brine management strategy is for a given situation. Therefore, by creating a criteria master list the decision-makers can quickly organise those criteria that are suitable for a given scenario. The master list was adapted to a hypothetical case study in WA, as there was very little literature specific to WA with regards to brine management. This case study made use of 4 brine treatment technologies, namely membrane distillation (MD), forward osmosis (FO), osmotically-assisted reverse osmosis (OARO) and eutectic freeze crystallisation (EFC). Based on the information provided to the DDS from literature, the DDS suggested that the most preferred to least preferred options are as follows, MD, FO, EFC and OARO.

In order to test the robustness of the DDS, two sensitivity analyses were undertaken using a Monte Carlo simulation. The first method assigned random crisp weightings by using triangular, normal and uniform input distributions. The findings suggest that MD was the most suitable technology across all three distribution types. There was uncertainty between 1$^{st}$ and 2$^{nd}$ rankings between MD and FO, ranging from 2% to 6.6%. The second sensitivity analysis method looked at the effects of individual aspects (economic, environmental, technical and social) on the outputs (rankings and closeness degree). Individually altering the aspect weightings for the economic, environmental and technical aspects had very little influence on the dominance of MD as the most preferred brine management technology. However, the social aspect with a uniform distribution significantly increased FO's chances at ranking 1$^{st}$ to 22%. Which indicates that sufficiently high social aspect weighting can significantly influence MD's ranking. For OARO and EFC the most confusion was seen when altering the technical and social aspects.

The DSS created can be adapted to any brine management scenario and is not limited to WA. Although this thesis has a focus on brine treatment, it can be adapted for selecting an appropriate brine disposal method. Further work can be done to refine and validate the DDS.

## 6.1 Recommendations

In order to better understand the model, potential additional tasks include:

1. Further validation of the interval AHP, especially for matrices larger than 2 by 2. This would also include further understanding of the matrix calculations being used in interval AHP.
2. Develop or find a method of measuring the consistency in the decision-maker's interval AHP comparison matrix, which indicates to the user if there is potential error.
3. Sensitivity analysis on the influence of the distance between ideal best and worst solution. One scenario in which this could be applied is that a client only wants to go up to a certain TDS limit and feels like there is no benefit going higher. Therefore, technologies that greatly exceed the clients limit would be restricted, however, the influence on the final results wouldn't be known unless a sensitivity analysis is conducted. Because TOPSIS works on distance between the ideal best and worst solutions to determine the proportion of the weights that are assigned to each technology.
4. Incorporation of more brine management technologies to the TOPSIS hybrid information table, allowing for every technology added be included or excluded for any given scenario.
5. Sensitivity analysis of the complete model once the previously mentioned tasks are complete.

# 7 References

[1] K. Elsaid, E. T. Sayed, M. A. Abdelkareem, A. Baroutaji, and A. G. Olabi, "Environmental impact of desalination processes: Mitigation and control strategies," *Science of the Total Environment*, vol. 740, Oct. 2020, doi: 10.1016/j.scitotenv.2020.140125.

[2] Bureau of Reclamation, "Water Facts - Worldwide Water Supply," 2020. https://www.usbr.gov/mp/arwec/water-facts-ww-water-sup.html#:~:text=2.5%25%20of%20the%20earth's%20fresh,water%20is%20available%20fresh%20water. (accessed May 28, 2021).

[3] Z. Huang, X. Liu, S. Sun, Y. Tang, X. Yuan, and Q. Tang, "Global assessment of future sectoral water scarcity under adaptive inner-basin water allocation measures," *Science of The Total Environment*, vol. 783, p. 146973, Aug. 2021, doi: 10.1016/j.scitotenv.2021.146973.

[4] A. Panagopoulos, K. J. Haralambous, and M. Loizidou, "Desalination brine disposal methods and treatment technologies - A review," *Science of the Total Environment*, vol. 693. Elsevier B.V., Nov. 25, 2019. doi: 10.1016/j.scitotenv.2019.07.351.

[5] C. Fritzmann, J. Löwenberg, T. Wintgens, and T. Melin, "State-of-the-art of reverse osmosis desalination," *Desalination*, vol. 216, no. 1–3, pp. 1–76, Oct. 2007, doi: 10.1016/j.desal.2006.12.009.

[6] E. Jones, M. Qadir, M. T. H. van Vliet, V. Smakhtin, and S. mu Kang, "The state of desalination and brine production: A global outlook," *Science of the Total Environment*, vol. 657. Elsevier B.V., pp. 1343–1356, Mar. 20, 2019. doi: 10.1016/j.scitotenv.2018.12.076.

[7] M. M. Mekonnen and A. Y. Hoekstra, "Sustainability: Four billion people facing severe water scarcity," *Science Advances*, vol. 2, no. 2, Feb. 2016, doi: 10.1126/sciadv.1500323.

[8] Lenntech, “Brine Treatment (ZLD).” https://www.lenntech.com/processes/brine-treatment-ZLD.htm (accessed May 28, 2021).

[9] M. A. Alghoul, P. Poovanaesvaran, K. Sopian, and M. Y. Sulaiman, “Review of brackish water reverse osmosis (BWRO) system designs,” *Renewable and Sustainable Energy Reviews*, vol. 13, no. 9. pp. 2661–2667, Dec. 2009. doi: 10.1016/j.rser.2009.03.013.

[10] A. Panagopoulos and K. J. Haralambous, “Minimal Liquid Discharge (MLD) and Zero Liquid Discharge (ZLD) strategies for wastewater management and resource recovery-Analysis, challenges and prospects,” *Journal of Environmental Chemical Engineering*, vol. 8, no. 5, Oct. 2020, doi: 10.1016/j.jece.2020.104418.

[11] A. Ruiz-García, I. Nuez, M. D. Carrascosa-Chisvert, and J. J. Santana, “Simulations of BWRO systems under different feedwater characteristics. Analysis of operation windows and optimal operating points,” *Desalination*, vol. 491, Oct. 2020, doi: 10.1016/j.desal.2020.114582.

[12] D. M. Warsinger, E. W. Tow, L. A. Maswadeh, G. B. Connors, J. Swaminathan, and J. H. Lienhard V, “Inorganic fouling mitigation by salinity cycling in batch reverse osmosis,” *Water Research*, vol. 137, pp. 384–394, Jun. 2018, doi: 10.1016/j.watres.2018.01.060.

[13] H. Alnajjar, A. Tabatabai, A. Alpatova, T. Leiknes, and N. Ghaffour, “Organic fouling control in reverse osmosis (RO) by effective membrane cleaning using saturated CO2 solution,” *Separation and Purification Technology*, vol. 264, Jun. 2021, doi: 10.1016/j.seppur.2021.118410.

[14] P. S. Goh, W. J. Lau, M. H. D. Othman, and A. F. Ismail, “Membrane fouling in desalination and its mitigation strategies,” *Desalination*, vol. 425. Elsevier B.V., pp. 130–155, Jan. 01, 2018. doi: 10.1016/j.desal.2017.10.018.

[15] Y. M. Kim, S. J. Kim, Y. S. Kim, S. Lee, I. S. Kim, and J. H. Kim, “Presented at the IWA Overview of systems engineering approaches for a large-scale seawater desalination

plant with a reverse osmosis network,” *DES*, vol. 238, pp. 312–332, 2009, doi: 10.1016/j.desal.200.

[16] G. U. Semblante, J. Z. Lee, L. Y. Lee, S. L. Ong, and H. Y. Ng, “Brine pre-treatment technologies for zero liquid discharge systems,” *Desalination*, vol. 441. Elsevier B.V., pp. 96–111, Sep. 01, 2018. doi: 10.1016/j.desal.2018.04.006.

[17] R. Kaplan, D. Mamrosh, H. H. Salih, and S. A. Dastgheib, “Assessment of desalination technologies for treatment of a highly saline brine from a potential CO2 storage site,” *Desalination*, vol. 404, pp. 87–101, Feb. 2017, doi: 10.1016/j.desal.2016.11.018.

[18] V. G. Gude, “Desalination and sustainability - An appraisal and current perspective,” *Water Research*, vol. 89. Elsevier Ltd, pp. 87–106, Feb. 01, 2016. doi: 10.1016/j.watres.2015.11.012.

[19] D. Ariono, M. Purwasasmita, and I. G. Wenten, “Brine effluents: Characteristics, environmental impacts, and their handling,” *Journal of Engineering and Technological Sciences*, vol. 48, no. 4, pp. 367–387, 2016, doi: 10.5614/j.eng.technol.sci.2016.48.4.1.

[20] A. Giwa, V. Dufour, F. al Marzooqi, M. al Kaabi, and S. W. Hasan, “Brine management methods: Recent innovations and current status,” *Desalination*, vol. 407. Elsevier B.V., pp. 1–23, Apr. 01, 2017. doi: 10.1016/j.desal.2016.12.008.

[21] K. Elsaid, M. Kamil, T. Sayed, M. A. Abdelkareem, T. Wilberforce, and A. Olabi, “Environmental impact of desalination technologies: A review,” 2020, doi: 10.1016/j.scitotenv.2020.141528.

[22] I. Ihsanullah, M. A. Atieh, M. Sajid, and M. K. Nazal, “Desalination and environment: A critical analysis of impacts, mitigation strategies, and greener desalination technologies,” *Science of The Total Environment*, vol. 780, p. 146585, Aug. 2021, doi: 10.1016/j.scitotenv.2021.146585.

[23] Department of Primary Industries and Regional Development and Government of Western Australia, “Dryland salinity in Western Australia,” 2021. https://www.agric.wa.gov.au/soil-salinity/dryland-salinity-western-australia-0 (accessed May 28, 2021).

[24] H. Chen, Y. Ma, A. Zhu, Z. Wang, G. Zhao, and Y. Wei, “Soil salinity inversion based on differentiated fusion of satellite image and ground spectra,” *International Journal of Applied Earth Observation and Geoinformation*, vol. 101, p. 102360, Sep. 2021, doi: 10.1016/j.jag.2021.102360.

[25] H. Akbarimoghaddum, M. Galavi, and A. Ghanbari, “Salinity effects on seed germination and seedling growth of bread wheat cultivars,” 2011. [Online]. Available: http://www.uni-sz.bg

[26] N. Kumar Arora *et al.*, “Halo-tolerant plant growth promoting rhizobacteria for improving productivity and remediation of saline soils,” *Journal of Advanced Research*, vol. 26. Elsevier B.V., pp. 69–82, Nov. 01, 2020. doi: 10.1016/j.jare.2020.07.003.

[27] L. Xiong and J.-K. Zhu, “Molecular and genetic aspects of plant responses to osmotic stress,” 2002.

[28] F. Tian, M. Hou, Y. Qiu, T. Zhang, and Y. Yuan, “Salinity stress effects on transpiration and plant growth under different salinity soil levels based on thermal infrared remote (TIR) technique,” *Geoderma*, vol. 357, Jan. 2020, doi: 10.1016/j.geoderma.2019.113961.

[29] P. Shrivastava and R. Kumar, “Soil salinity: A serious environmental issue and plant growth promoting bacteria as one of the tools for its alleviation,” *Saudi Journal of Biological Sciences*, vol. 22, no. 2. Elsevier, pp. 123–131, Mar. 01, 2015. doi: 10.1016/j.sjbs.2014.12.001.

[30] R. Huang *et al.*, “Effects of plant growth regulator and chelating agent on the phytoextraction of heavy metals by Pfaffia glomerata and on the soil microbial community,” *Environmental Pollution*, vol. 283, Aug. 2021, doi: 10.1016/j.envpol.2021.117159.

[31] P. Zhuang, H. Lu, Z. Li, B. Zou, and M. B. McBride, “Multiple exposure and effects assessment of heavy metals in the population near mining area in South China,” *PLoS ONE*, vol. 9, no. 4, Apr. 2014, doi: 10.1371/journal.pone.0094484.

[32] M. O. Mavukkandy, C. M. Chabib, I. Mustafa, A. al Ghaferi, and F. AlMarzooqi, “Brine management in desalination industry: From waste to resources generation,” *Desalination*, vol. 472. Elsevier B.V., Dec. 15, 2019. doi: 10.1016/j.desal.2019.114187.

[33] I. Sola *et al.*, “Sustainable desalination: Long-term monitoring of brine discharge in the marine environment,” *Marine Pollution Bulletin*, vol. 161, Dec. 2020, doi: 10.1016/j.marpolbul.2020.111813.

[34] J. Aparicio, L. Candela, O. Alfranca, and J. L. García-Aróstegui, “Economic evaluation of small desalination plants from brackish aquifers. Application to Campo de Cartagena (SE Spain),” *Desalination*, vol. 411, pp. 38–44, 2017, doi: 10.1016/j.desal.2017.02.004.

[35] G. F. Clark *et al.*, “First large-scale ecological impact study of desalination outfall reveals trade-offs in effects of hypersalinity and hydrodynamics,” *Water Research*, vol. 145, pp. 757–768, Nov. 2018, doi: 10.1016/j.watres.2018.08.071.

[36] T. M. Missimer and R. G. Maliva, “Environmental issues in seawater reverse osmosis desalination: Intakes and outfalls,” *Desalination*, vol. 434. Elsevier B.V., pp. 198–215, May 15, 2018. doi: 10.1016/j.desal.2017.07.012.

[37] M. Ahmed, W. H. Shayya, D. Hoey, A. Mahendran, R. Morris, and J. A1-Handaly, “Use of evaporation ponds for brine disposal in desalination plants,” 2000. [Online]. Available: www.elsevier.com/locate/desal

[38] G. al Bazedi, R. S. Ettouney, S. R. Tewfik, M. H. Sorour, and M. A. El-Rifai, “Salt recovery from brine generated by large-scale seawater desalination plants,” *Desalination and Water Treatment*, vol. 52, no. 25–27, pp. 4689–4697, Jul. 2014, doi: 10.1080/19443994.2013.810381.

[39] A. S. Sánchez, I. B. R. Nogueira, and R. A. Kalid, “Uses of the reject brine from inland desalination for fish farming, Spirulina cultivation, and irrigation of forage shrub and crops,” *Desalination*, vol. 364, pp. 96–107, May 2015, doi: 10.1016/j.desal.2015.01.034.

[40] M. N. Soliman, F. Z. Guen, S. A. Ahmed, H. Saleem, M. J. Khalil, and S. J. Zaidi, “Energy consumption and environmental impact assessment of desalination plants and brine disposal strategies,” *Process Safety and Environmental Protection*, vol. 147. Institution of Chemical Engineers, pp. 589–608, Mar. 01, 2021. doi: 10.1016/j.psep.2020.12.038.

[41] A. Izady *et al.*, “Risk-based Stochastic Optimization of Evaporation Ponds as a Cost-Effective and Environmentally-Friendly Solution for the Disposal of Oil-Produced Water,” *Journal of Water Process Engineering*, vol. 38, Dec. 2020, doi: 10.1016/j.jwpe.2020.101607.

[42] F. J. Díaz, S. E. Benes, and S. R. Grattan, “Field performance of halophytic species under irrigation with saline drainage water in the San Joaquin Valley of California,” *Agricultural Water Management*, vol. 118, pp. 59–69, Feb. 2013, doi: 10.1016/j.agwat.2012.11.017.

[43] R. S. Al-Absi, M. Abu-Dieyeh, and M. A. Al-Ghouti, “Brine management strategies, technologies, and recovery using adsorption processes,” *Environmental Technology and Innovation*, vol. 22. Elsevier B.V., May 01, 2021. doi: 10.1016/j.eti.2021.101541.

[44] B. Ladewig and B. Asquith, *Desalination Concentrate management*. 2011.

[45] D. Jiménez-Arias *et al.*, “Rejected brine recycling in hydroponic and thermo-solar evaporation systems for leisure and tourist facilities. Changing waste into raw material,” *Desalination*, vol. 496, Dec. 2020, doi: 10.1016/j.desal.2020.114443.

[46] Y. Liang *et al.*, “Constructed wetlands for saline wastewater treatment: A review,” *Ecological Engineering*, vol. 98. Elsevier B.V., pp. 275–285, Jan. 01, 2017. doi: 10.1016/j.ecoleng.2016.11.005.

[47] M. Mickley, “Desalination and Water Purification Research and Development Program Report No. 207,” 2018. [Online]. Available: https://www.usbr.gov/research/dwpr/DWPR_Reports.html

[48] M. K. K. Nassar, R. M. El-Damak, and A. H. M. Ghanem, “Impact of desalination plants brine injection wells on coastal aquifers,” in *Environmental Geology*, Apr. 2008, vol. 54, no. 3, pp. 445–454. doi: 10.1007/s00254-007-0849-9.

[49] A. Putri Pertiwi, D. Samuel Hutajalu, H. Imanuddin, and I. Amanda, “AN ENVIRONMENTAL PROTECTION (ZERO DISCHARGE) UTILIZING IDLE WELLS TO INJECT PRODUCED WATER FOR PRESSURE MAINTANANCE WITH DEEP WELL INJECTION METHOD,” 2015.

[50] H. He, Y. Chen, X. Li, Y. Cheng, C. Yang, and G. Zeng, “Influence of salinity on microorganisms in activated sludge processes: A review,” *International Biodeterioration and Biodegradation*, vol. 119, pp. 520–527, Apr. 2017, doi: 10.1016/j.ibiod.2016.10.007.

[51] A. S. Bello, N. Zouari, D. A. Da’ana, J. N. Hahladakis, and M. A. Al-Ghouti, “An overview of brine management: Emerging desalination technologies, life cycle assessment, and metal recovery methodologies,” *Journal of Environmental Management*, vol. 288. Academic Press, Jun. 15, 2021. doi: 10.1016/j.jenvman.2021.112358.

[52] Q. Chen *et al.*, "A zero liquid discharge system integrating multi-effect distillation and evaporative crystallization for desalination brine treatment," *Desalination*, vol. 502, Apr. 2021, doi: 10.1016/j.desal.2020.114928.

[53] D. M. Davenport, A. Deshmukh, J. R. Werber, and M. Elimelech, "High-Pressure Reverse Osmosis for Energy-Efficient Hypersaline Brine Desalination: Current Status, Design Considerations, and Research Needs," *Environmental Science and Technology Letters*, vol. 5, no. 8, pp. 467–475, Aug. 2018, doi: 10.1021/acs.estlett.8b00274.

[54] D. M. Davenport *et al.*, "Thin film composite membrane compaction in high-pressure reverse osmosis," *Journal of Membrane Science*, vol. 610, p. 118268, Sep. 2020, doi: 10.1016/j.memsci.2020.118268.

[55] Y. Okamoto and J. H. Lienhard, "How RO membrane permeability and other performance factors affect process cost and energy use: A review," *Desalination*, vol. 470. Elsevier B.V., p. 114064, Nov. 15, 2019. doi: 10.1016/j.desal.2019.07.004.

[56] Saltworks, "Applying Ultra-High pressure Reverse Osmosis in Brine Management," 2019. https://www.saltworkstech.com/articles/applying-ultra-high-pressure-reverse-osmosis-in-brine-management/ (accessed Jun. 01, 2021).

[57] Dupont, "Specialty Membranes XUS180808 Ultra-High Pressure RO Element." https://www.dupont.com/products/dupontspecialtymembranesxus180808ultrahighpressureroelement.html (accessed Jun. 01, 2021).

[58] A. B. Schantz, B. Xiong, E. Dees, D. R. Moore, X. Yang, and M. Kumar, "Prospects and challenges for high-pressure reverse osmosis in minimizing concentrated waste streams," 2018.

[59] S. M. Iskander, S. Zou, B. Brazil, J. T. Novak, and Z. He, "Energy consumption by forward osmosis treatment of landfill leachate for water recovery," *Waste Management*, vol. 63, pp. 284–291, May 2017, doi: 10.1016/j.wasman.2017.03.026.

[60] M. T. Vu, W. E. Price, T. He, X. Zhang, and L. D. Nghiem, “Seawater-driven forward osmosis for pre-concentrating nutrients in digested sludge centrate,” *Journal of Environmental Management*, vol. 247, pp. 135–139, Oct. 2019, doi: 10.1016/j.jenvman.2019.06.082.

[61] H. S. Son *et al.*, “Impact of osmotic and thermal isolation barrier on concentration and temperature polarization and energy efficiency in a novel FO-MD integrated module,” *Journal of Membrane Science*, vol. 620, p. 118811, Feb. 2021, doi: 10.1016/j.memsci.2020.118811.

[62] F. Parveen and N. Hankins, “Integration of Forward Osmosis Membrane Bioreactor (FO-MBR) and Membrane Distillation (MD) units for water reclamation and regeneration of draw solutions,” *Journal of Water Process Engineering*, vol. 41, p. 102045, Jun. 2021, doi: 10.1016/j.jwpe.2021.102045.

[63] G. Kolliopoulos, J. T. Martin, and V. G. Papangelakis, “Energy requirements in the separation-regeneration step in forward osmosis using TMA–CO2–H2O as the draw solution,” *Chemical Engineering Research and Design*, vol. 140, pp. 166–174, Dec. 2018, doi: 10.1016/j.cherd.2018.10.015.

[64] K. Nakagawa *et al.*, “Multistage osmotically assisted reverse osmosis process for concentrating solutions using hollow fiber membrane modules,” *Chemical Engineering Research and Design*, vol. 162, pp. 117–124, Oct. 2020, doi: 10.1016/j.cherd.2020.07.029.

[65] B. Al-Najar, C. D. Peters, H. Albuflasa, and N. P. Hankins, “Pressure and osmotically driven membrane processes: A review of the benefits and production of nano-enhanced membranes for desalination,” *Desalination*, vol. 479. Elsevier B.V., p. 114323, Apr. 01, 2020. doi: 10.1016/j.desal.2020.114323.

[66] C. D. Peters and N. P. Hankins, “Osmotically assisted reverse osmosis (OARO): Five approaches to dewatering saline brines using pressure-driven membrane processes,” *Desalination*, vol. 458, pp. 1–13, May 2019, doi: 10.1016/j.desal.2019.01.025.

[67] C. D. Peters and N. P. Hankins, “The synergy between osmotically assisted reverse osmosis (OARO) and the use of thermo-responsive draw solutions for energy efficient, zero-liquid discharge desalination,” *Desalination*, vol. 493, p. 114630, Nov. 2020, doi: 10.1016/j.desal.2020.114630.

[68] M. Askari, C. Z. Liang, L. T. (Simon) Choong, and T. S. Chung, “Optimization of TFC-PES hollow fiber membranes for reverse osmosis (RO) and osmotically assisted reverse osmosis (OARO) applications,” *Journal of Membrane Science*, vol. 625, p. 119156, May 2021, doi: 10.1016/j.memsci.2021.119156.

[69] T. v. Bartholomew, L. Mey, J. T. Arena, N. S. Siefert, and M. S. Mauter, “Osmotically assisted reverse osmosis for high salinity brine treatment,” *Desalination*, vol. 421, pp. 3–11, Nov. 2017, doi: 10.1016/j.desal.2017.04.012.

[70] A. A. Atia, N. Y. Yip, and V. Fthenakis, “Pathways for minimal and zero liquid discharge with enhanced reverse osmosis technologies: Module-scale modeling and techno-economic assessment,” *Desalination*, vol. 509, p. 115069, Aug. 2021, doi: 10.1016/j.desal.2021.115069.

[71] J. Arena, N. Siefert, T. Bartholomew, and M. Mauter, “Dewatering of High Salinity Brines by Osmotically Assisted Reverse Osmosis,” 2018, Accessed: Jun. 02, 2021. [Online]. Available: https://netl.doe.gov/sites/default/files/event-proceedings/2017/crosscutting/20170323-Track-A/20170323_0930A_Presentation_Arena_NETL.pdf

[72] S. Liang, H. Zheng, X. Ma, F. Liu, G. Wang, and Z. Zhao, “Study on a passive concentrating photovoltaic-membrane distillation integrated system,” *Energy Conversion and Management*, vol. 242, p. 114332, Aug. 2021, doi: 10.1016/j.enconman.2021.114332.

[73] O. Alrehaili, F. Perreault, S. Sinha, and P. Westerhoff, “Increasing net water recovery of reverse osmosis with membrane distillation using natural thermal differentials

between brine and co-located water sources: Impacts at large reclamation facilities," *Water Research*, vol. 184, p. 116134, Oct. 2020, doi: 10.1016/j.watres.2020.116134.

[74] S. Zare and A. Kargari, "Membrane properties in membrane distillation," in *Emerging Technologies for Sustainable Desalination Handbook*, Elsevier, 2018, pp. 107–156. doi: 10.1016/B978-0-12-815818-0.00004-7.

[75] I.- Noor, A. Martin, and O. Dahl, "Techno-economic system analysis of membrane distillation process for treatment of chemical mechanical planarization wastewater in nano-electronics industries," *Separation and Purification Technology*, vol. 248, Oct. 2020, doi: 10.1016/j.seppur.2020.117013.

[76] Y. Wang *et al.*, "Treatment of coal gasification brine by membrane distillation: Effect of mixed fouling and pretreatment on process performance," *Desalination*, vol. 499, p. 114820, Feb. 2021, doi: 10.1016/j.desal.2020.114820.

[77] R. Bahar and K. C. Ng, "Fresh water production by membrane distillation (MD) using marine engine's waste heat," *Sustainable Energy Technologies and Assessments*, vol. 42, Dec. 2020, doi: 10.1016/j.seta.2020.100860.

[78] F. E. Ahmed, B. S. Lalia, R. Hashaikeh, and N. Hilal, "Alternative heating techniques in membrane distillation: A review," *Desalination*, vol. 496. Elsevier B.V., p. 114713, Dec. 15, 2020. doi: 10.1016/j.desal.2020.114713.

[79] I. A. Said, T. R. Chomiak, Z. He, and Q. Li, "Low-cost high-efficiency solar membrane distillation for treatment of oil produced waters," *Separation and Purification Technology*, vol. 250, p. 117170, Nov. 2020, doi: 10.1016/j.seppur.2020.117170.

[80] M. Bindels, J. Carvalho, C. B. Gonzalez, N. Brand, and B. Nelemans, "Techno-economic assessment of seawater reverse osmosis (SWRO) brine treatment with air gap membrane distillation (AGMD)," *Desalination*, vol. 489, p. 114532, Sep. 2020, doi: 10.1016/j.desal.2020.114532.

[81] D. González, J. Amigo, and F. Suárez, “Membrane distillation: Perspectives for sustainable and improved desalination,” *Renewable and Sustainable Energy Reviews*, vol. 80. Elsevier Ltd, pp. 238–259, Dec. 01, 2017. doi: 10.1016/j.rser.2017.05.078.

[82] M. C. Sparenberg, I. Ruiz Salmón, and P. Luis, “Economic evaluation of salt recovery from wastewater via membrane distillation-crystallization,” *Separation and Purification Technology*, vol. 235, p. 116075, Mar. 2020, doi: 10.1016/j.seppur.2019.116075.

[83] N. Mir and Y. Bicer, “Integration of electrodialysis with renewable energy sources for sustainable freshwater production: A review,” *Journal of Environmental Management*, vol. 289. Academic Press, p. 112496, Jul. 01, 2021. doi: 10.1016/j.jenvman.2021.112496.

[84] M. I. Khan *et al.*, “Preparation of anion exchange membranes from BPPO and dimethylethanolamine for electrodialysis,” *Desalination*, vol. 402, pp. 10–18, Jan. 2017, doi: 10.1016/j.desal.2016.09.019.

[85] Lenntech, “Electrodialysis reversal (EDR).” https://www.lenntech.com/Data-sheets/ED-ZLD-interactive.pdf (accessed Jun. 03, 2021).

[86] K. M. Chehayeb, D. M. Farhat, K. G. Nayar, and J. H. Lienhard, “Optimal design and operation of electrodialysis for brackish-water desalination and for high-salinity brine concentration,” *Desalination*, vol. 420, pp. 167–182, Oct. 2017, doi: 10.1016/j.desal.2017.07.003.

[87] B. F. Severin and T. D. Hayes, “Electrodialysis of concentrated brines: Effects of multivalent cations,” *Separation and Purification Technology*, vol. 218, pp. 227–241, Jul. 2019, doi: 10.1016/j.seppur.2019.02.039.

[88] M. Herrero-Gonzalez, P. Diaz-Guridi, A. Dominguez-Ramos, A. Irabien, and R. Ibañez, “Highly concentrated HCl and NaOH from brines using electrodialysis with bipolar

membranes," *Separation and Purification Technology*, vol. 242, p. 116785, Jul. 2020, doi: 10.1016/j.seppur.2020.116785.

[89] A. Pérez-González, A. M. Urtiaga, R. Ibáñez, and I. Ortiz, "State of the art and review on the treatment technologies of water reverse osmosis concentrates," *Water Research*, vol. 46, no. 2. Elsevier Ltd, pp. 267–283, 2012. doi: 10.1016/j.watres.2011.10.046.

[90] D. Zhao, L. Y. Lee, S. L. Ong, P. Chowdhury, K. B. Siah, and H. Y. Ng, "Electrodialysis reversal for industrial reverse osmosis brine treatment," *Separation and Purification Technology*, vol. 213, Apr. 2019, doi: 10.1016/j.seppur.2018.12.056.

[91] T. Tong and M. Elimelech, "The Global Rise of Zero Liquid Discharge for Wastewater Management: Drivers, Technologies, and Future Directions," *Environmental Science and Technology*, vol. 50, no. 13, pp. 6846–6855, 2016, doi: 10.1021/acs.est.6b01000.

[92] M. M. Shah, "A General Correlation for Heat Transfer During Evaporation of Falling Films on Single Horizontal Plain Tubes," *International Journal of Refrigeration*, Apr. 2021, doi: 10.1016/j.ijrefrig.2021.04.025.

[93] R. Battisti, R. A. F. Machado, and C. Marangoni, "A background review on falling film distillation in wetted-wall columns: From fundamentals towards intensified technologies," *Chemical Engineering and Processing - Process Intensification*, vol. 150. Elsevier B.V., p. 107873, Apr. 01, 2020. doi: 10.1016/j.cep.2020.107873.

[94] H. Zheng, "Fundamental Relationships of Heat and Mass Transfer in Solar Seawater Desalination Systems," in *Solar Energy Desalination Technology*, Elsevier, 2017, pp. 173–258. doi: 10.1016/b978-0-12-805411-6.00003-8.

[95] Z. Berk, "Evaporation," in *Food Process Engineering and Technology*, Elsevier, 2009, pp. 429–458. doi: 10.1016/B978-0-12-373660-4.00021-1.

[96] Astrolex Industries, "Evaporation Technology."

[97] D. von Eiff, P. W. Wong, Y. Gao, S. Jeong, and A. K. An, “Technical and economic analysis of an advanced multi-stage flash crystallizer for the treatment of concentrated brine,” *Desalination*, vol. 503, p. 114925, May 2021, doi: 10.1016/j.desal.2020.114925.

[98] A. Panagopoulos, M. Loizidou, and K.-J. Haralambous, “Stainless Steel in Thermal Desalination and Brine Treatment: Current Status and Prospects,” *Metals and Materials International*, vol. 26, no. 10, Oct. 2020, doi: 10.1007/s12540-019-00398-w.

[99] Y. Ghalavand, M. S. Hatamipour, and A. Rahimi, “A review on energy consumption of desalination processes,” *Desalination and Water Treatment*, vol. 54, no. 6, pp. 1526–1541, 2015, doi: 10.1080/19443994.2014.892837.

[100] I. Baniasad Askari and M. Ameri, “A techno-economic review of multi effect desalination systems integrated with different solar thermal sources,” *Applied Thermal Engineering*, vol. 185, p. 116323, Feb. 2021, doi: 10.1016/j.applthermaleng.2020.116323.

[101] A. Al-Karaghouli and L. L. Kazmerski, “Energy consumption and water production cost of conventional and renewable-energy-powered desalination processes,” *Renewable and Sustainable Energy Reviews*, vol. 24, Aug. 2013, doi: 10.1016/j.rser.2012.12.064.

[102] S. M. Jafari, C. Arpagaus, M. A. Cerqueira, and K. Samborska, “Nano spray drying of food ingredients; materials, processing and applications,” *Trends in Food Science and Technology*, vol. 109. Elsevier Ltd, pp. 632–646, Mar. 01, 2021. doi: 10.1016/j.tifs.2021.01.061.

[103] G. Nasr, A. Yule, and lothar Bendig, *Industrial Sprays and Atomization: Design, Analysis and Applications*. 2013. Accessed: Jun. 29, 2021. [Online]. Available: https://books.google.com.au/books?hl=en&lr=&id=AuzjBwAAQBAJ&oi=fnd&pg=PR15&ots=JX9SZN88vp&sig=-oKE9cgRH_ImSkBb-WbZFJezAOw&redir_esc=y#v=onepage&q&f=false

[104] G. L. Stepakoff, D. Siegelman, R. Johnson, and W. Gibson, “Development of a eutectic freezing process for brine disposal,” *Desalination*, vol. 15, no. 1, pp. 25–38, Aug. 1974, doi: 10.1016/S0011-9164(00)82061-5.

[105] P. M. Williams, M. Ahmad, B. S. Connolly, and D. L. Oatley-Radcliffe, “Technology for freeze concentration in the desalination industry,” *Desalination*, vol. 356. Elsevier, pp. 314–327, Jan. 05, 2015. doi: 10.1016/j.desal.2014.10.023.

[106] D. G. Randall, J. Nathoo, and A. E. Lewis, “A case study for treating a reverse osmosis brine using Eutectic Freeze Crystallization-Approaching a zero waste process,” *Desalination*, vol. 266, no. 1–3, pp. 256–262, Jan. 2011, doi: 10.1016/j.desal.2010.08.034.

[107] R. J. C. Vaessen, B. J. H. Janse, M. M. Seckler, and G. J. Witkamp, “Evaluation of the Performance of a Newly Developed Eutectic Freeze Crystallizer: Scraped Cooled Wall Crystallizer,” *Chemical Engineering Research and Design*, vol. 81, no. 10, pp. 1363–1372, Nov. 2003, doi: 10.1205/026387603771339573.

[108] R. Halde, “Concentration of impurities by progressive freezing,” *Water Research*, vol. 14, no. 6, pp. 575–580, Jan. 1980, doi: 10.1016/0043-1354(80)90115-3.

[109] G. Q. Chen, S. L. Gras, and S. E. Kentish, “Eutectic freeze crystallization of saline dairy effluent,” *Desalination*, vol. 480, p. 114349, Apr. 2020, doi: 10.1016/j.desal.2020.114349.

[110] J. Gilron, Y. Folkman, R. Savliev, M. Waisman, and O. Kedem, “WAIV — wind aided intensified evaporation for reduction of desalination brine volume,” *Desalination*, vol. 158, no. 1–3, pp. 205–214, Aug. 2003, doi: 10.1016/S0011-9164(03)00453-3.

[111] G. J. Millar, S. J. Couperthwaite, and C. D. Moodliar, “Strategies for the management and treatment of coal seam gas associated water,” *Renewable and Sustainable Energy Reviews*, vol. 57, pp. 669–691, May 2016, doi: 10.1016/J.RSER.2015.12.087.

[112] A. Subramani and J. G. Jacangelo, “Treatment technologies for reverse osmosis concentrate volume minimization: A review,” *Separation and Purification Technology*, vol. 122, pp. 472–489, Feb. 2014, doi: 10.1016/J.SEPPUR.2013.12.004.

[113] M. F. Kaddoura, M. Chosa, P. Bhalekar, and N. C. Wright, “Mathematical modeling of a modular convection-enhanced evaporation system,” *Desalination*, vol. 510, p. 115057, Aug. 2021, doi: 10.1016/J.DESAL.2021.115057.

[114] J. Gilron, E. Ramon, N. Assaf, and O. Kedem, “Wind-aided intensified evaporation (WAIV): An environmentally sustainable method for brine management,” in *Current Trends and Future Developments on (Bio-) Membranes: Membrane Desalination Systems: The Next Generation*, Elsevier, 2018, pp. 215–241. doi: 10.1016/B978-0-12-813551-8.00009-7.

[115] M. Poch, J. Comas, I. Rodríguez-Roda, M. Sànchez-Marrè, and U. Cortés, “Designing and building real environmental decision support systems,” in *Environmental Modelling and Software*, Sep. 2004, vol. 19, no. 9, pp. 857–873. doi: 10.1016/j.envsoft.2003.03.007.

[116] A. Ullah, S. Hussain, A. Wasim, and M. Jahanzaib, “Development of a decision support system for the selection of wastewater treatment technologies,” *Science of The Total Environment*, vol. 731, p. 139158, Aug. 2020, doi: 10.1016/J.SCITOTENV.2020.139158.

[117] G. Mannina, T. F. Rebouças, A. Cosenza, M. Sànchez-Marrè, and K. Gibert, “Decision support systems (DSS) for wastewater treatment plants – A review of the state of the art,” *Bioresource Technology*, vol. 290, p. 121814, Oct. 2019, doi: 10.1016/J.BIORTECH.2019.121814.

[118] V. Villanueva *et al.*, “Identifying key unmet needs and value drivers in the treatment of focal-onset seizures (FOS) in patients with drug-resistant epilepsy (DRE) in Spain through Multi-Criteria Decision Analysis (MCDA),” *Epilepsy & Behavior*, vol. 122, p. 108222, Sep. 2021, doi: 10.1016/J.YEBEH.2021.108222.

[119] Ankana and G. Dhanaraj, “Study of selected influential criteria on groundwater potential storage using geospatial technology and multi-criteria decision analysis (MCDA) approach: A case study,” *The Egyptian Journal of Remote Sensing and Space Science*, Jul. 2021, doi: 10.1016/J.EJRS.2021.06.004.

[120] D. Nicklin and H. Gohari Darabkhani, “Techniques to measure particulate matter emissions from stationary sources: A critical technology review using Multi Criteria Decision Analysis (MCDA),” *Journal of Environmental Management*, vol. 296, p. 113167, Oct. 2021, doi: 10.1016/J.JENVMAN.2021.113167.

[121] D. A. Cunha, M. Andrade, L. A. Prado, L. O. Santana, and M. P. Gonçalves da Silv, “RISK assessment in airport maintenance runway condition using MCDA-C,” *Journal of Air Transport Management*, vol. 90, p. 101948, Jan. 2021, doi: 10.1016/J.JAIRTRAMAN.2020.101948.

[122] E. Ustaoglu, S. Sisman, and A. C. Aydınoglu, “Determining agricultural suitable land in peri-urban geography using GIS and Multi Criteria Decision Analysis (MCDA) techniques,” *Ecological Modelling*, vol. 455, p. 109610, Sep. 2021, doi: 10.1016/J.ECOLMODEL.2021.109610.

[123] M. Sahabuddin and I. Khan, “Multi-criteria decision analysis methods for energy sector’s sustainability assessment: Robustness analysis through criteria weight change,” *Sustainable Energy Technologies and Assessments*, vol. 47, p. 101380, Oct. 2021, doi: 10.1016/J.SETA.2021.101380.

[124] F. Dweiri, S. A. Khan, and A. Almulla, “A multi-criteria decision support system to rank sustainable desalination plant location criteria,” *Desalination*, vol. 444, pp. 26–34, Oct. 2018, doi: 10.1016/j.desal.2018.07.007.

[125] S. A. Ghassemi and S. Danesh, “A hybrid fuzzy multi-criteria decision making approach for desalination process selection,” *Desalination*, vol. 313, pp. 44–50, Mar. 2013, doi: 10.1016/j.desal.2012.12.008.

[126] D. Georgiou, E. S. Mohammed, and S. Rozakis, “Multi-criteria decision making on the energy supply configuration of autonomous desalination units,” *Renewable Energy*, vol. 75, pp. 459–467, Mar. 2015, doi: 10.1016/j.renene.2014.09.036.

[127] M. Erbaş, M. Kabak, E. Özceylan, and C. Çetinkaya, “Optimal siting of electric vehicle charging stations: A GIS-based fuzzy Multi-Criteria Decision Analysis,” *Energy*, vol. 163, pp. 1017–1031, Nov. 2018, doi: 10.1016/j.energy.2018.08.140.

[128] J. Vishnupriyan, D. Arumugam, N. M. Kumar, S. S. Chopra, and P. Partheeban, “Multi-criteria decision analysis for optimal planning of desalination plant feasibility in different urban cities in India,” *Journal of Cleaner Production*, vol. 315, p. 128146, Sep. 2021, doi: 10.1016/J.JCLEPRO.2021.128146.

[129] Z. Wang, Y. Wang, G. Xu, and J. Ren, “Sustainable desalination process selection: Decision support framework under hybrid information,” *Desalination*, vol. 465, pp. 44–57, Sep. 2019, doi: 10.1016/J.DESAL.2019.04.022.

[130] B. Purvis, Y. Mao, and D. Robinson, “Three pillars of sustainability: in search of conceptual origins,” *Sustainability Science*, vol. 14, no. 3, May 2019, doi: 10.1007/s11625-018-0627-5.

[131] J. J. Wang, Y. Y. Jing, C. F. Zhang, and J. H. Zhao, “Review on multi-criteria decision analysis aid in sustainable energy decision-making,” *Renewable and Sustainable Energy Reviews*, vol. 13, no. 9. pp. 2263–2278, Dec. 2009. doi: 10.1016/j.rser.2009.06.021.

[132] Sustainable Business Council, “Social-Licence-to-Operate-Paper”.

[133] R. W. Saaty, “The analytic hierarchy process—what it is and how it is used,” *Mathematical Modelling*, vol. 9, no. 3–5, pp. 161–176, Jan. 1987, doi: 10.1016/0270-0255(87)90473-8.

[134] V. Ravisankar, “Correspondence with Murdoch University Research Officer.” Perth, 2021.

[135] Sigma-Aldrich, “NaCl”, Accessed: Oct. 05, 2021. [Online]. Available: https://www.sigmaaldrich.com/deepweb/assets/sigmaaldrich/product/documents/404/031/71376dat.pdf

[136] D. Price, A. Maile, J. Peterson-Droogh, and D. Blight, “A methodology for uncertainty quantification and sensitivity analysis for responses subject to Monte Carlo uncertainty with application to fuel plate characteristics in the ATRC,” *Nuclear Engineering and Technology*, Sep. 2021, doi: 10.1016/J.NET.2021.09.010.

[137] H. el ganich, O. el rhazouani, A. Halimi, M. Mkimel, Y. Ait Ahmed, and E. Saad, “Magnetic properties of the perovskite GdCuO3: Monte Carlo simulation,” *Physics Letters A*, vol. 412, p. 127587, Oct. 2021, doi: 10.1016/J.PHYSLETA.2021.127587.

[138] P. S. Dąbrowski and M. Hubert Zienkiewicz, “Impact of cross-section CENTERS estimation on the accuracy of the Point cloud spatial expansion using robust m-estimation and monte carlo simulation,” *Measurement*, p. 110436, Nov. 2021, doi: 10.1016/J.MEASUREMENT.2021.110436.

[139] M. Błażkiewicz and A. Konefał, “The Monte Carlo simulation approach to verification of the attenuation factors k for isotropic gamma-ray sources commonly used in industry, medicine and science,” *Radiation Physics and Chemistry*, vol. 190, p. 109816, Jan. 2022, doi: 10.1016/J.RADPHYSCHEM.2021.109816.

[140] J. De-la-Colina, J. Valdés-González, and F. Manzanarez Morones, “Accidental torsion within the frame of nonlinear dynamic analysis using code accidental eccentricities and Monte Carlo simulations,” *Engineering Structures*, vol. 248, p. 113196, Dec. 2021, doi: 10.1016/J.ENGSTRUCT.2021.113196.

[141] A. Sabry *et al.*, “DFT study, Mean-Field Approximation and Monte-Carlo simulation of physical properties of Fe and Cr doped and co-doped GaN,” *Solid State Communications*, vol. 340, p. 114509, Dec. 2021, doi: 10.1016/J.SSC.2021.114509.

[142] v. Shyamprasad and P. Kousalya, “Role of Consistency and Random Index in Analytic Hierarchy Process—A New Measure,” 2020, pp. 233–239. doi: 10.1007/978-981-15-3215-3_22.

[143] A. Saltelli *et al.*, *Global Sensitivity Analysis. The Primer*. 2007.

[144] Glen Stephanie, “Empirical Rule and Research,” 2021. https://www.statisticshowto.com/probability-and-statistics/statistics-definitions/empirical-rule-2/ (accessed Nov. 21, 2021).

[145] O. Shechtman, “The Coefficient of Variation as an Index of Measurement Reliability,” 2013, pp. 39–49. doi: 10.1007/978-3-642-37131-8_4.

# 8 Appendix

The appendix shows intermediate results and pre-processed raw data for the Monte Carlo simulations.

## 8.1 TOPSIS hybrid information decision making matrices

Shows the intermediate results of step 2 (normalised decision making matrix) and 3 (weighted normalised decision making matrix) of the TOPSIS process.

*Table 20: Normalised data from the hybrid information decision-making matrix.*

| Criteria | Global crisp weightings | MD | | | FO with regeneration | | | OARO | | | EFC | | | Calculation type |
|---|---|---|---|---|---|---|---|---|---|---|---|---|---|---|
| Capital Cost | 0.1666 | 1.0000 | | | 0.5000 | | | 0.1250 | | | 0.0000 | | | cost type |
| Production Cost | 0.1208 | 0.6949 | | | 1.0000 | | | 0.0000 | | | 0.5537 | | | cost type |
| TDS Limitation | 0.1346 | 1.0000 | 1.0000 | | 0.0000 | 0.3333 | | 0.0476 | 0.0476 | | 1.0000 | 1.0000 | | benefit type |
| Energy consumption | 0.2121 | 0.5685 | 0.7603 | | 0.9130 | 0.9808 | | 0.8973 | 0.9863 | | 0.0000 | 1.0000 | | cost type |
| Footprint | 0.0566 | 0.3333 | 1.0000 | | 0.0000 | 0.6667 | | 0.3333 | 0.6667 | | 0.3333 | 1.0000 | | cost type |
| Technology maturity | 0.0199 | 0.3333 | 0.5000 | 0.6667 | 0.0000 | 0.1667 | 0.3333 | 0.0000 | 0.1667 | 0.3333 | 0.6667 | 0.8333 | 1.0000 | benefit type |
| Technology Reliability | 0.0497 | 0.7143 | 0.8571 | 1.0000 | 0.4286 | 0.5714 | 0.7143 | 0.4286 | 0.5714 | 0.7143 | 0.0000 | 0.1429 | 0.2857 | benefit type |
| Flexibility | 0.0426 | 0.6667 | 0.8333 | 1.0000 | 0.0000 | 0.1667 | 0.3333 | 0.3333 | 0.5000 | 0.6667 | 0.6667 | 0.8333 | 1.0000 | benefit type |
| Company Image | 0.0831 | 0.3333 | 0.5000 | 0.6667 | 0.6667 | 0.8333 | 1.0000 | 0.6667 | 0.8333 | 1.0000 | 0.0000 | 0.1667 | 0.3333 | benefit type |
| Skill req | 0.1139 | 0.0000 | 0.2500 | 0.5000 | 0.5000 | 0.7500 | 1.0000 | 0.0000 | 0.2500 | 0.5000 | 0.0000 | 0.2500 | 0.5000 | benefit type |

*Table 21: Weighted normalised hybrid information decision-making matrix.*

| Criteria | Global crisp weightings | MD | | | FO with regeneration | | | OARO | | | EFC | | |
|---|---|---|---|---|---|---|---|---|---|---|---|---|---|
| Capital Cost | 0.1666 | 0.1666 | | | 0.0833 | | | 0.0208 | | | 0.0000 | | |
| Production Cost | 0.1208 | 0.0840 | | | 0.1208 | | | 0.0000 | | | 0.0669 | | |
| TDS Limitation | 0.1346 | 0.1346 | 0.1346 | | 0.0000 | 0.0449 | | 0.0064 | 0.0064 | | 0.1346 | 0.1346 | |
| Energy consumption | 0.2121 | 0.1206 | 0.1612 | | 0.1936 | 0.2080 | | 0.1903 | 0.2092 | | 0.0000 | 0.2121 | |
| Footprint | 0.0566 | 0.0189 | 0.0566 | | 0.0000 | 0.0377 | | 0.0189 | 0.0377 | | 0.0189 | 0.0566 | |
| Technology maturity | 0.0199 | 0.0066 | 0.0099 | 0.0133 | 0.0000 | 0.0033 | 0.0066 | 0.0000 | 0.0033 | 0.0066 | 0.0133 | 0.0166 | 0.0199 |
| Technology Reliability | 0.0497 | 0.0355 | 0.0426 | 0.0497 | 0.0213 | 0.0284 | 0.0355 | 0.0213 | 0.0284 | 0.0355 | 0.0000 | 0.0071 | 0.0142 |
| Flexibility | 0.0426 | 0.0284 | 0.0355 | 0.0426 | 0.0000 | 0.0071 | 0.0142 | 0.0142 | 0.0213 | 0.0284 | 0.0284 | 0.0355 | 0.0426 |
| Company Image | 0.0831 | 0.0277 | 0.0415 | 0.0554 | 0.0554 | 0.0692 | 0.0831 | 0.0554 | 0.0692 | 0.0831 | 0.0000 | 0.0138 | 0.0277 |
| Skill req | 0.1139 | 0.0000 | 0.0285 | 0.0570 | 0.0570 | 0.0854 | 0.1139 | 0.0000 | 0.0285 | 0.0570 | 0.0000 | 0.0285 | 0.0570 |

## 8.2 Frequency distribution graphs

The frequency distribution graphs shown in the following 2 sections are a visual representation of the final rankings of each of the 10,000 Monte Carlo simulations conducted for each input type and input location.

### 8.2.1 Varying Global Interval Weightings Directly

#### 8.2.1.1 Triangular Input Distribution

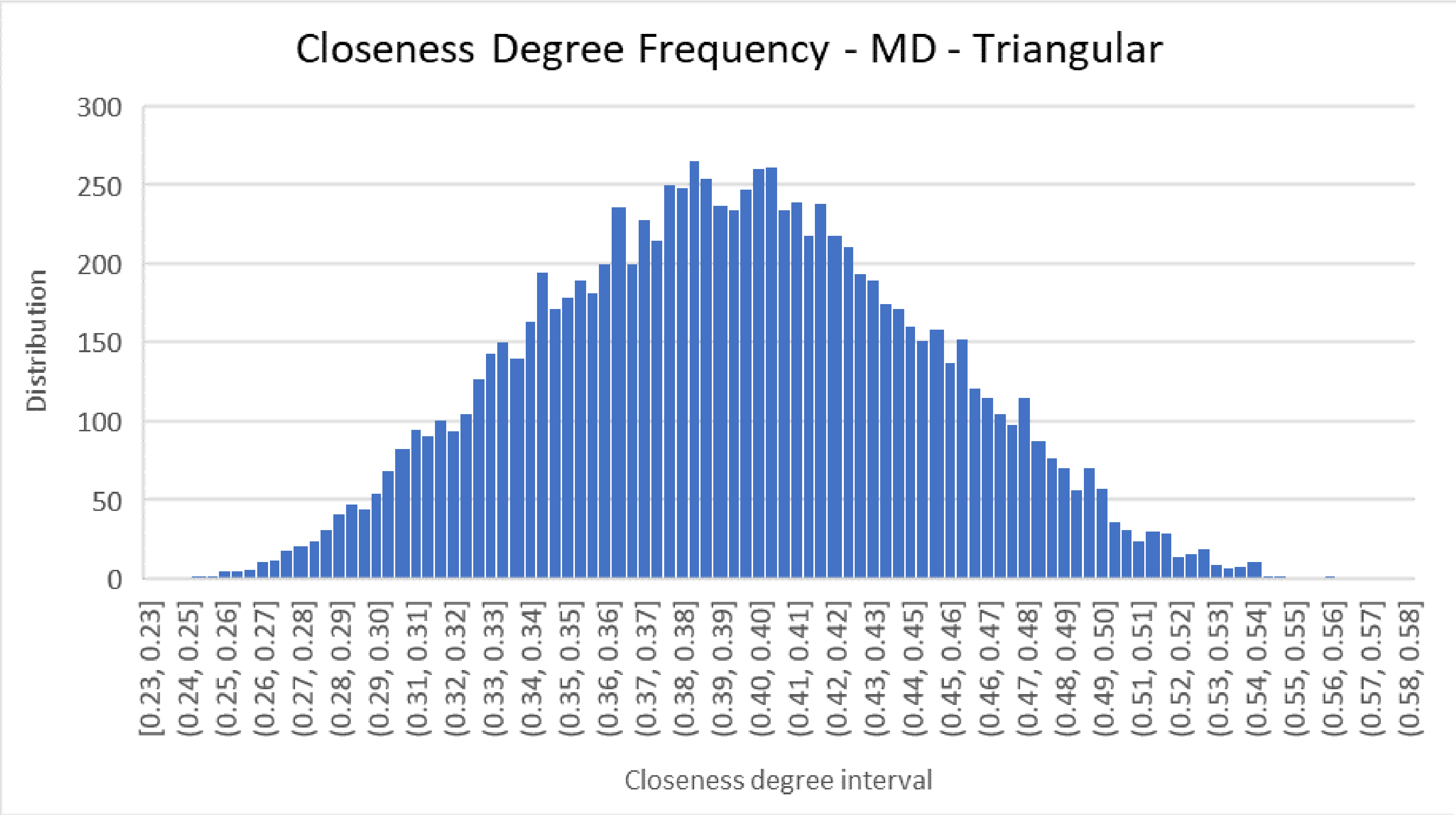

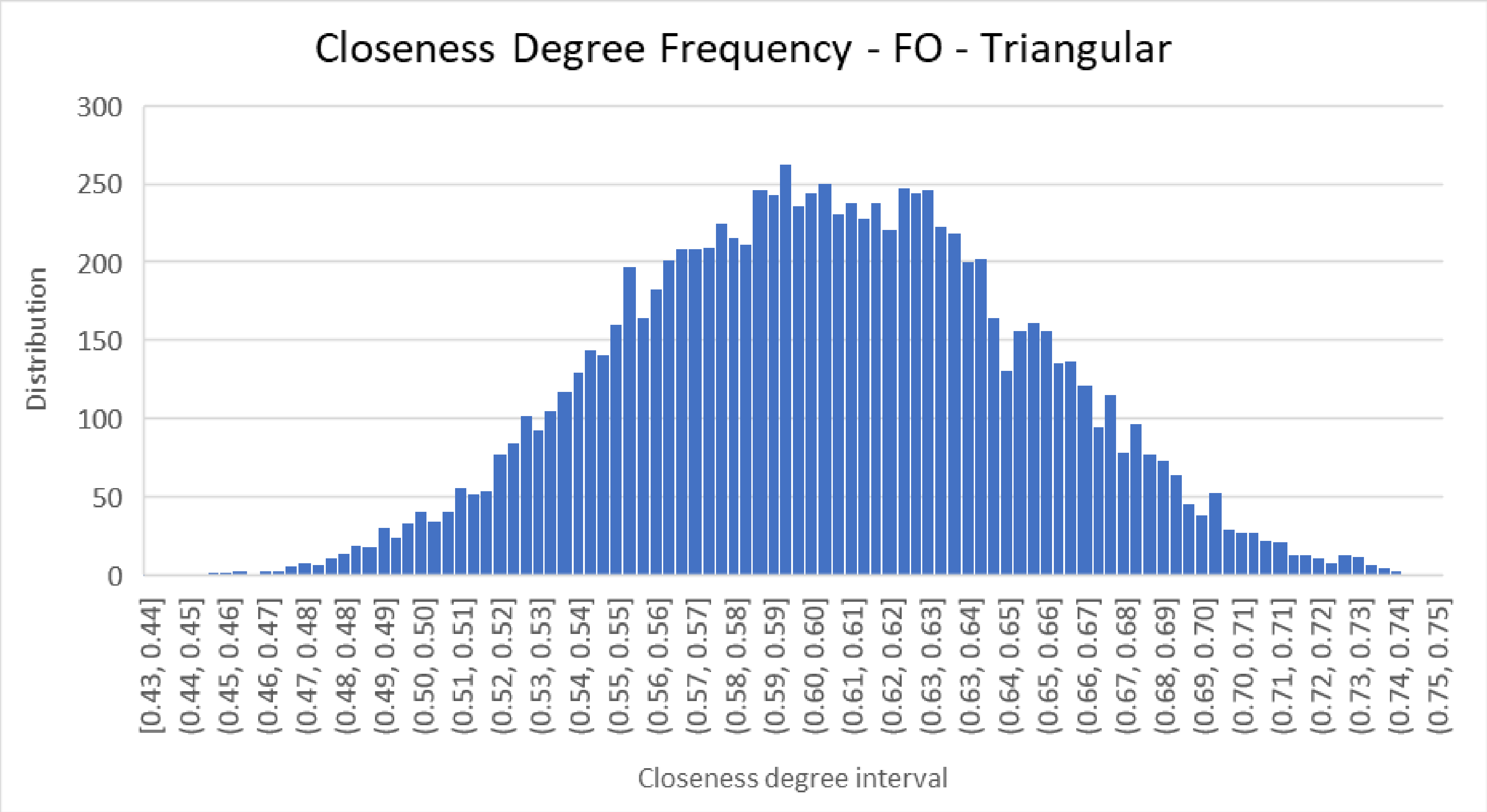

Closeness Degree Frequency - FO - Triangular
Distribution
300
250
200
150
100
50
0
[0.43, 0.44]
(0.44, 0.45]
(0.45, 0.46]
(0.46, 0.47]
(0.47, 0.48]
(0.48, 0.48]
(0.49, 0.49]
(0.50, 0.50]
(0.51, 0.51]
(0.52, 0.52]
(0.53, 0.53]
(0.54, 0.54]
(0.55, 0.55]
(0.56, 0.56]
(0.57, 0.57]
(0.58, 0.58]
(0.59, 0.59]
(0.60, 0.60]
(0.61, 0.61]
(0.62, 0.62]
(0.63, 0.63]
(0.63, 0.64]
(0.64, 0.65]
(0.65, 0.66]
(0.66, 0.67]
(0.67, 0.68]
(0.68, 0.69]
(0.69, 0.70]
(0.70, 0.71]
(0.71, 0.71]
(0.72, 0.72]
(0.73, 0.73]
(0.74, 0.74]
(0.75, 0.75]
Closeness degree interval

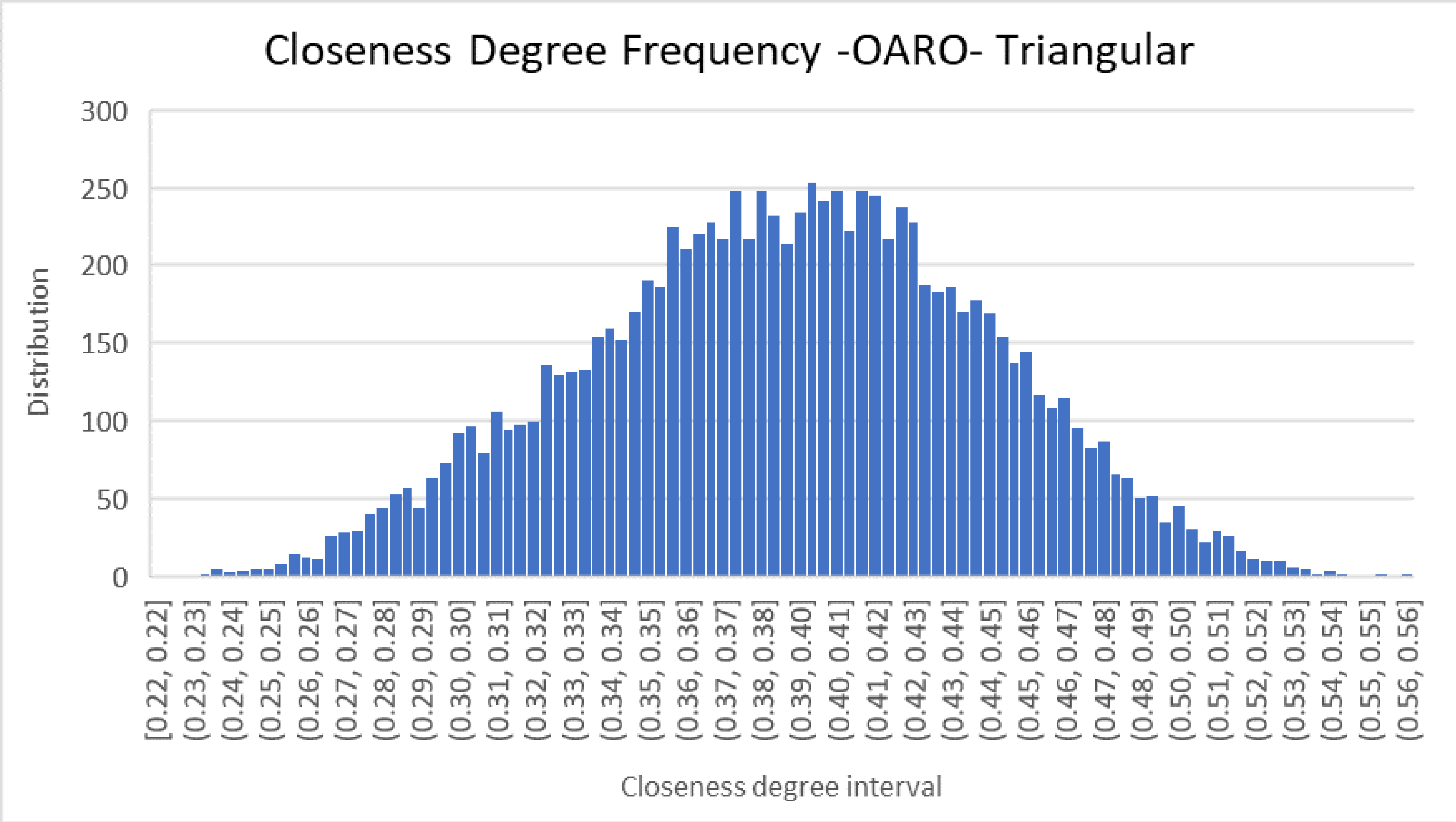
Closeness Degree Frequency -OARO- Triangular
Distribution
300
250
200
150
100
50
0
[0.22, 0.22]
(0.23, 0.23]
(0.24, 0.24]
(0.25, 0.25]
(0.26, 0.26]
(0.27, 0.27]
(0.28, 0.28]
(0.29, 0.29]
(0.30, 0.30]
(0.31, 0.31]
(0.32, 0.32]
(0.33, 0.33]
(0.34, 0.34]
(0.35, 0.35]
(0.36, 0.36]
(0.37, 0.37]
(0.38, 0.38]
(0.39, 0.40]
(0.40, 0.41]
(0.41, 0.42]
(0.42, 0.43]
(0.43, 0.44]
(0.44, 0.45]
(0.45, 0.46]
(0.46, 0.47]
(0.47, 0.48]
(0.48, 0.49]
(0.50, 0.50]
(0.51, 0.51]
(0.52, 0.52]
(0.53, 0.53]
(0.54, 0.54]
(0.55, 0.55]
(0.56, 0.56]
Closeness degree interval

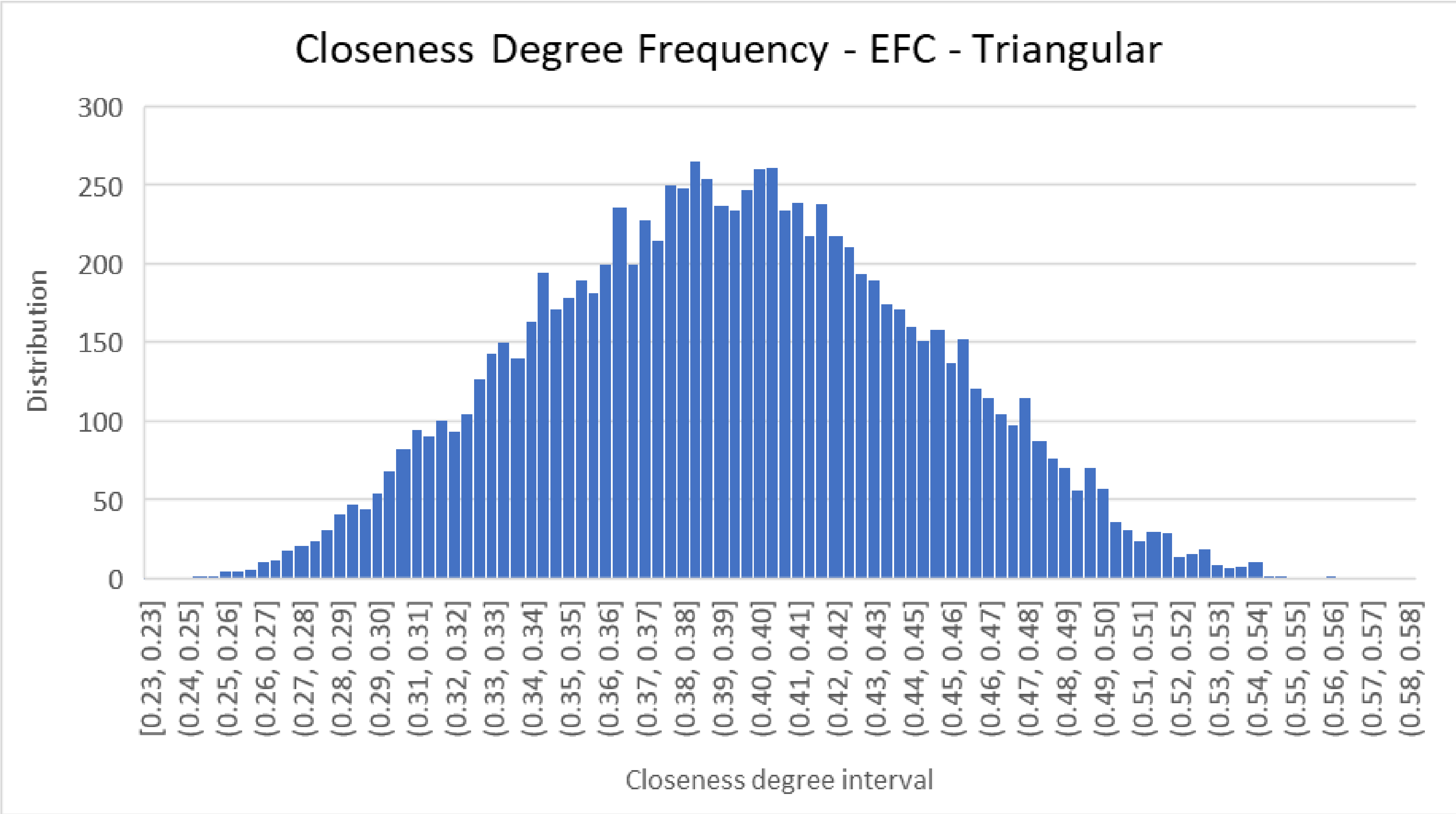
Closeness Degree Frequency - EFC - Triangular
Distribution
300
250
200
150
100
50
0
[0.23, 0.23]
(0.24, 0.25]
(0.25, 0.26]
(0.26, 0.27]
(0.27, 0.28]
(0.28, 0.29]
(0.29, 0.30]
(0.30, 0.31]
(0.31, 0.31]
(0.32, 0.32]
(0.33, 0.33]
(0.34, 0.34]
(0.35, 0.35]
(0.36, 0.36]
(0.37, 0.37]
(0.38, 0.38]
(0.39, 0.39]
(0.40, 0.40]
(0.41, 0.41]
(0.42, 0.42]
(0.43, 0.43]
(0.44, 0.45]
(0.45, 0.46]
(0.46, 0.47]
(0.47, 0.48]
(0.48, 0.49]
(0.49, 0.50]
(0.51, 0.51]
(0.52, 0.52]
(0.53, 0.53]
(0.54, 0.54]
(0.55, 0.55]
(0.56, 0.56]
(0.57, 0.57]
(0.58, 0.58]
Closeness degree interval

8.2.1.2 Uniform Input Distribution

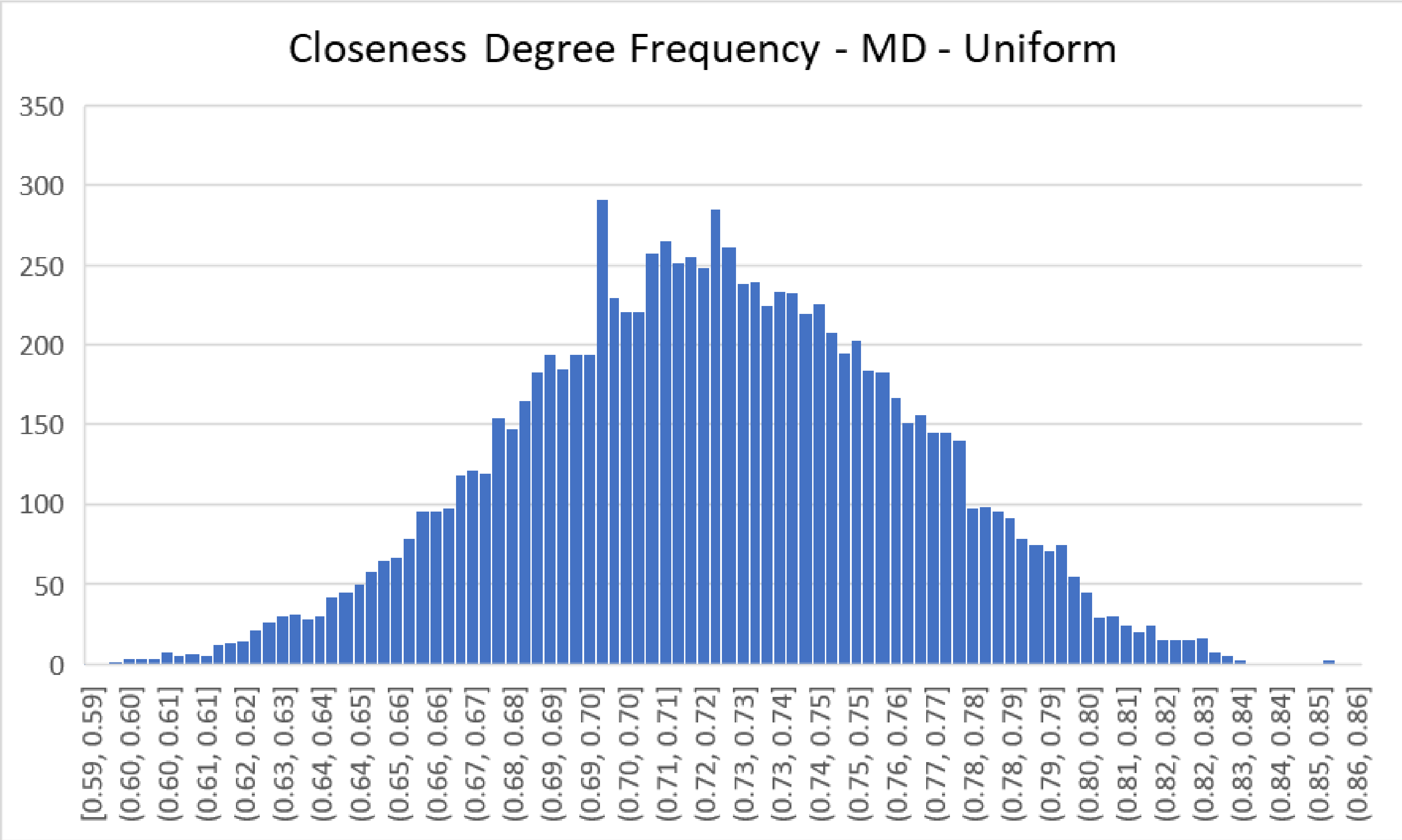

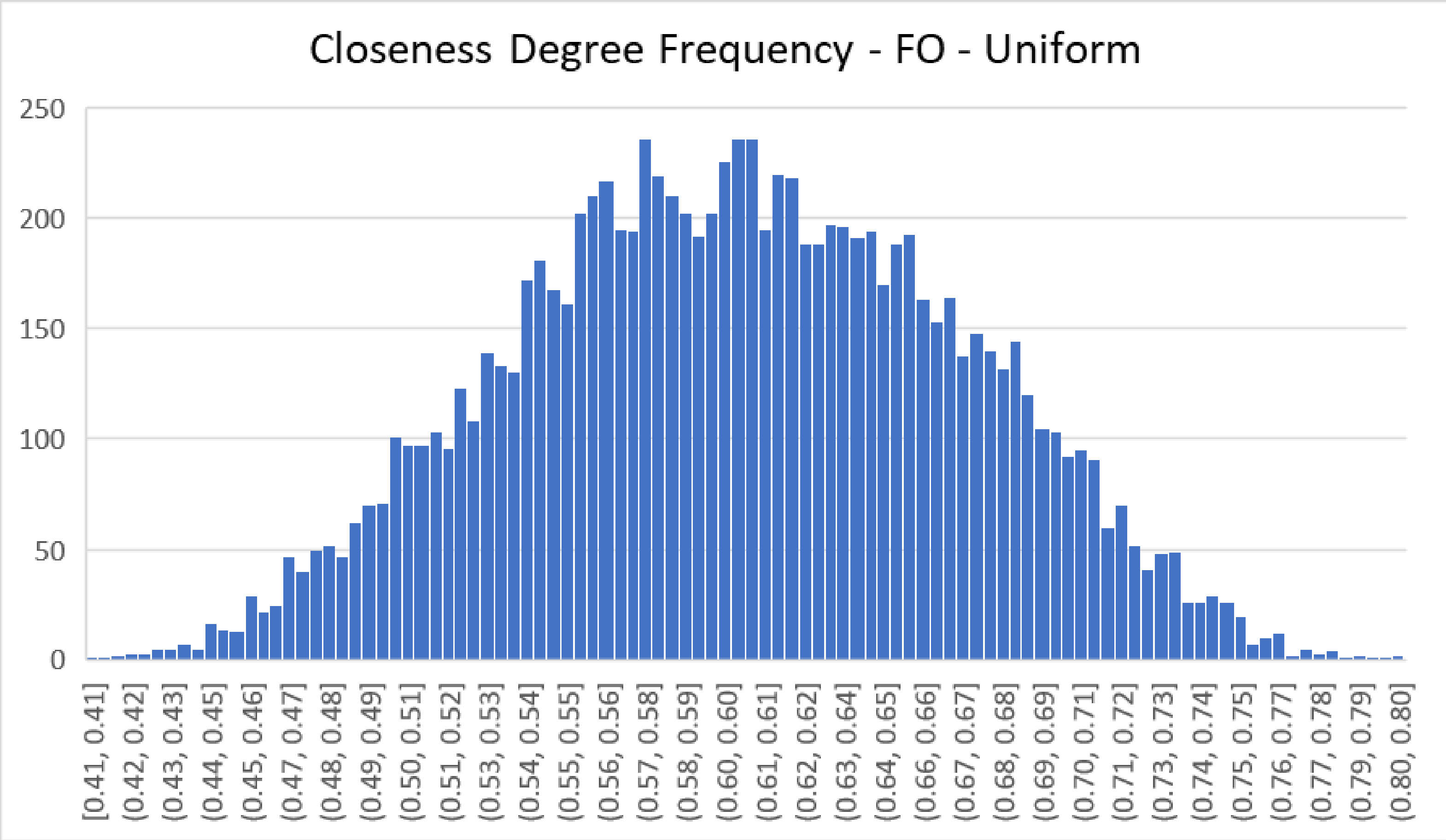
Closeness Degree Frequency - FO - Uniform
250
200
150
100
50
0
[0.41, 0.41]
(0.42, 0.42]
(0.43, 0.43]
(0.44, 0.45]
(0.45, 0.46]
(0.47, 0.47]
(0.48, 0.48]
(0.49, 0.49]
(0.50, 0.51]
(0.51, 0.52]
(0.53, 0.53]
(0.54, 0.54]
(0.55, 0.55]
(0.56, 0.56]
(0.57, 0.58]
(0.58, 0.59]
(0.60, 0.60]
(0.61, 0.61]
(0.62, 0.62]
(0.63, 0.64]
(0.64, 0.65]
(0.66, 0.66]
(0.67, 0.67]
(0.68, 0.68]
(0.69, 0.69]
(0.70, 0.71]
(0.71, 0.72]
(0.73, 0.73]
(0.74, 0.74]
(0.75, 0.75]
(0.76, 0.77]
(0.77, 0.78]
(0.79, 0.79]
(0.80, 0.80]

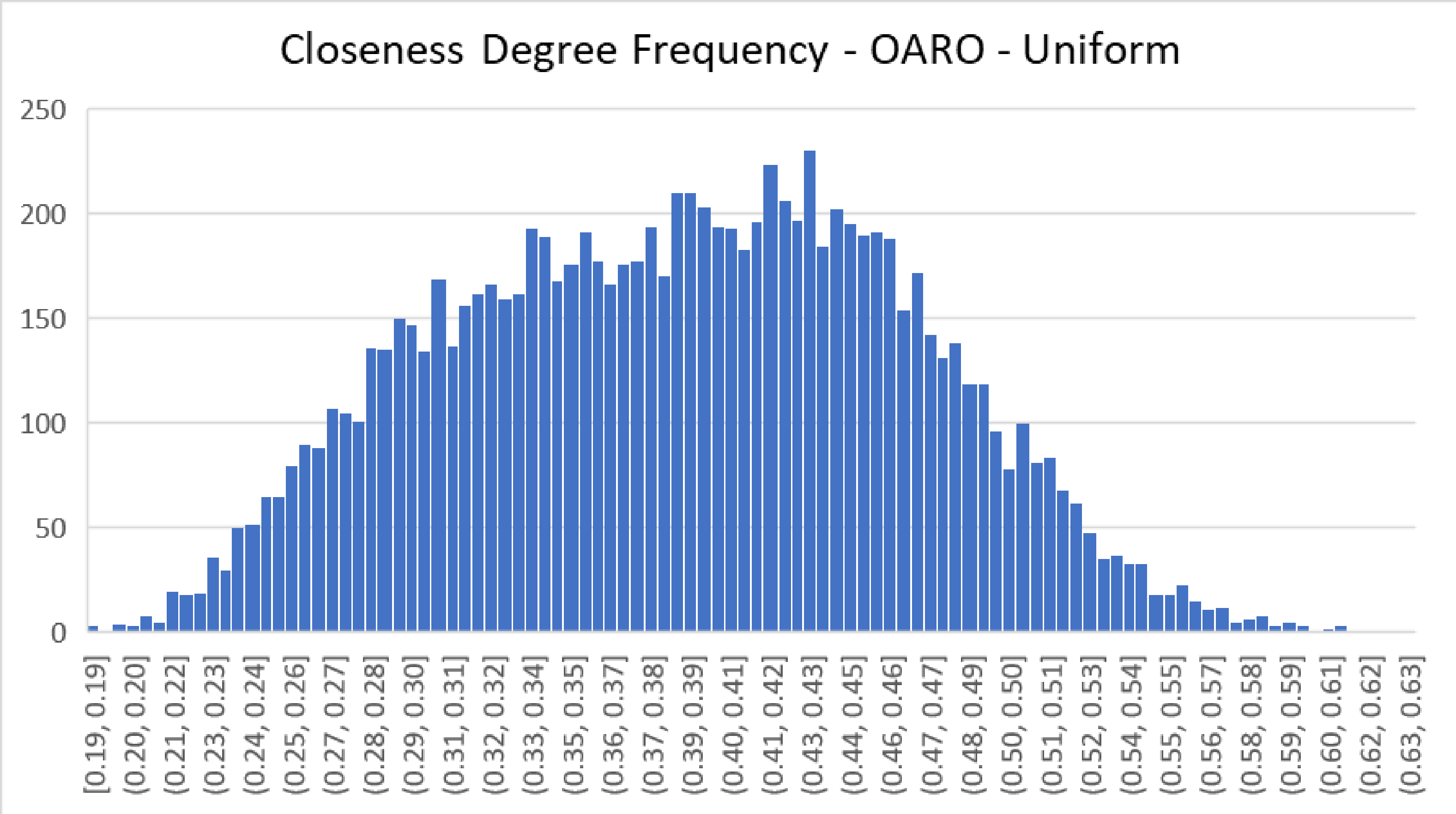
Closeness Degree Frequency - OARO - Uniform
250
200
150
100
50
0
[0.19, 0.19]
(0.20, 0.20]
(0.21, 0.22]
(0.23, 0.23]
(0.24, 0.24]
(0.25, 0.26]
(0.27, 0.27]
(0.28, 0.28]
(0.29, 0.30]
(0.31, 0.31]
(0.32, 0.32]
(0.33, 0.34]
(0.35, 0.35]
(0.36, 0.37]
(0.37, 0.38]
(0.39, 0.39]
(0.40, 0.41]
(0.41, 0.42]
(0.43, 0.43]
(0.44, 0.45]
(0.46, 0.46]
(0.47, 0.47]
(0.48, 0.49]
(0.50, 0.50]
(0.51, 0.51]
(0.52, 0.53]
(0.54, 0.54]
(0.55, 0.55]
(0.56, 0.57]
(0.58, 0.58]
(0.59, 0.59]
(0.60, 0.61]
(0.62, 0.62]
(0.63, 0.63]

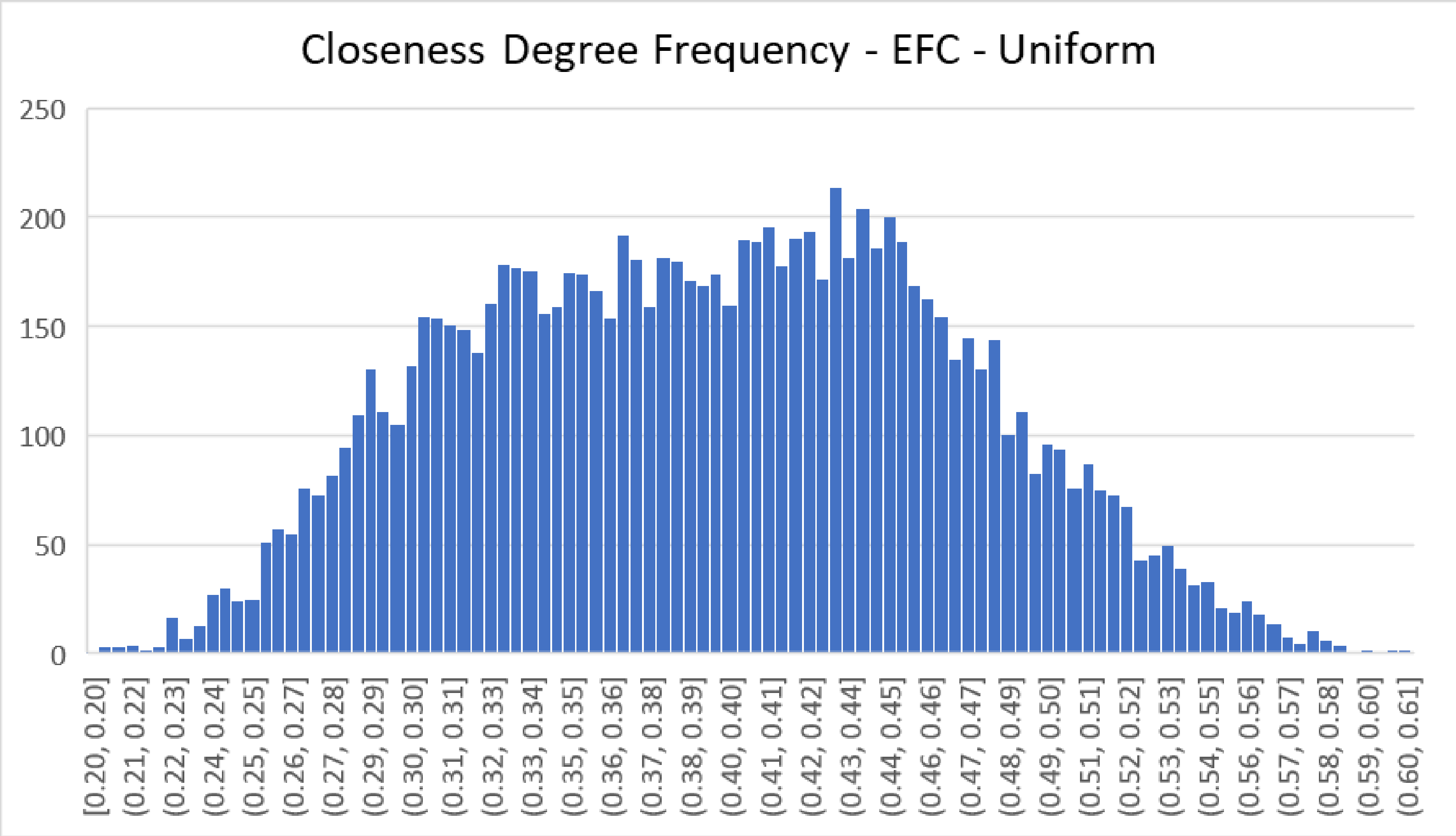
Closeness Degree Frequency - EFC - Uniform
250
200
150
100
50
0
[0.20, 0.20]
(0.21, 0.22]
(0.22, 0.23]
(0.24, 0.24]
(0.25, 0.25]
(0.26, 0.27]
(0.27, 0.28]
(0.29, 0.29]
(0.30, 0.30]
(0.31, 0.31]
(0.32, 0.33]
(0.33, 0.34]
(0.35, 0.35]
(0.36, 0.36]
(0.37, 0.38]
(0.38, 0.39]
(0.40, 0.40]
(0.41, 0.41]
(0.42, 0.42]
(0.43, 0.44]
(0.44, 0.45]
(0.46, 0.46]
(0.47, 0.47]
(0.48, 0.49]
(0.49, 0.50]
(0.51, 0.51]
(0.52, 0.52]
(0.53, 0.53]
(0.54, 0.55]
(0.56, 0.56]
(0.57, 0.57]
(0.58, 0.58]
(0.59, 0.60]
(0.60, 0.61]

#### 8.2.1.3 Normal input Distribution

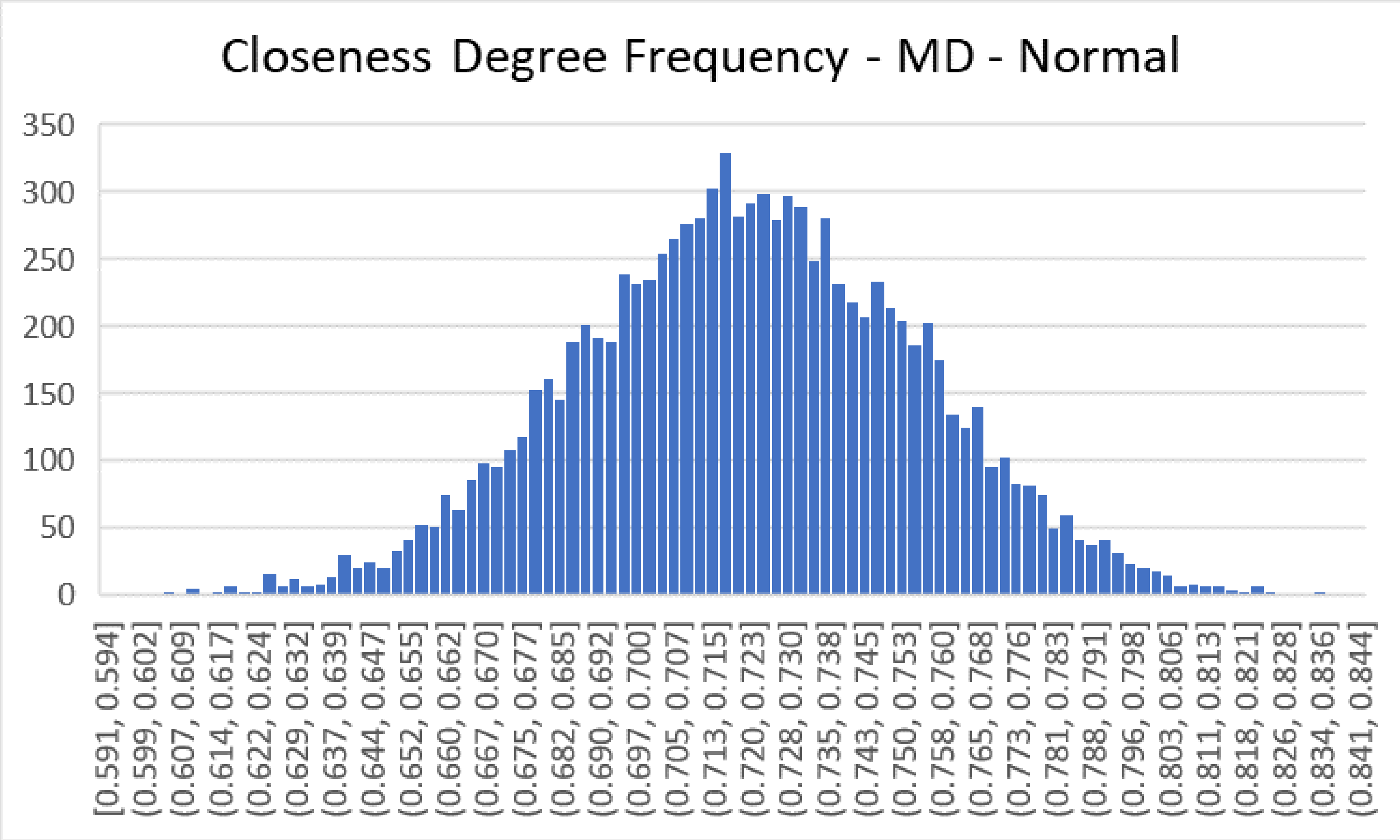

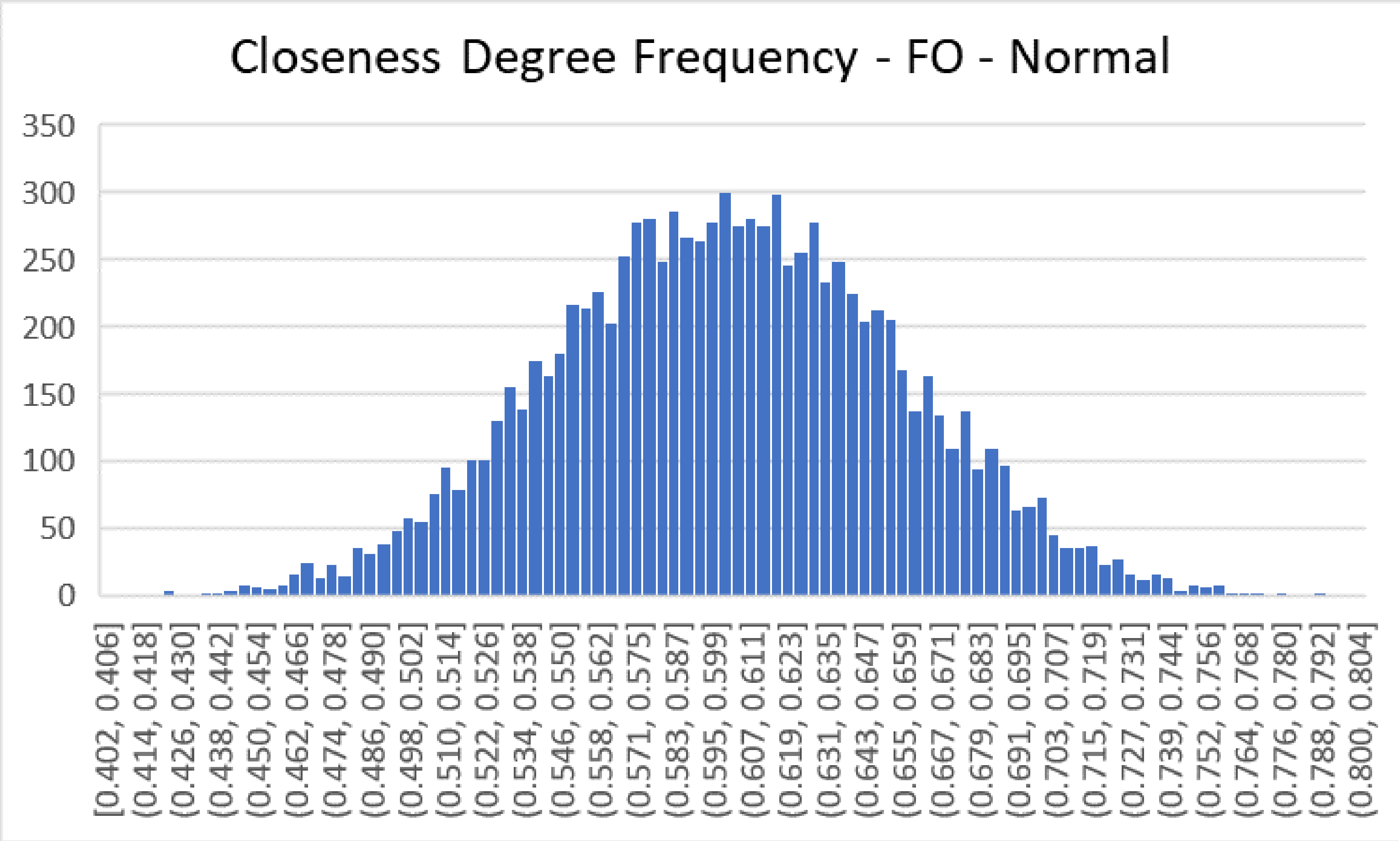
Closeness Degree Frequency - FO - Normal
0
50
100
150
200
250
300
350
[0.402, 0.406]
(0.414, 0.418]
(0.426, 0.430]
(0.438, 0.442]
(0.450, 0.454]
(0.462, 0.466]
(0.474, 0.478]
(0.486, 0.490]
(0.498, 0.502]
(0.510, 0.514]
(0.522, 0.526]
(0.534, 0.538]
(0.546, 0.550]
(0.558, 0.562]
(0.571, 0.575]
(0.583, 0.587]
(0.595, 0.599]
(0.607, 0.611]
(0.619, 0.623]
(0.631, 0.635]
(0.643, 0.647]
(0.655, 0.659]
(0.667, 0.671]
(0.679, 0.683]
(0.691, 0.695]
(0.703, 0.707]
(0.715, 0.719]
(0.727, 0.731]
(0.739, 0.744]
(0.752, 0.756]
(0.764, 0.768]
(0.776, 0.780]
(0.788, 0.792]
(0.800, 0.804]

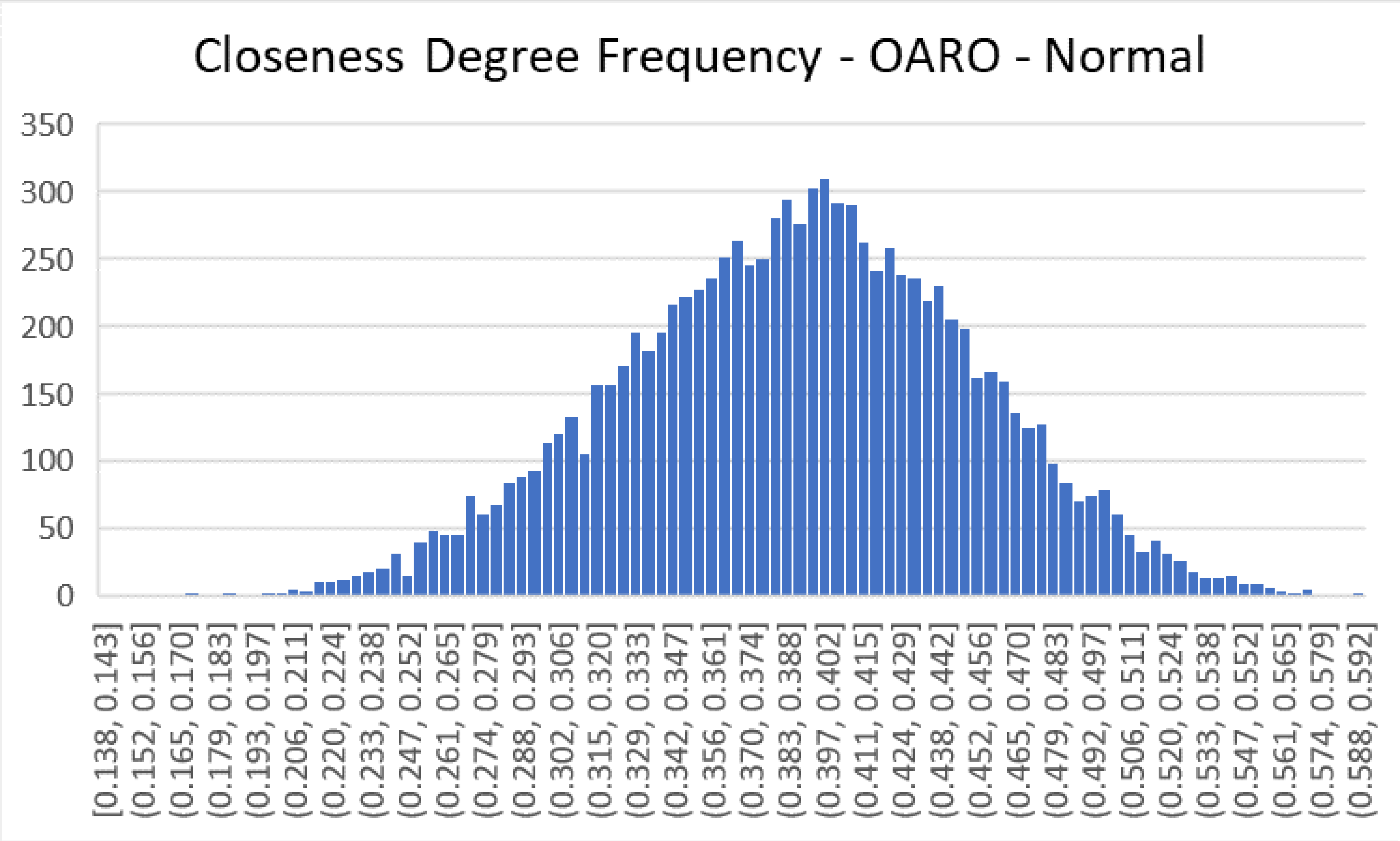
Closeness Degree Frequency - OARO - Normal
350
300
250
200
150
100
50
0
[0.138, 0.143]
(0.152, 0.156]
(0.165, 0.170]
(0.179, 0.183]
(0.193, 0.197]
(0.206, 0.211]
(0.220, 0.224]
(0.233, 0.238]
(0.247, 0.252]
(0.261, 0.265]
(0.274, 0.279]
(0.288, 0.293]
(0.302, 0.306]
(0.315, 0.320]
(0.329, 0.333]
(0.342, 0.347]
(0.356, 0.361]
(0.370, 0.374]
(0.383, 0.388]
(0.397, 0.402]
(0.411, 0.415]
(0.424, 0.429]
(0.438, 0.442]
(0.452, 0.456]
(0.465, 0.470]
(0.479, 0.483]
(0.492, 0.497]
(0.506, 0.511]
(0.520, 0.524]
(0.533, 0.538]
(0.547, 0.552]
(0.561, 0.565]
(0.574, 0.579]
(0.588, 0.592]

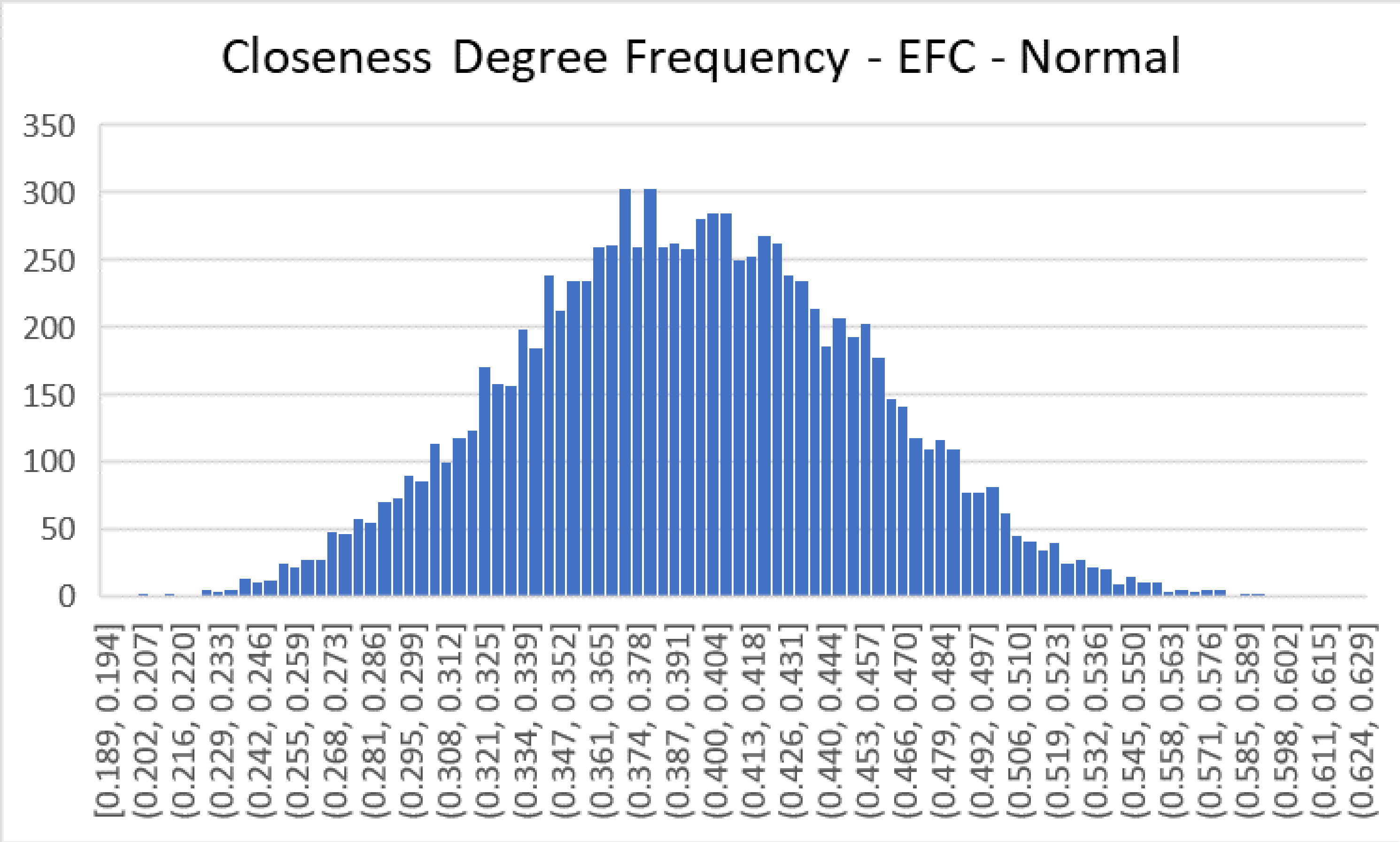
Closeness Degree Frequency - EFC - Normal
350
300
250
200
150
100
50
0
[0.189, 0.194]
(0.202, 0.207]
(0.216, 0.220]
(0.229, 0.233]
(0.242, 0.246]
(0.255, 0.259]
(0.268, 0.273]
(0.281, 0.286]
(0.295, 0.299]
(0.308, 0.312]
(0.321, 0.325]
(0.334, 0.339]
(0.347, 0.352]
(0.361, 0.365]
(0.374, 0.378]
(0.387, 0.391]
(0.400, 0.404]
(0.413, 0.418]
(0.426, 0.431]
(0.440, 0.444]
(0.453, 0.457]
(0.466, 0.470]
(0.479, 0.484]
(0.492, 0.497]
(0.506, 0.510]
(0.519, 0.523]
(0.532, 0.536]
(0.545, 0.550]
(0.558, 0.563]
(0.571, 0.576]
(0.585, 0.589]
(0.598, 0.602]
(0.611, 0.615]
(0.624, 0.629]

### 8.2.2 Distribution of simulation closeness degree results while only varying the economic aspect

#### 8.2.2.1 Normal input Distribution

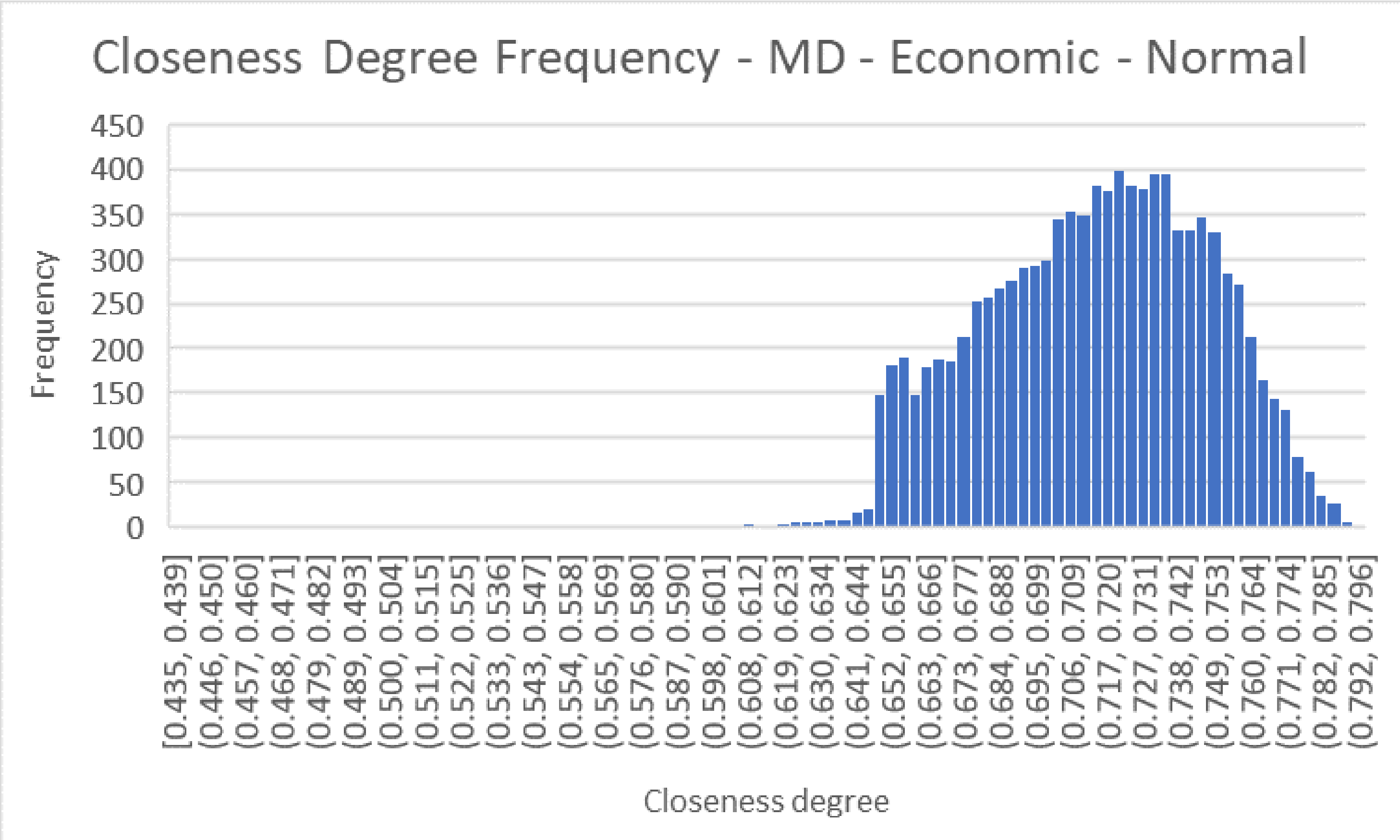

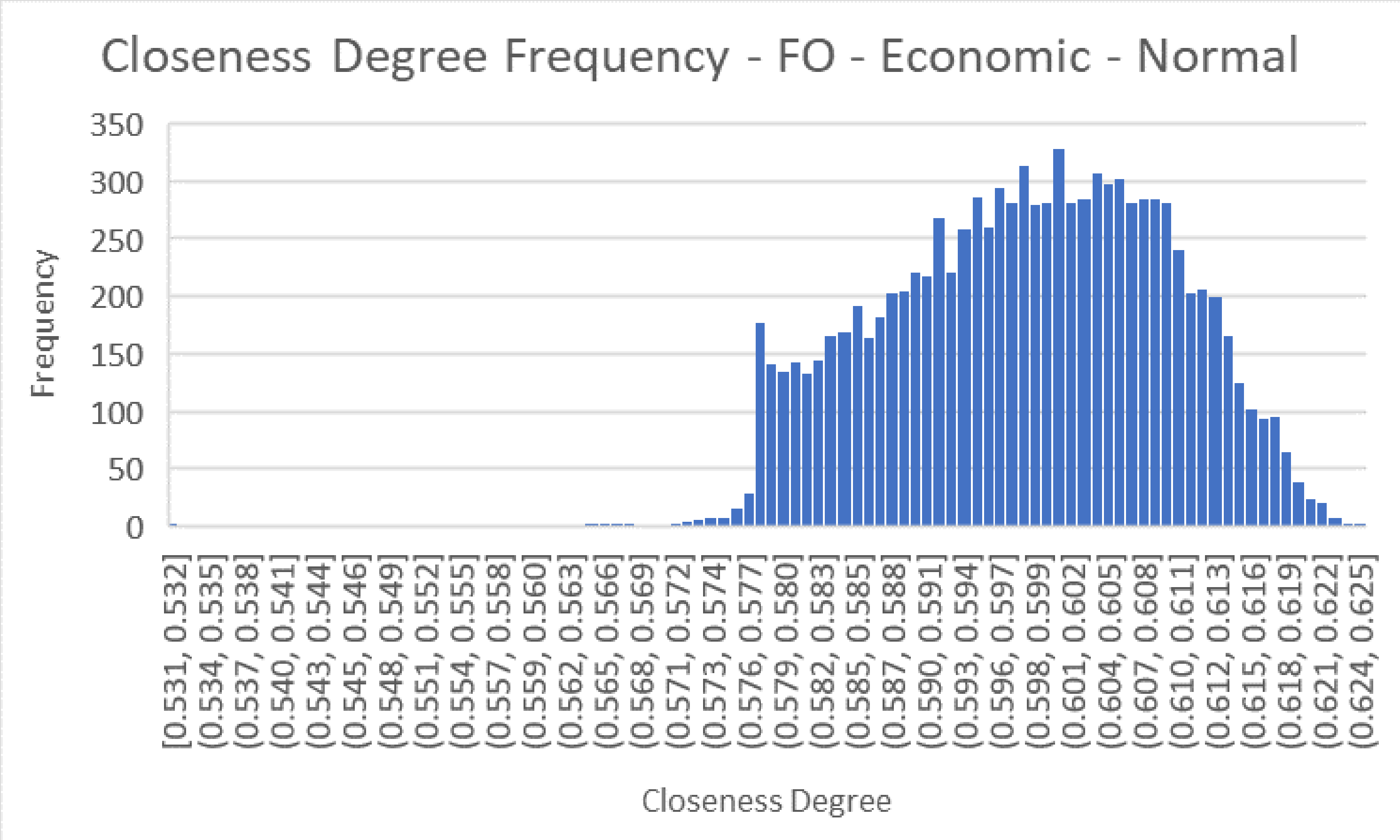
Closeness Degree Frequency - FO - Economic - Normal
Frequency
Closeness Degree
0
50
100
150
200
250
300
350
[0.531, 0.532]
(0.534, 0.535]
(0.537, 0.538]
(0.540, 0.541]
(0.543, 0.544]
(0.545, 0.546]
(0.548, 0.549]
(0.551, 0.552]
(0.554, 0.555]
(0.557, 0.558]
(0.559, 0.560]
(0.562, 0.563]
(0.565, 0.566]
(0.568, 0.569]
(0.571, 0.572]
(0.573, 0.574]
(0.576, 0.577]
(0.579, 0.580]
(0.582, 0.583]
(0.585, 0.585]
(0.587, 0.588]
(0.590, 0.591]
(0.593, 0.594]
(0.596, 0.597]
(0.598, 0.599]
(0.601, 0.602]
(0.604, 0.605]
(0.607, 0.608]
(0.610, 0.611]
(0.612, 0.613]
(0.615, 0.616]
(0.618, 0.619]
(0.621, 0.622]
(0.624, 0.625]

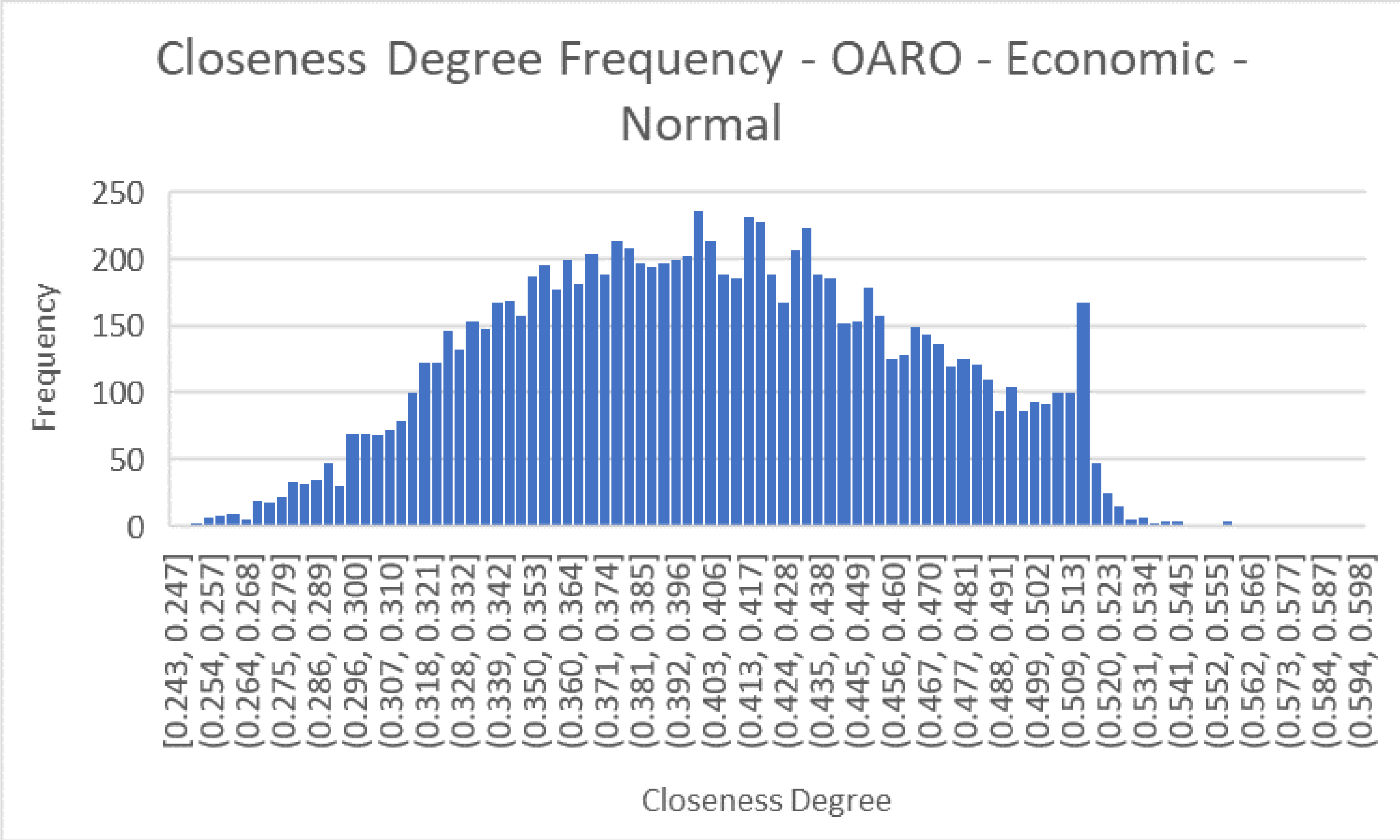

Closeness Degree Frequency - OARO - Economic - Normal
Frequency
0
50
100
150
200
250
[0.243, 0.247]
(0.254, 0.257]
(0.264, 0.268]
(0.275, 0.279]
(0.286, 0.289]
(0.296, 0.300]
(0.307, 0.310]
(0.318, 0.321]
(0.328, 0.332]
(0.339, 0.342]
(0.350, 0.353]
(0.360, 0.364]
(0.371, 0.374]
(0.381, 0.385]
(0.392, 0.396]
(0.403, 0.406]
(0.413, 0.417]
(0.424, 0.428]
(0.435, 0.438]
(0.445, 0.449]
(0.456, 0.460]
(0.467, 0.470]
(0.477, 0.481]
(0.488, 0.491]
(0.499, 0.502]
(0.509, 0.513]
(0.520, 0.523]
(0.531, 0.534]
(0.541, 0.545]
(0.552, 0.555]
(0.562, 0.566]
(0.573, 0.577]
(0.584, 0.587]
(0.594, 0.598]
Closeness Degree

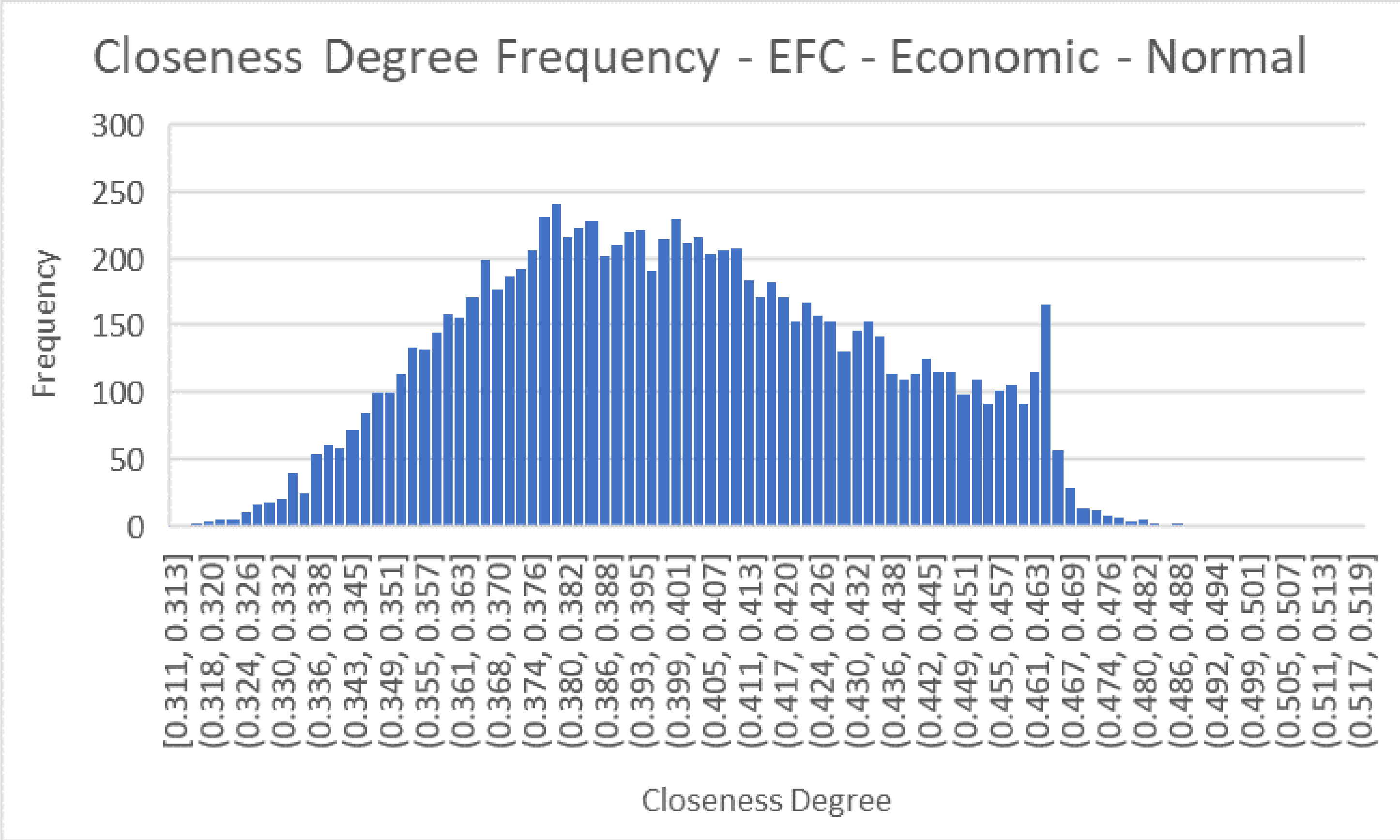

Closeness Degree Frequency - EFC - Economic - Normal
Frequency
Closeness Degree
300
250
200
150
100
50
0
[0.311, 0.313]
(0.318, 0.320]
(0.324, 0.326]
(0.330, 0.332]
(0.336, 0.338]
(0.343, 0.345]
(0.349, 0.351]
(0.355, 0.357]
(0.361, 0.363]
(0.368, 0.370]
(0.374, 0.376]
(0.380, 0.382]
(0.386, 0.388]
(0.393, 0.395]
(0.399, 0.401]
(0.405, 0.407]
(0.411, 0.413]
(0.417, 0.420]
(0.424, 0.426]
(0.430, 0.432]
(0.436, 0.438]
(0.442, 0.445]
(0.449, 0.451]
(0.455, 0.457]
(0.461, 0.463]
(0.467, 0.469]
(0.474, 0.476]
(0.480, 0.482]
(0.486, 0.488]
(0.492, 0.494]
(0.499, 0.501]
(0.505, 0.507]
(0.511, 0.513]
(0.517, 0.519]

#### 8.2.2.2 Uniform Input Distribution

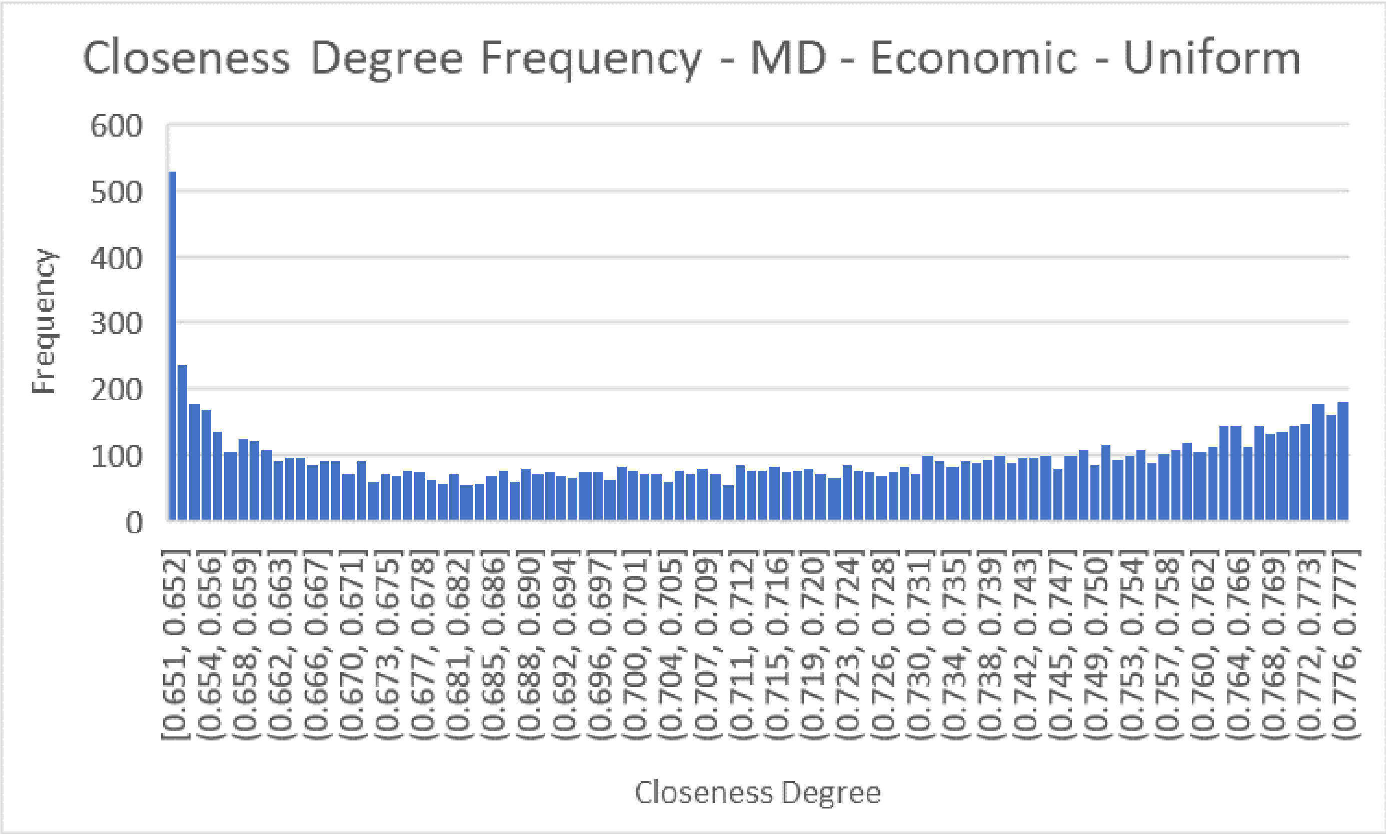

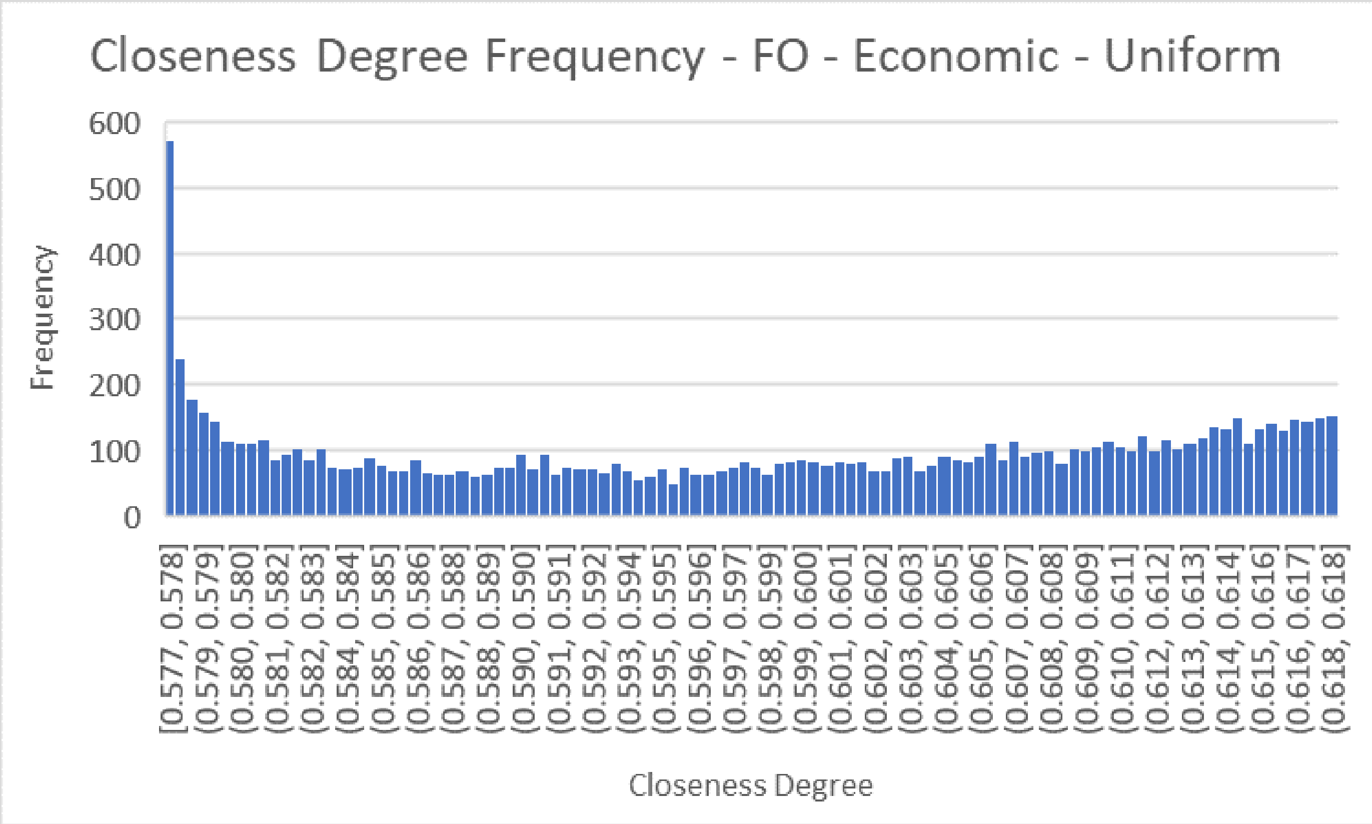
Closeness Degree Frequency - FO - Economic - Uniform
Frequency
Closeness Degree

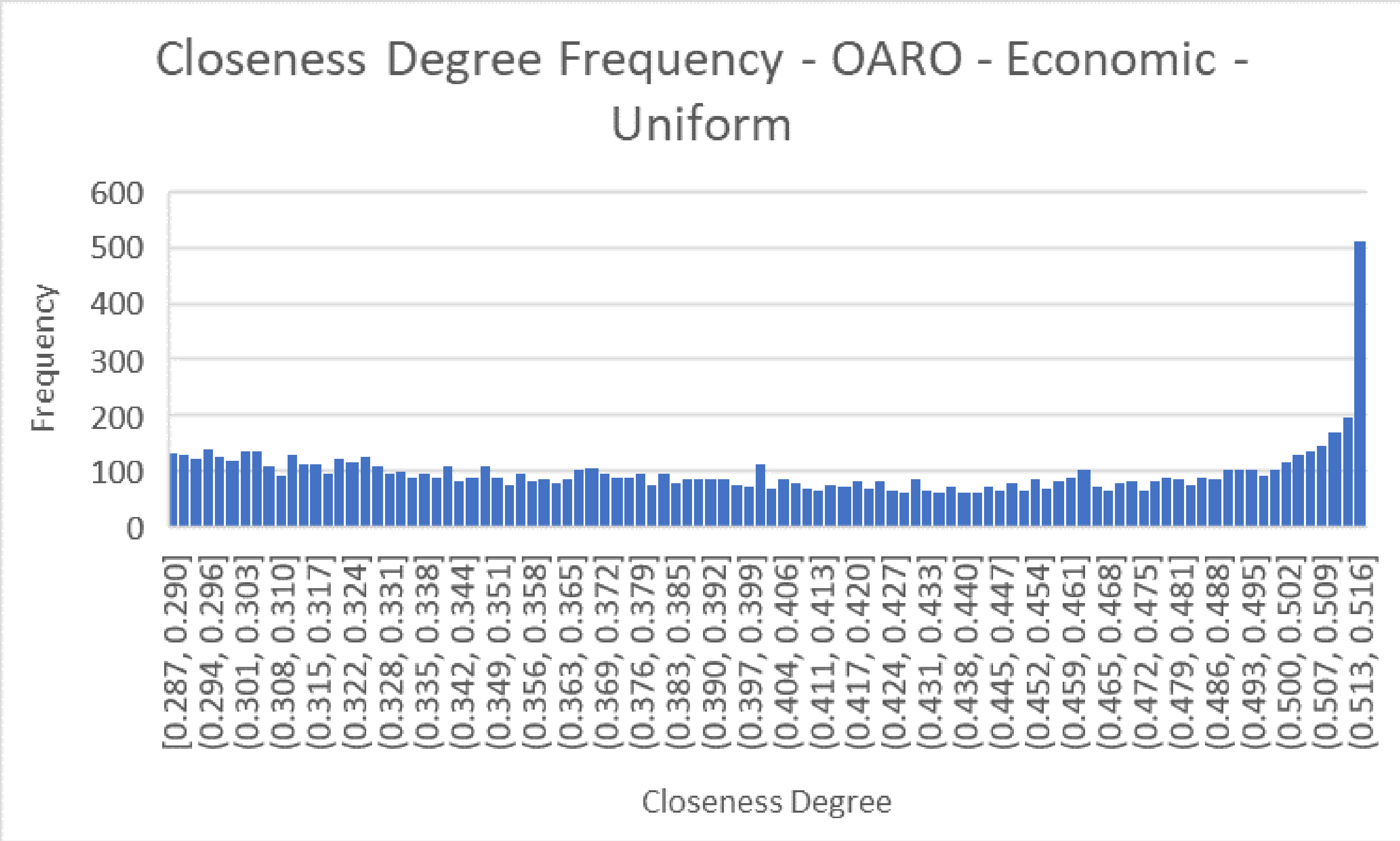
Closeness Degree Frequency - OARO - Economic - Uniform
Frequency
600
500
400
300
200
100
0
Closeness Degree

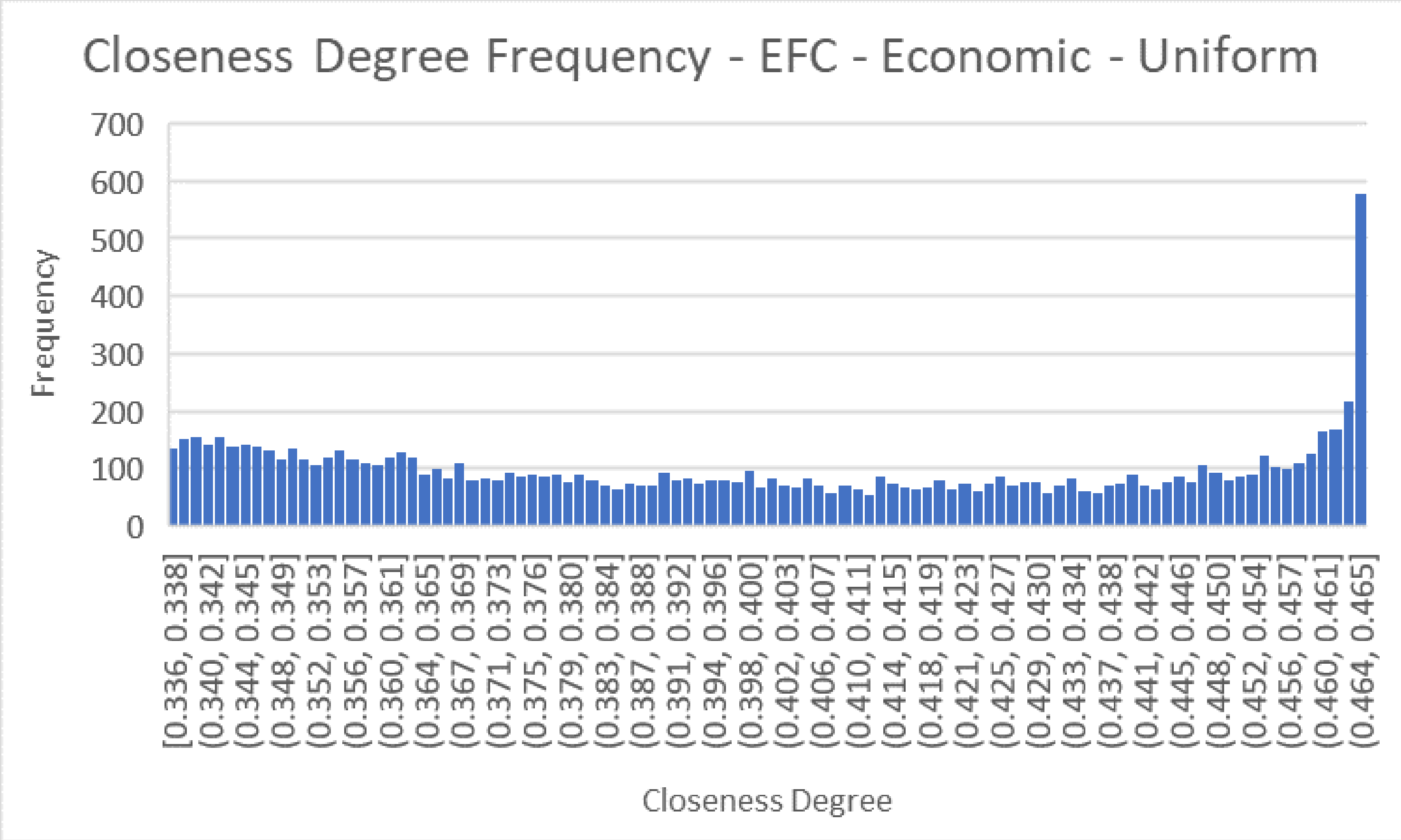
Closeness Degree Frequency - EFC - Economic - Uniform
Frequency
700
600
500
400
300
200
100
0
Closeness Degree

8.2.3 Distribution of simulation closeness degree results while only varying the environmental aspect

8.2.3.1 Normal Input Distribution

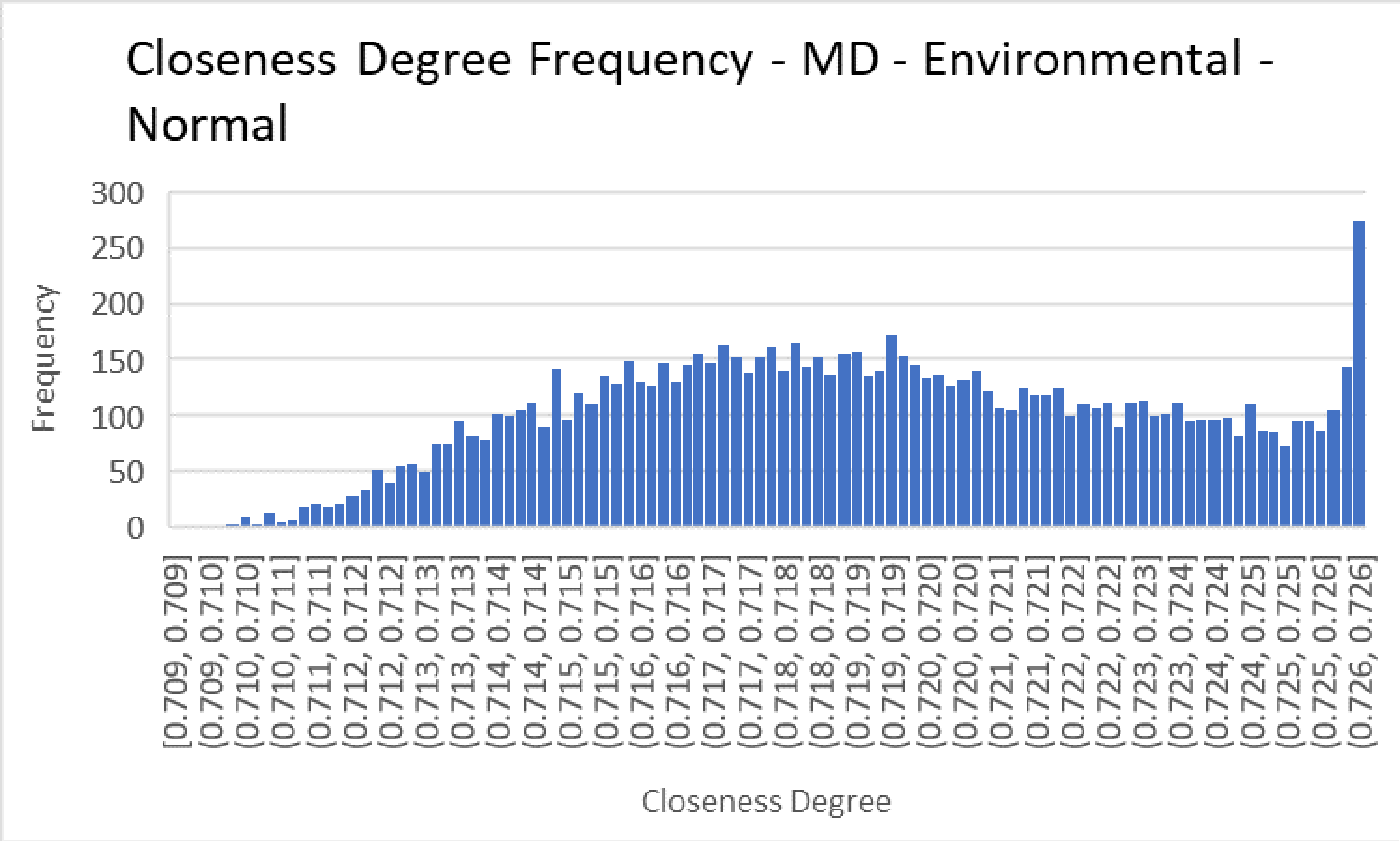

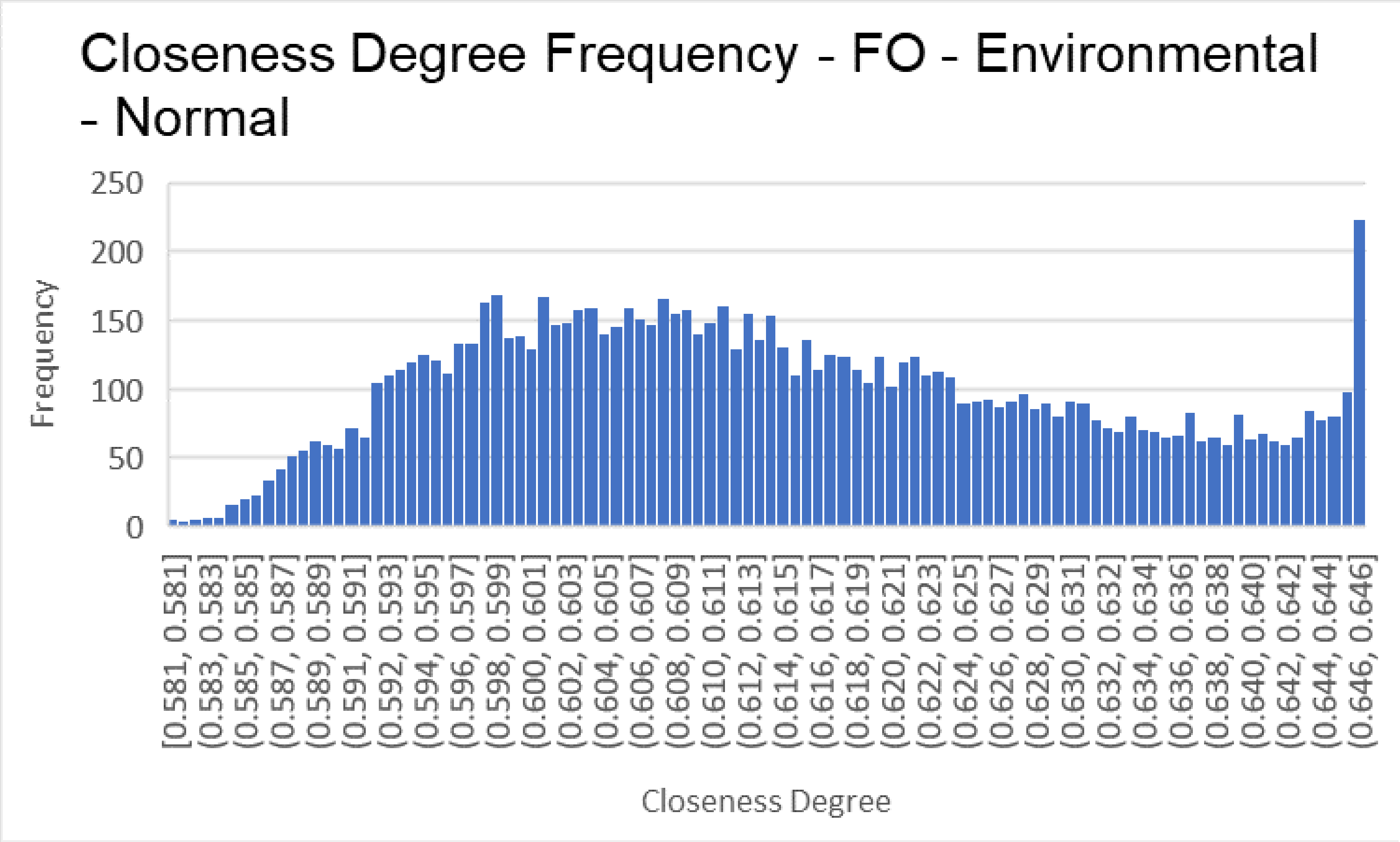
Closeness Degree Frequency - FO - Environmental - Normal
Frequency
250
200
150
100
50
0
[0.581, 0.581]
(0.581, 0.583]
(0.583, 0.585]
(0.585, 0.587]
(0.587, 0.589]
(0.589, 0.591]
(0.591, 0.592]
(0.592, 0.594]
(0.594, 0.596]
(0.596, 0.598]
(0.598, 0.600]
(0.600, 0.602]
(0.602, 0.604]
(0.604, 0.606]
(0.606, 0.608]
(0.608, 0.610]
(0.610, 0.612]
(0.612, 0.614]
(0.614, 0.616]
(0.616, 0.618]
(0.618, 0.620]
(0.620, 0.622]
(0.622, 0.624]
(0.624, 0.626]
(0.626, 0.628]
(0.628, 0.630]
(0.630, 0.632]
(0.632, 0.634]
(0.634, 0.636]
(0.636, 0.638]
(0.638, 0.640]
(0.640, 0.642]
(0.642, 0.644]
(0.644, 0.646]
(0.646, 0.646]
Closeness Degree

Closeness Degree Frequency - OARO - Environmental - Normal

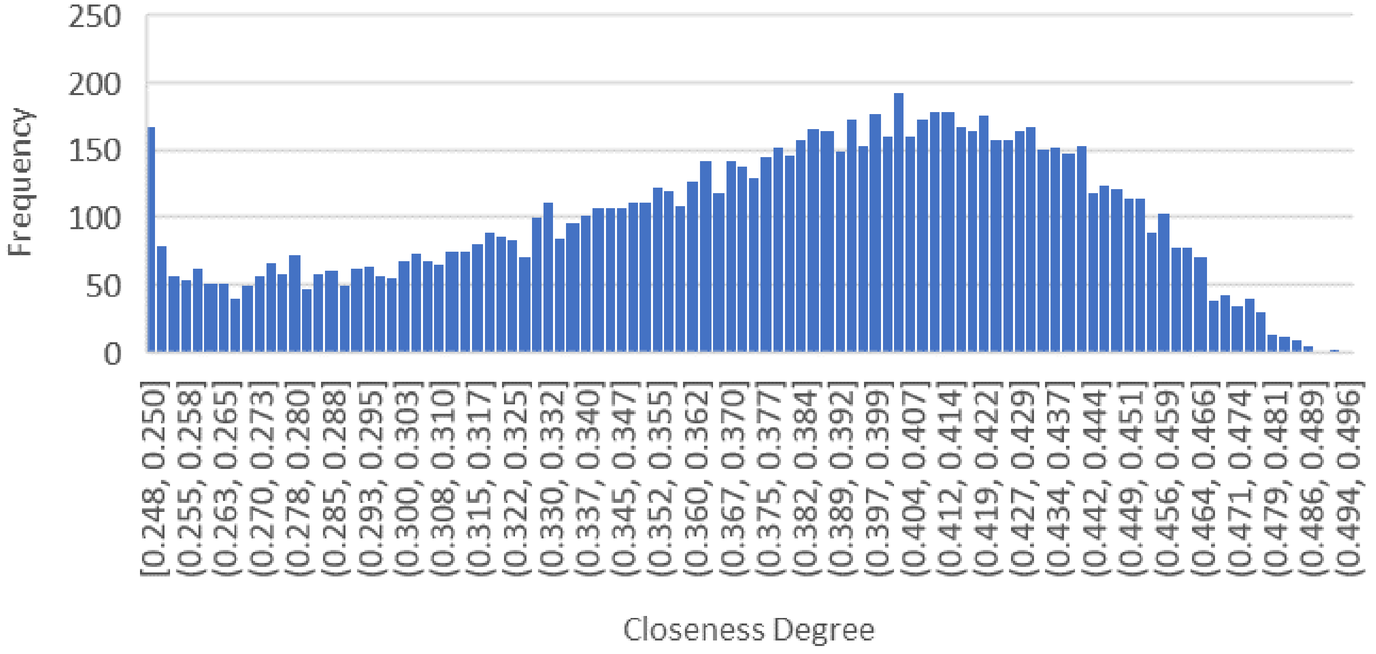

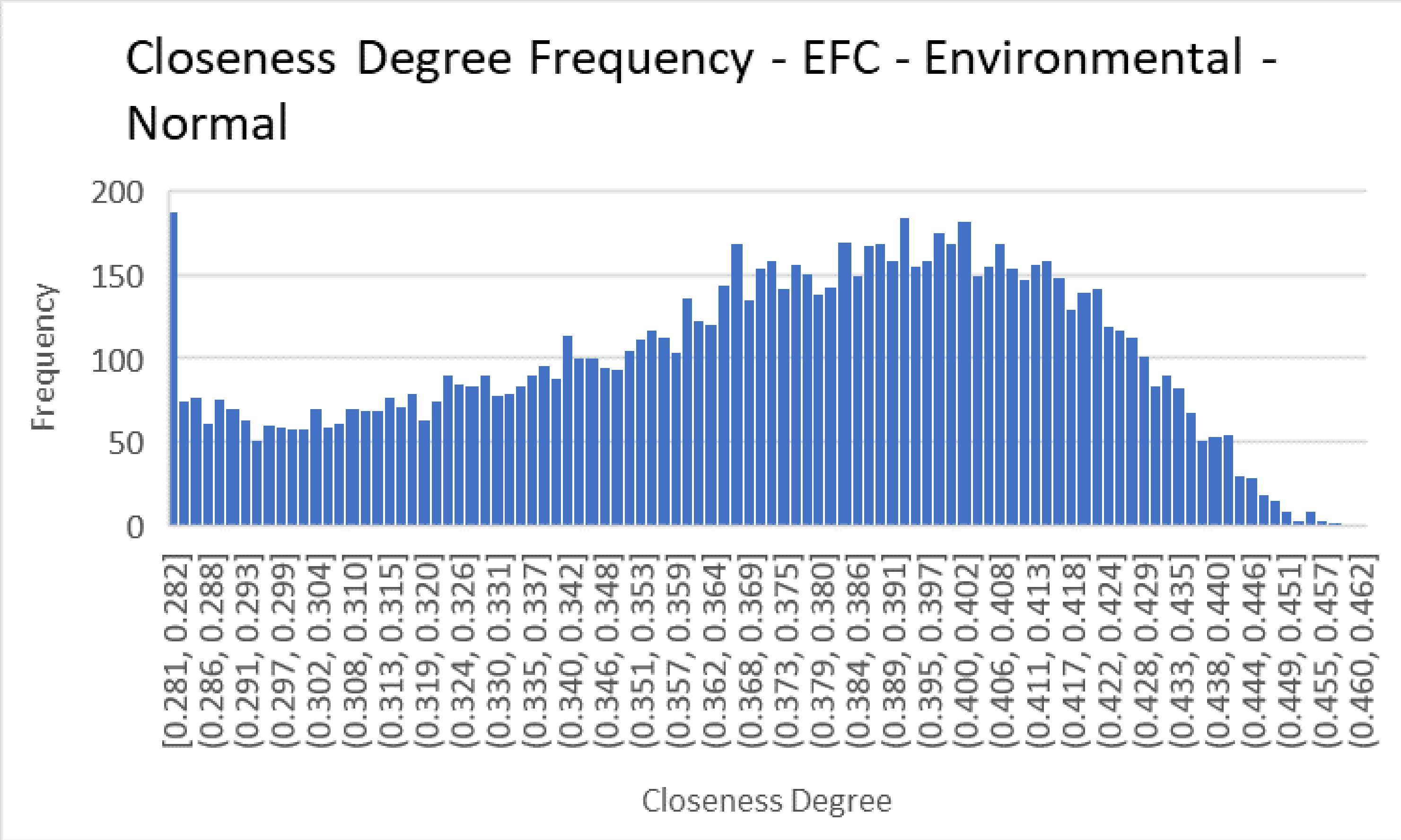
Closeness Degree Frequency - EFC - Environmental - Normal
Frequency
200
150
100
50
0
[0.281, 0.282]
(0.286, 0.288]
(0.291, 0.293]
(0.297, 0.299]
(0.302, 0.304]
(0.308, 0.310]
(0.313, 0.315]
(0.319, 0.320]
(0.324, 0.326]
(0.330, 0.331]
(0.335, 0.337]
(0.340, 0.342]
(0.346, 0.348]
(0.351, 0.353]
(0.357, 0.359]
(0.362, 0.364]
(0.368, 0.369]
(0.373, 0.375]
(0.379, 0.380]
(0.384, 0.386]
(0.389, 0.391]
(0.395, 0.397]
(0.400, 0.402]
(0.406, 0.408]
(0.411, 0.413]
(0.417, 0.418]
(0.422, 0.424]
(0.428, 0.429]
(0.433, 0.435]
(0.438, 0.440]
(0.444, 0.446]
(0.449, 0.451]
(0.455, 0.457]
(0.460, 0.462]
Closeness Degree

8.2.3.2 Uniform Input Distribution

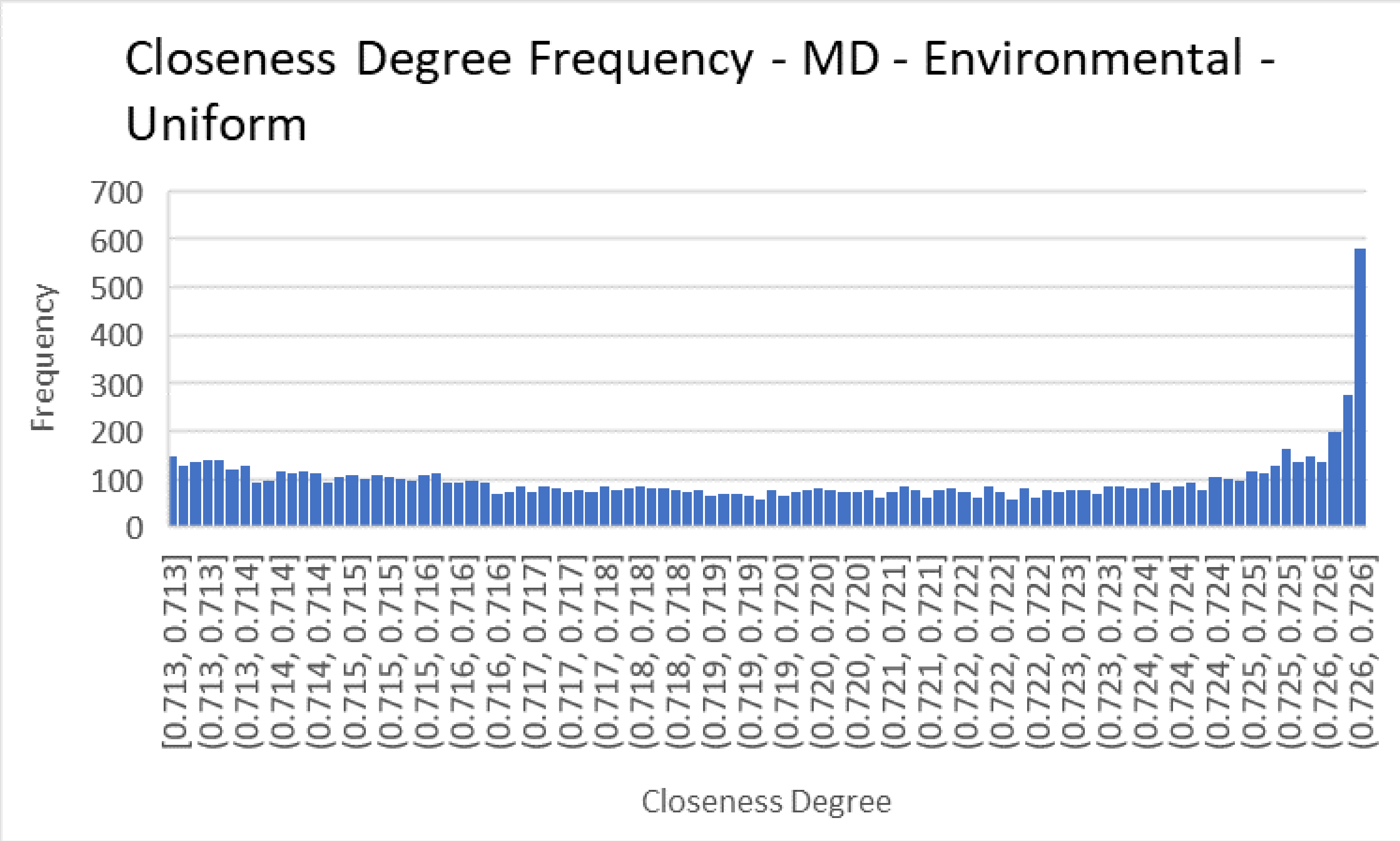

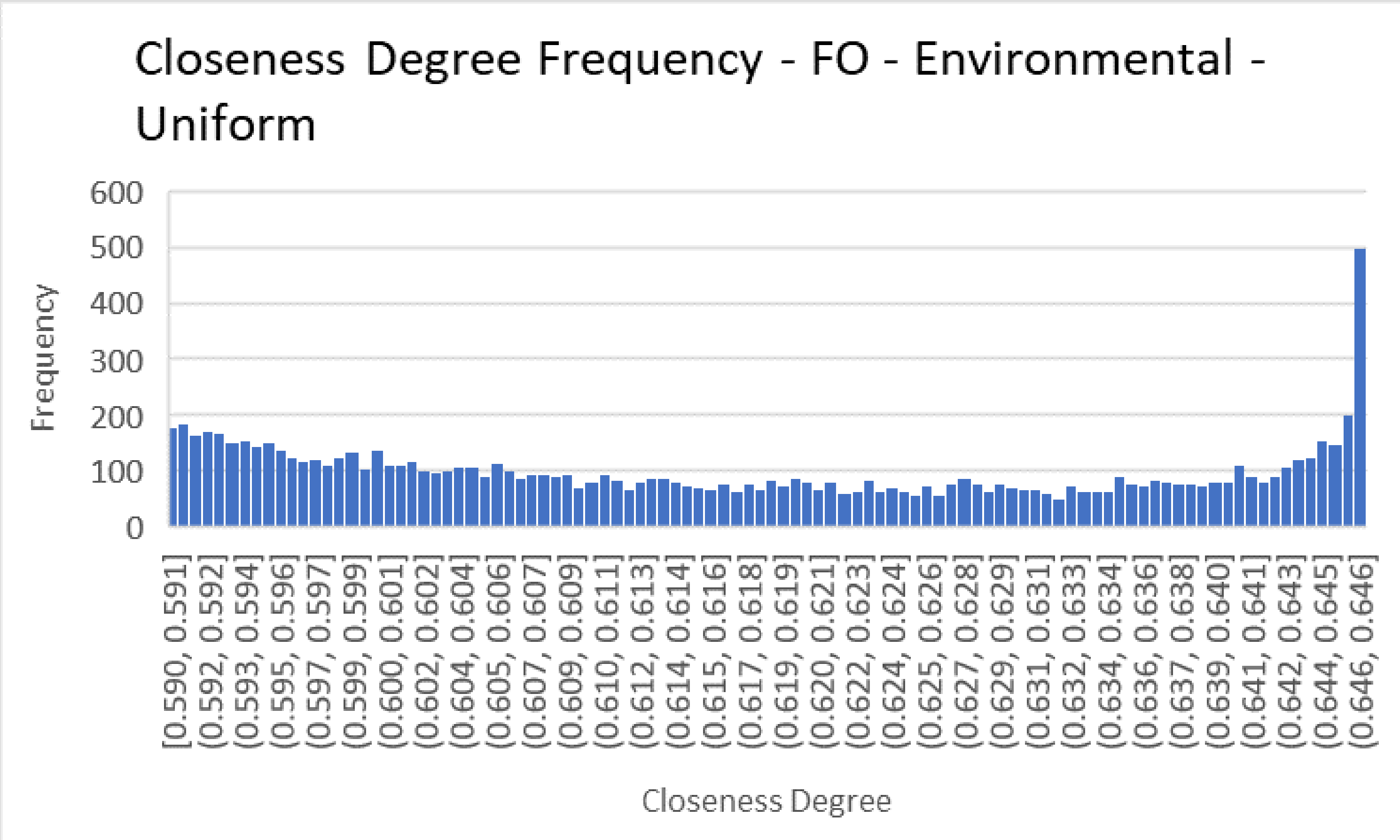
Closeness Degree Frequency - FO - Environmental - Uniform
Frequency
600
500
400
300
200
100
0
[0.590, 0.591]
(0.592, 0.592]
(0.593, 0.594]
(0.595, 0.596]
(0.597, 0.597]
(0.599, 0.599]
(0.600, 0.601]
(0.602, 0.602]
(0.604, 0.604]
(0.605, 0.606]
(0.607, 0.607]
(0.609, 0.609]
(0.610, 0.611]
(0.612, 0.613]
(0.614, 0.614]
(0.615, 0.616]
(0.617, 0.618]
(0.619, 0.619]
(0.620, 0.621]
(0.622, 0.623]
(0.624, 0.624]
(0.625, 0.626]
(0.627, 0.628]
(0.629, 0.629]
(0.631, 0.631]
(0.632, 0.633]
(0.634, 0.634]
(0.636, 0.636]
(0.637, 0.638]
(0.639, 0.640]
(0.641, 0.641]
(0.642, 0.643]
(0.644, 0.645]
(0.646, 0.646]
Closeness Degree

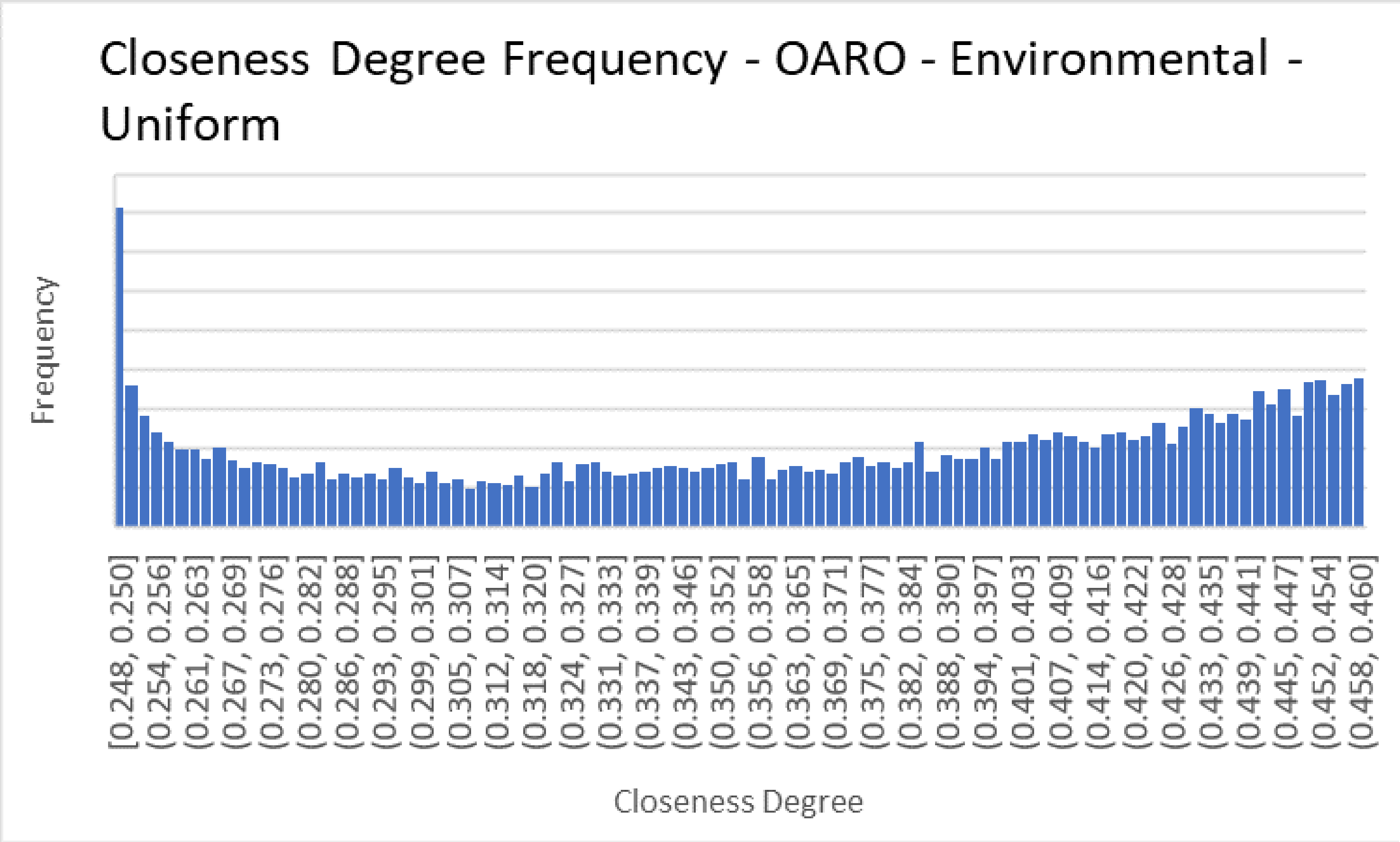

Closeness Degree Frequency - OARO - Environmental - Uniform
Frequency
[0.248, 0.250]
(0.254, 0.256]
(0.261, 0.263]
(0.267, 0.269]
(0.273, 0.276]
(0.280, 0.282]
(0.286, 0.288]
(0.293, 0.295]
(0.299, 0.301]
(0.305, 0.307]
(0.312, 0.314]
(0.318, 0.320]
(0.324, 0.327]
(0.331, 0.333]
(0.337, 0.339]
(0.343, 0.346]
(0.350, 0.352]
(0.356, 0.358]
(0.363, 0.365]
(0.369, 0.371]
(0.375, 0.377]
(0.382, 0.384]
(0.388, 0.390]
(0.394, 0.397]
(0.401, 0.403]
(0.407, 0.409]
(0.414, 0.416]
(0.420, 0.422]
(0.426, 0.428]
(0.433, 0.435]
(0.439, 0.441]
(0.445, 0.447]
(0.452, 0.454]
(0.458, 0.460]
Closeness Degree

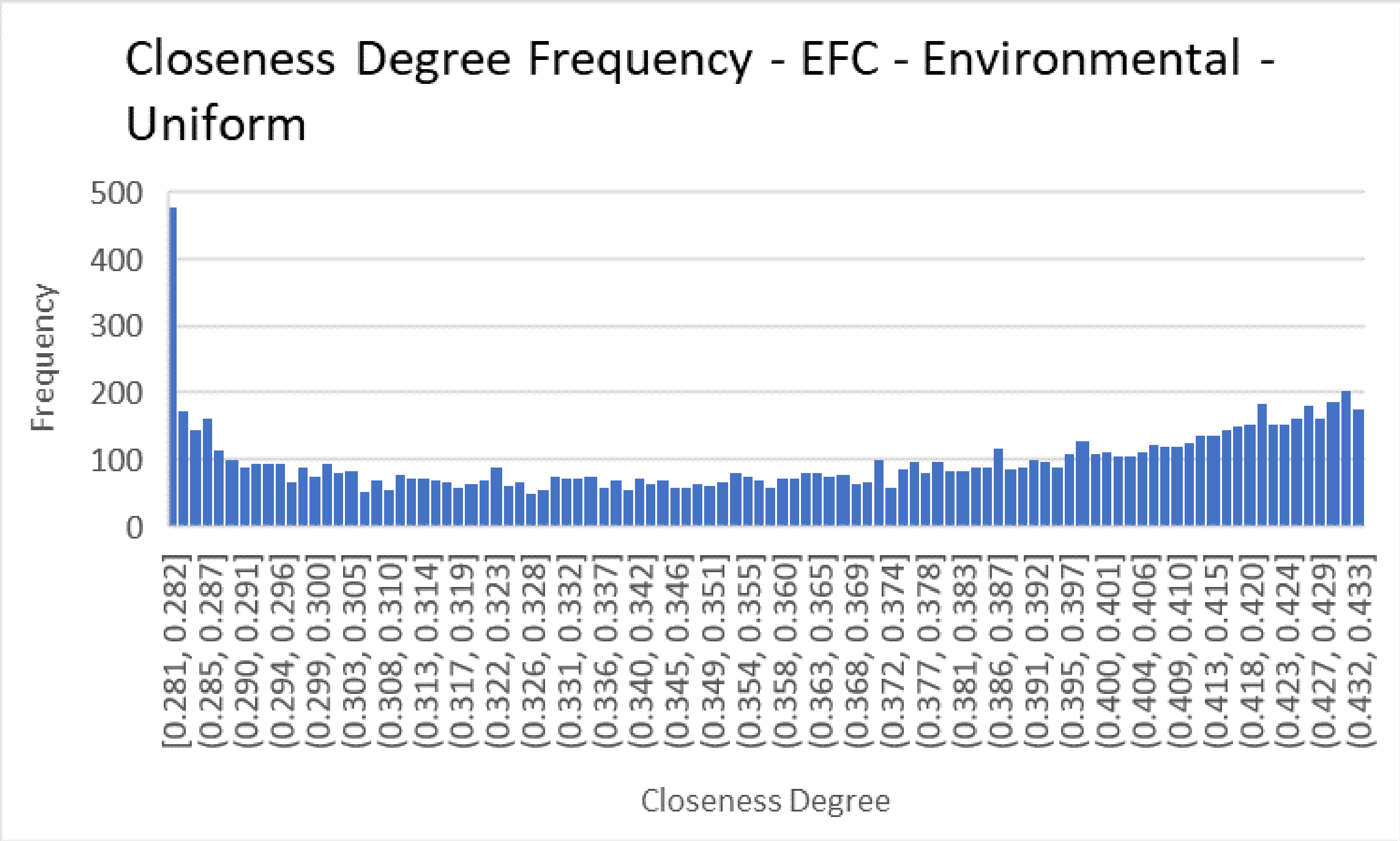

Closeness Degree Frequency - EFC - Environmental - Uniform
Frequency
500
400
300
200
100
0
[0.281, 0.282]
(0.285, 0.287]
(0.290, 0.291]
(0.294, 0.296]
(0.299, 0.300]
(0.303, 0.305]
(0.308, 0.310]
(0.313, 0.314]
(0.317, 0.319]
(0.322, 0.323]
(0.326, 0.328]
(0.331, 0.332]
(0.336, 0.337]
(0.340, 0.342]
(0.345, 0.346]
(0.349, 0.351]
(0.354, 0.355]
(0.358, 0.360]
(0.363, 0.365]
(0.368, 0.369]
(0.372, 0.374]
(0.377, 0.378]
(0.381, 0.383]
(0.386, 0.387]
(0.391, 0.392]
(0.395, 0.397]
(0.400, 0.401]
(0.404, 0.406]
(0.409, 0.410]
(0.413, 0.415]
(0.418, 0.420]
(0.423, 0.424]
(0.427, 0.429]
(0.432, 0.433]
Closeness Degree

### 8.2.4 Distribution of simulation closeness degree results while only varying the technical aspect

#### 8.2.4.1 Normal Input Distribution

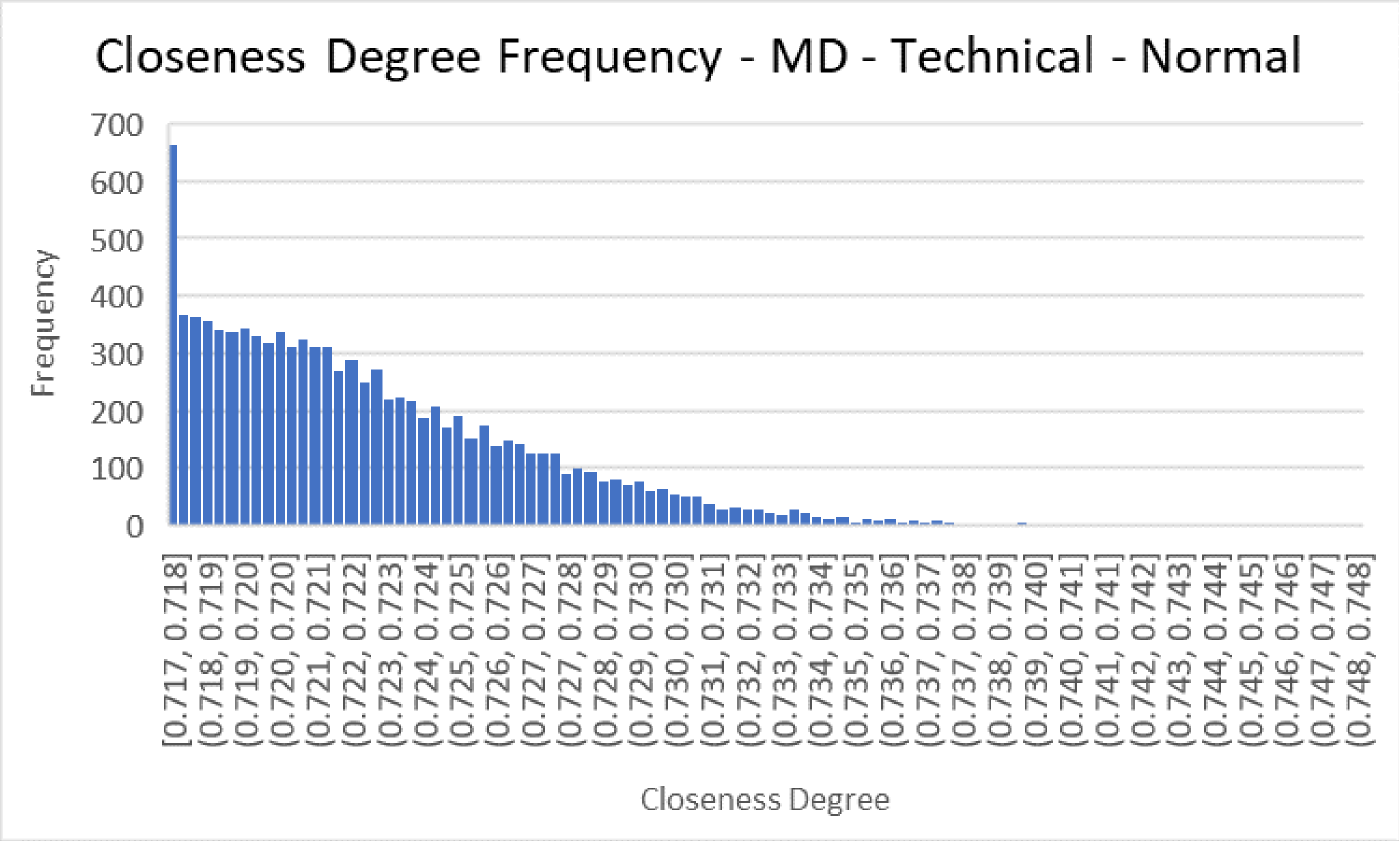

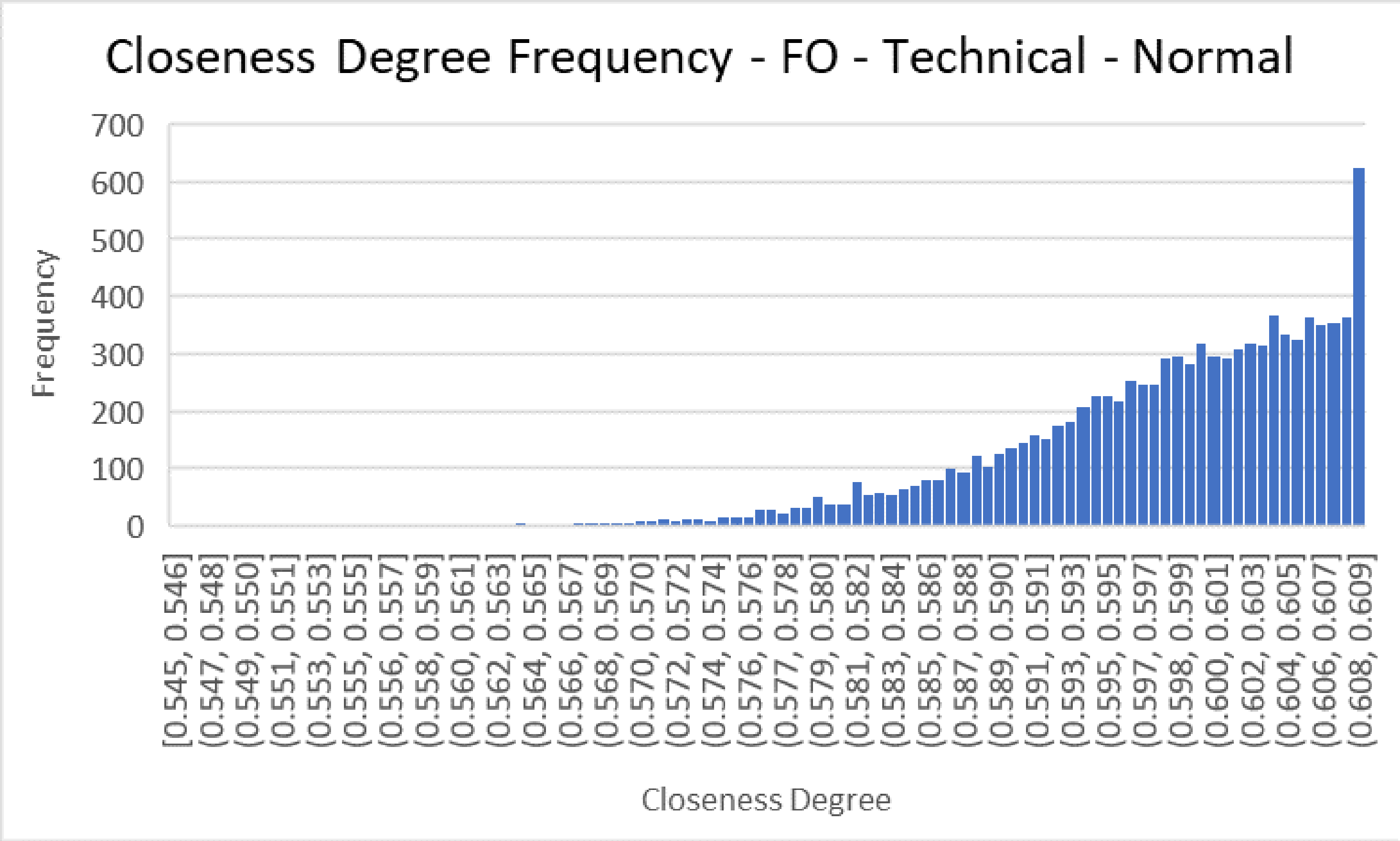
Closeness Degree Frequency - FO - Technical - Normal
Frequency
Closeness Degree

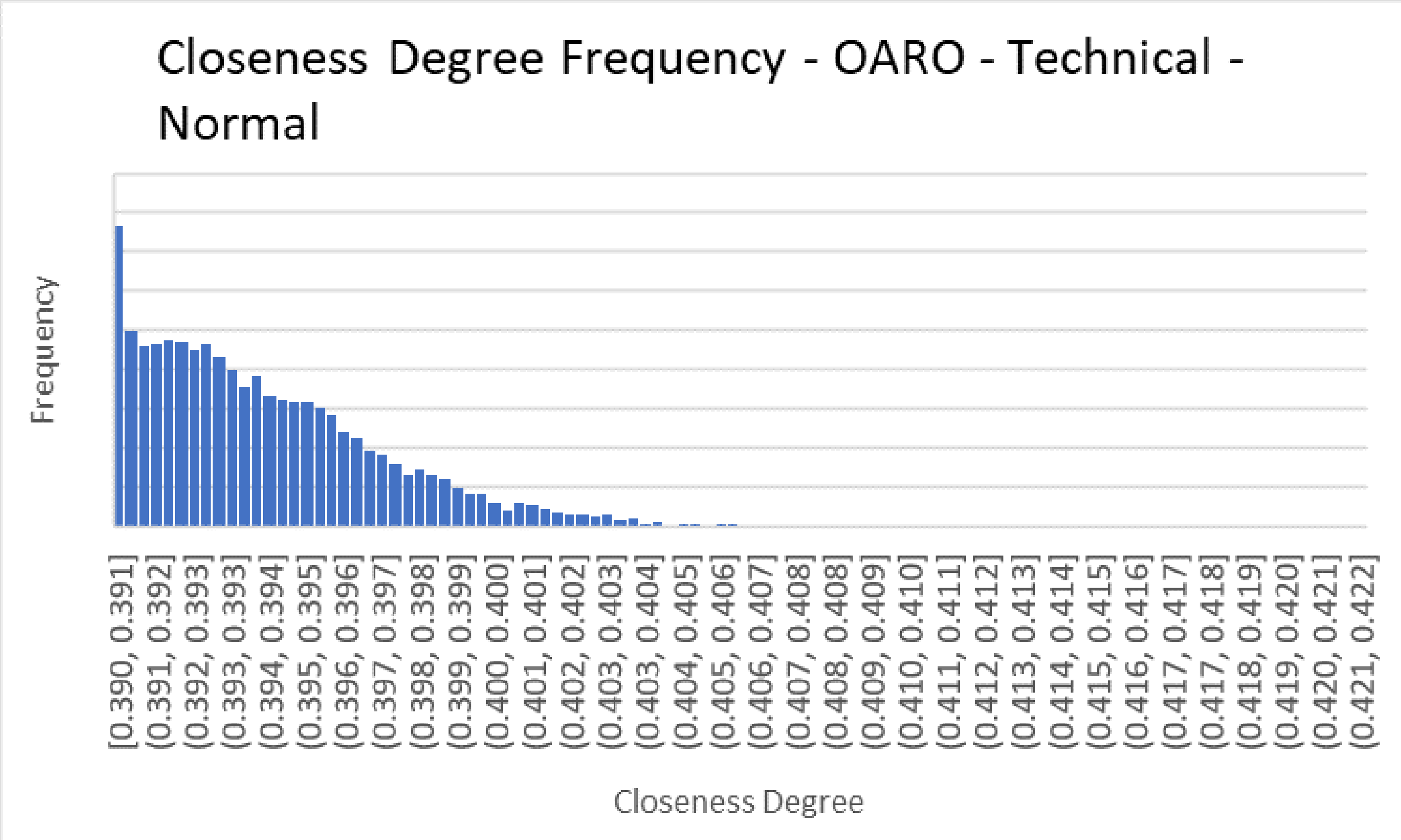
Closeness Degree Frequency - OARO - Technical - Normal
Frequency
Closeness Degree
[0.390, 0.391]
(0.391, 0.392]
(0.392, 0.393]
(0.393, 0.393]
(0.393, 0.394]
(0.394, 0.395]
(0.395, 0.396]
(0.396, 0.397]
(0.397, 0.398]
(0.398, 0.399]
(0.399, 0.400]
(0.400, 0.401]
(0.401, 0.402]
(0.402, 0.403]
(0.403, 0.404]
(0.404, 0.405]
(0.405, 0.406]
(0.406, 0.407]
(0.407, 0.408]
(0.408, 0.409]
(0.409, 0.410]
(0.410, 0.411]
(0.411, 0.412]
(0.412, 0.413]
(0.413, 0.414]
(0.414, 0.415]
(0.415, 0.416]
(0.416, 0.417]
(0.417, 0.418]
(0.418, 0.419]
(0.419, 0.420]
(0.420, 0.421]
(0.421, 0.422]

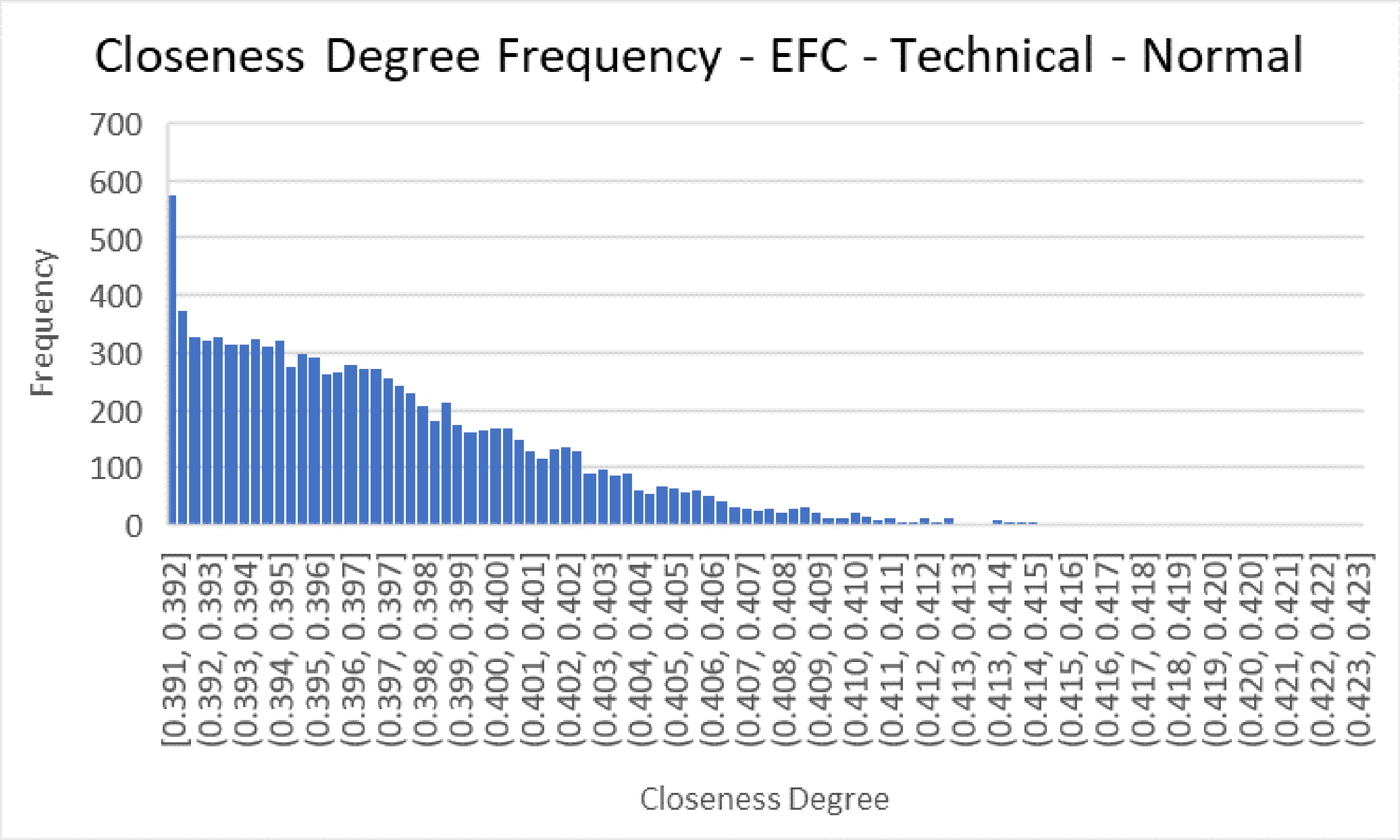
Closeness Degree Frequency - EFC - Technical - Normal
Frequency
700
600
500
400
300
200
100
0
[0.391, 0.392]
(0.392, 0.393]
(0.393, 0.394]
(0.394, 0.395]
(0.395, 0.396]
(0.396, 0.397]
(0.397, 0.397]
(0.398, 0.398]
(0.399, 0.399]
(0.400, 0.400]
(0.401, 0.401]
(0.402, 0.402]
(0.403, 0.403]
(0.404, 0.404]
(0.405, 0.405]
(0.406, 0.406]
(0.407, 0.407]
(0.408, 0.408]
(0.409, 0.409]
(0.410, 0.410]
(0.411, 0.411]
(0.412, 0.412]
(0.413, 0.413]
(0.413, 0.414]
(0.414, 0.415]
(0.415, 0.416]
(0.416, 0.417]
(0.417, 0.418]
(0.418, 0.419]
(0.419, 0.420]
(0.420, 0.420]
(0.421, 0.421]
(0.422, 0.422]
(0.423, 0.423]
Closeness Degree

8.2.4.2 Uniform Input Distribution

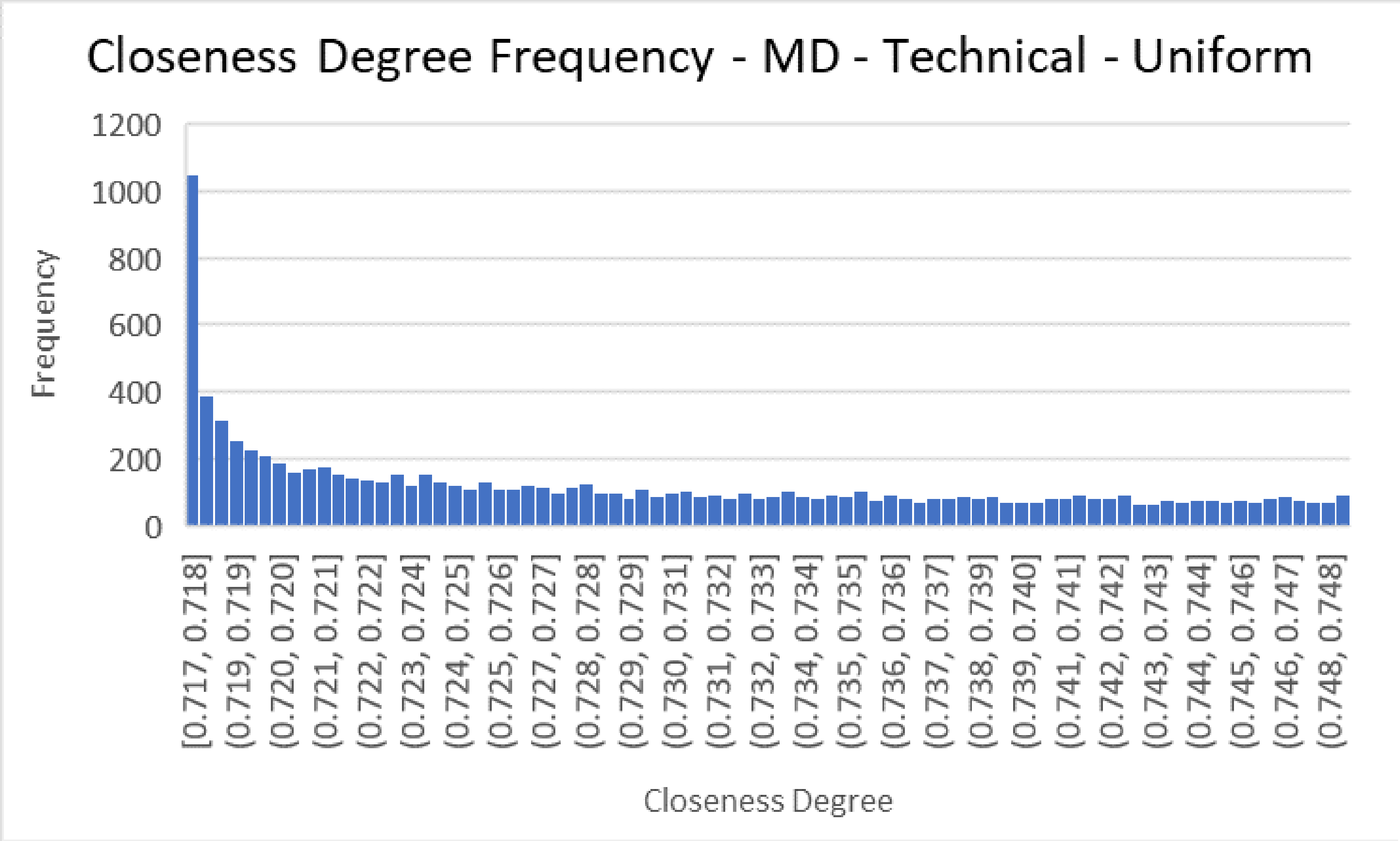

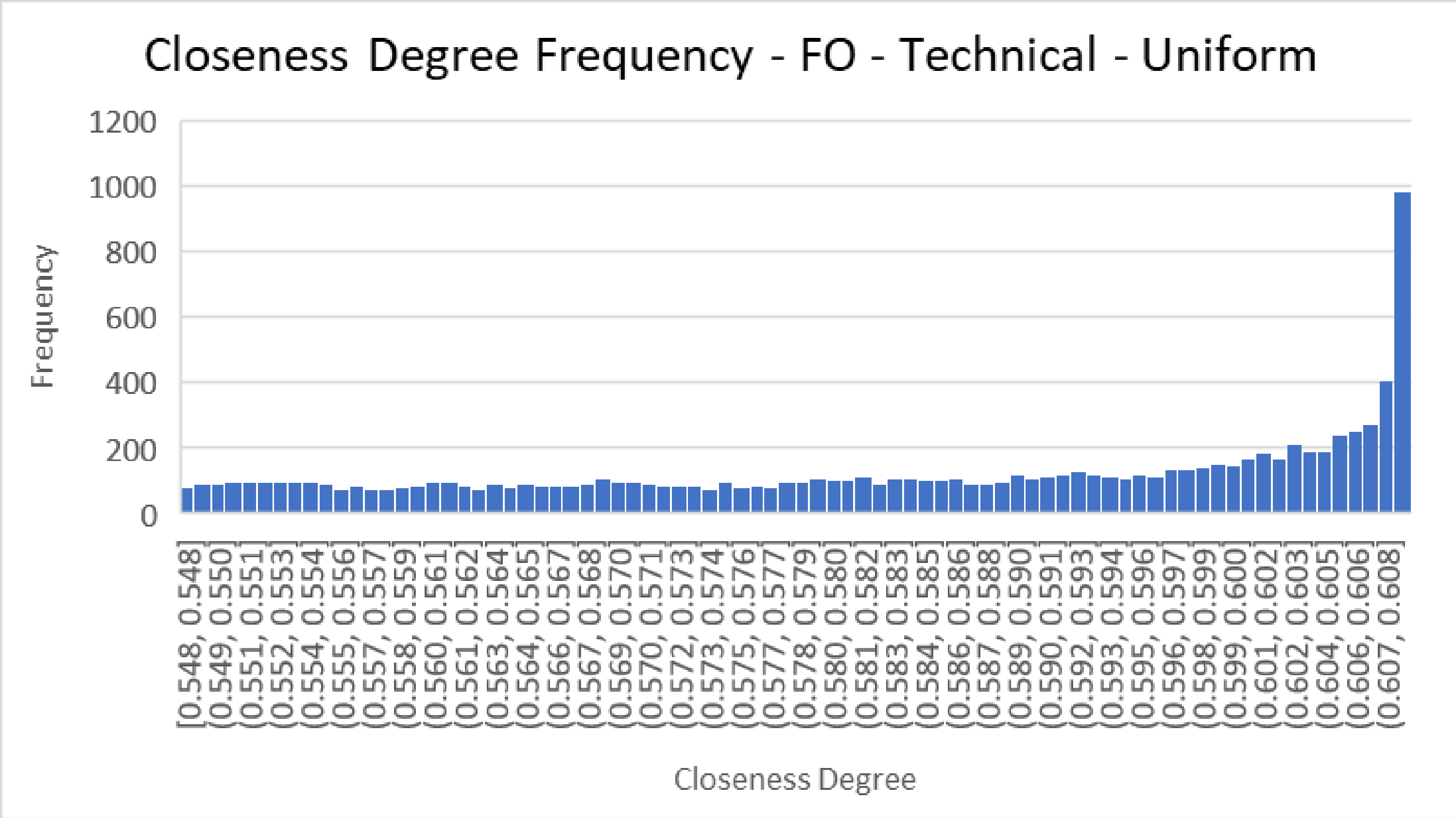

Closeness Degree Frequency - FO - Technical - Uniform
Frequency
0
200
400
600
800
1000
1200
[0.548, 0.548]
(0.549, 0.550]
(0.551, 0.551]
(0.552, 0.553]
(0.554, 0.554]
(0.555, 0.556]
(0.557, 0.557]
(0.558, 0.559]
(0.560, 0.561]
(0.561, 0.562]
(0.563, 0.564]
(0.564, 0.565]
(0.566, 0.567]
(0.567, 0.568]
(0.569, 0.570]
(0.570, 0.571]
(0.572, 0.573]
(0.573, 0.574]
(0.575, 0.576]
(0.577, 0.577]
(0.578, 0.579]
(0.580, 0.580]
(0.581, 0.582]
(0.583, 0.583]
(0.584, 0.585]
(0.586, 0.586]
(0.587, 0.588]
(0.589, 0.590]
(0.590, 0.591]
(0.592, 0.593]
(0.593, 0.594]
(0.595, 0.596]
(0.596, 0.597]
(0.598, 0.599]
(0.599, 0.600]
(0.601, 0.602]
(0.602, 0.603]
(0.604, 0.605]
(0.606, 0.606]
(0.607, 0.608]
Closeness Degree

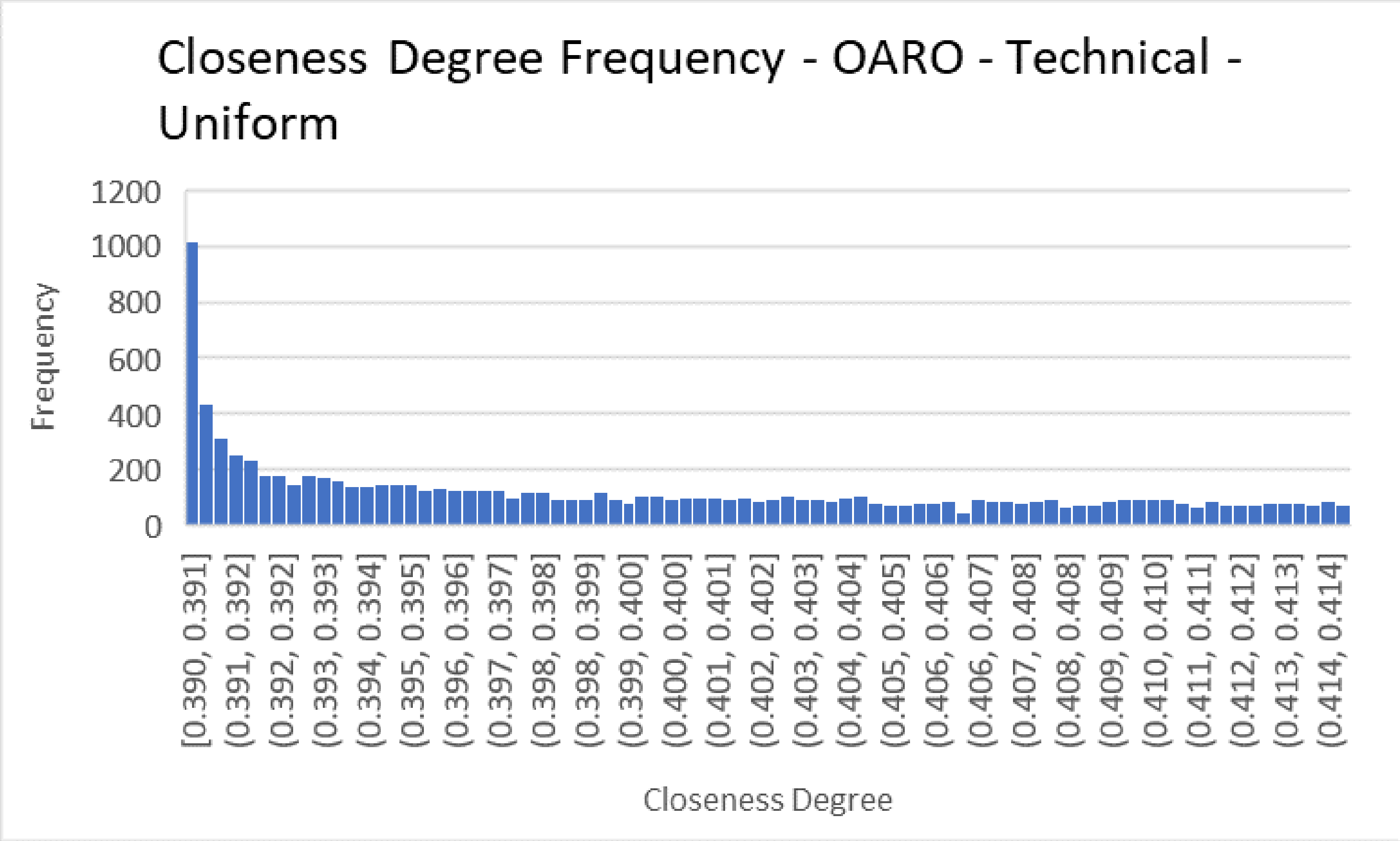
Closeness Degree Frequency - OARO - Technical - Uniform
Frequency
1200
1000
800
600
400
200
0
[0.390, 0.391]
(0.391, 0.392]
(0.392, 0.392]
(0.393, 0.393]
(0.394, 0.394]
(0.395, 0.395]
(0.396, 0.396]
(0.397, 0.397]
(0.398, 0.398]
(0.398, 0.399]
(0.399, 0.400]
(0.400, 0.400]
(0.401, 0.401]
(0.402, 0.402]
(0.403, 0.403]
(0.404, 0.404]
(0.405, 0.405]
(0.406, 0.406]
(0.406, 0.407]
(0.407, 0.408]
(0.408, 0.408]
(0.409, 0.409]
(0.410, 0.410]
(0.411, 0.411]
(0.412, 0.412]
(0.413, 0.413]
(0.414, 0.414]
Closeness Degree

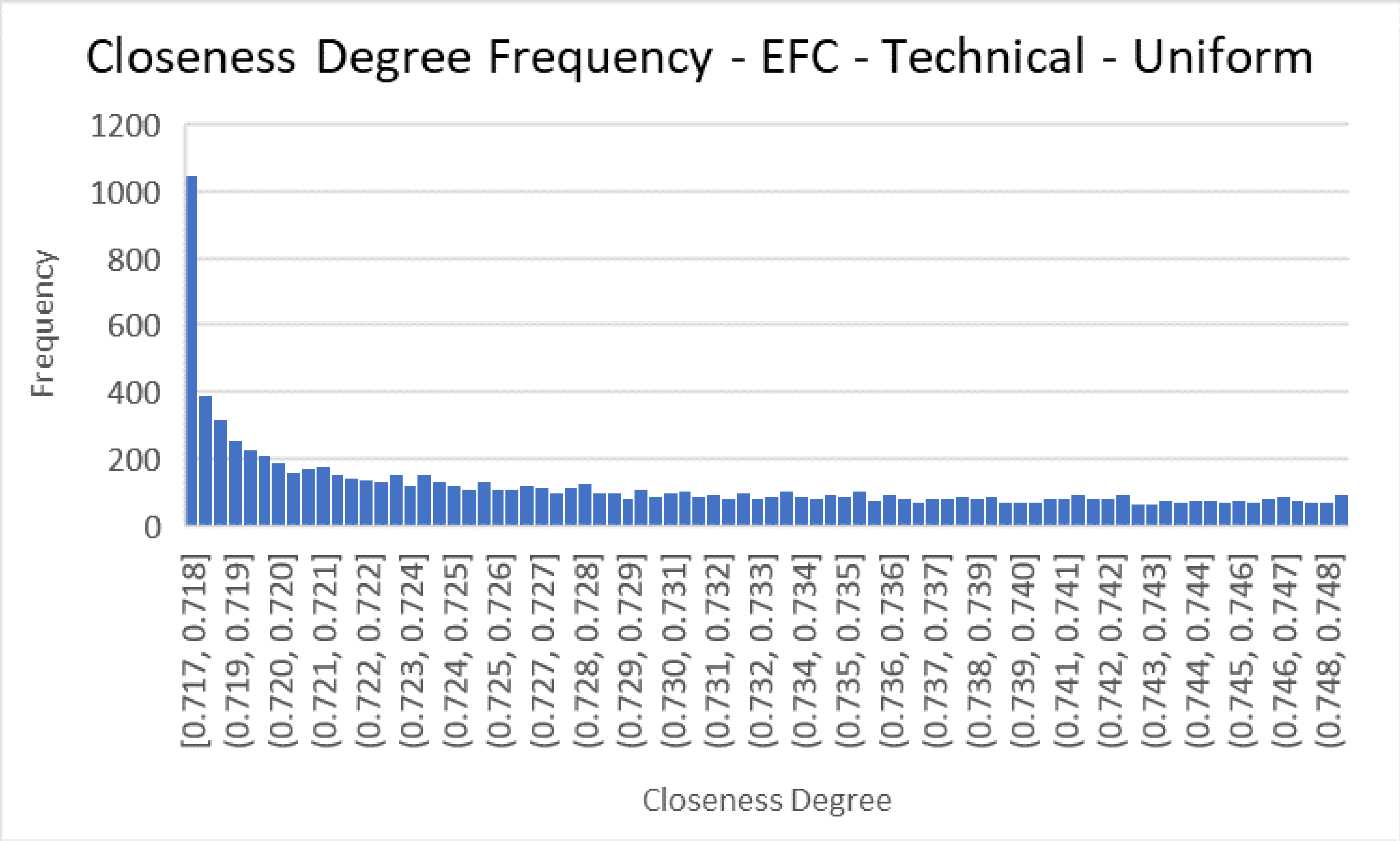
Closeness Degree Frequency - EFC - Technical - Uniform
Frequency
1200
1000
800
600
400
200
0
[0.717, 0.718]
(0.719, 0.719]
(0.720, 0.720]
(0.721, 0.721]
(0.722, 0.722]
(0.723, 0.724]
(0.724, 0.725]
(0.725, 0.726]
(0.727, 0.727]
(0.728, 0.728]
(0.729, 0.729]
(0.730, 0.731]
(0.731, 0.732]
(0.732, 0.733]
(0.734, 0.734]
(0.735, 0.735]
(0.736, 0.736]
(0.737, 0.737]
(0.738, 0.739]
(0.739, 0.740]
(0.741, 0.741]
(0.742, 0.742]
(0.743, 0.743]
(0.744, 0.744]
(0.745, 0.746]
(0.746, 0.747]
(0.748, 0.748]
Closeness Degree

### 8.2.5 Distribution of simulation closeness degree results while only varying the social aspect

#### 8.2.5.1 Normal Input Distribution

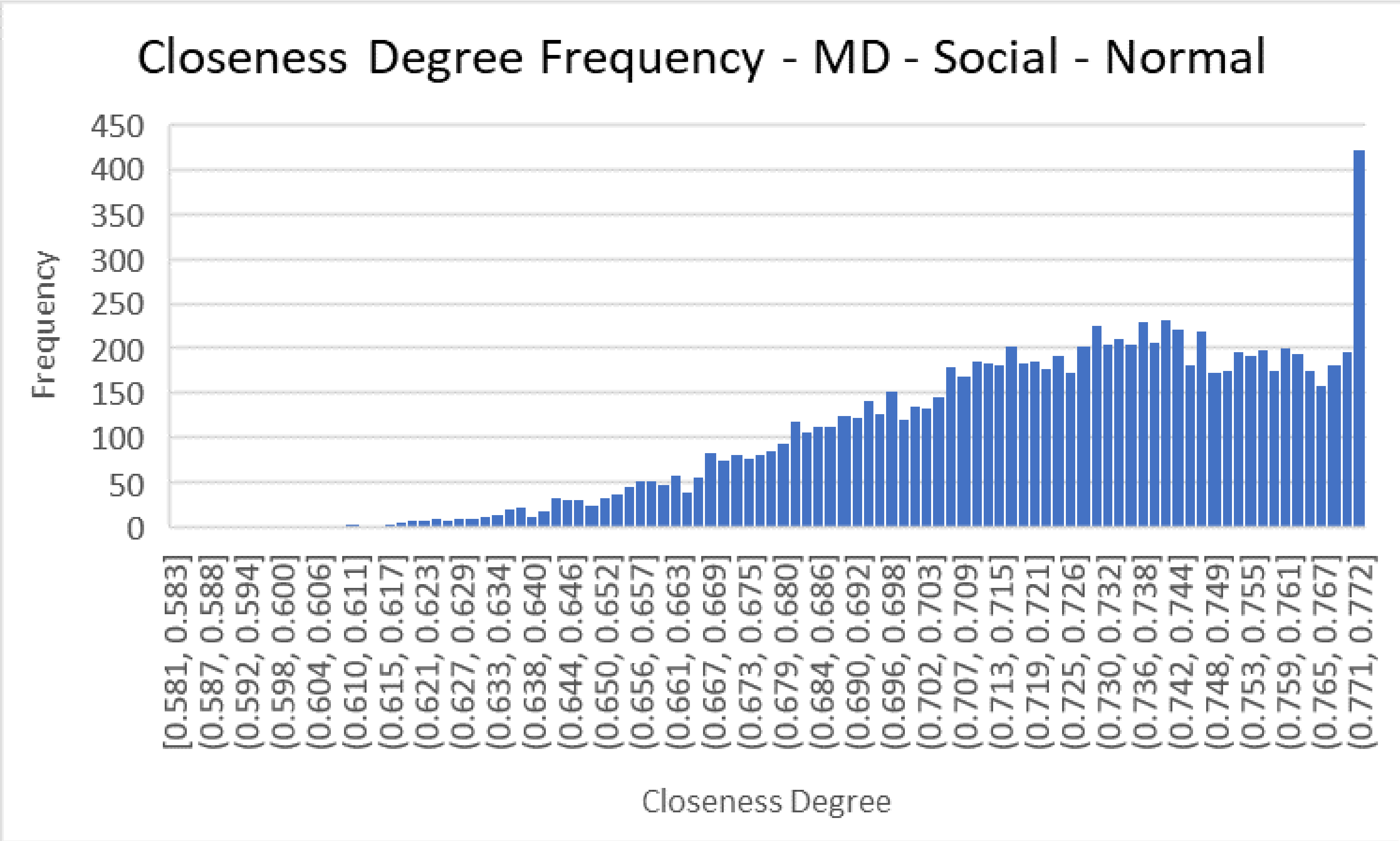

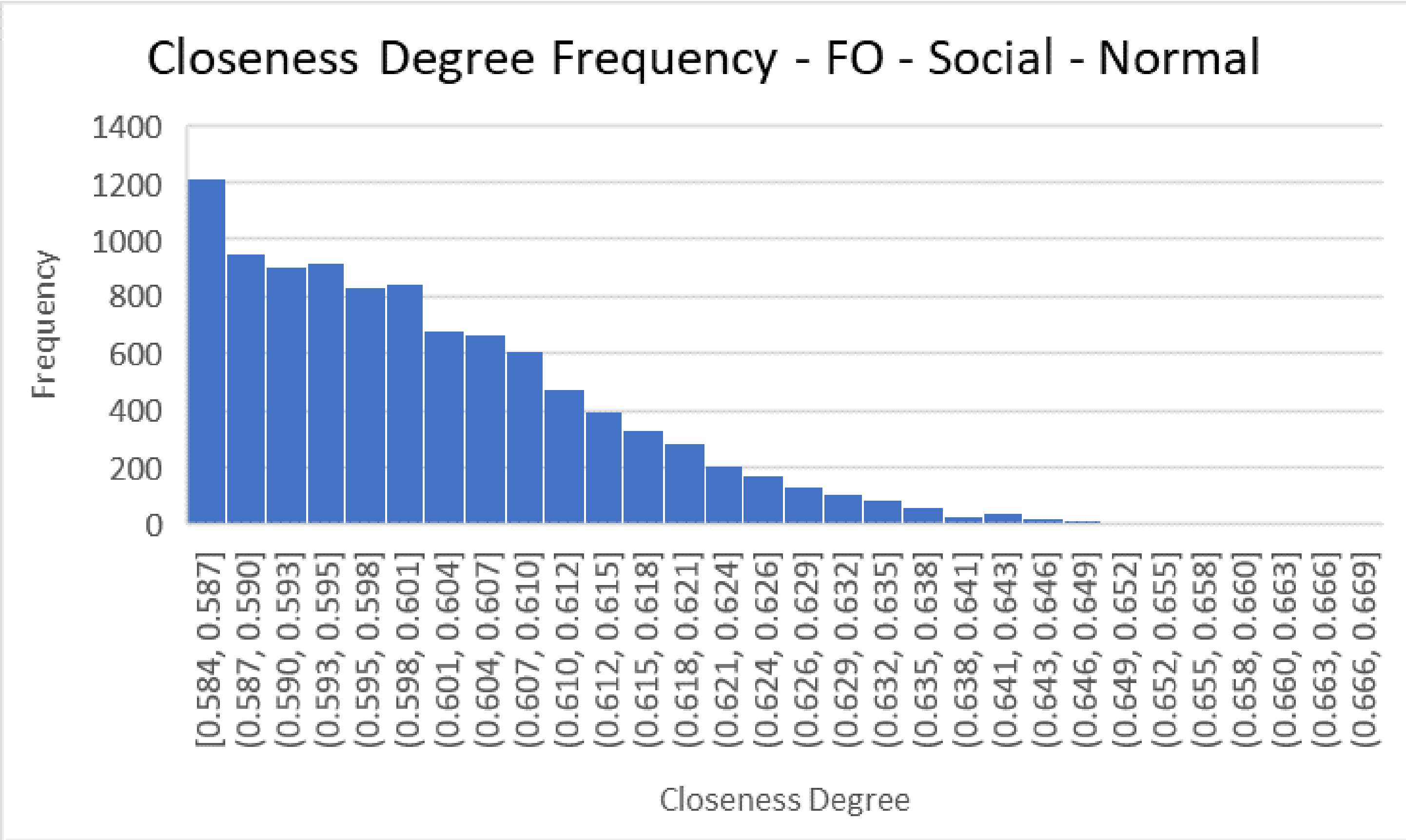
Closeness Degree Frequency - FO - Social - Normal
Frequency
1400
1200
1000
800
600
400
200
0
[0.584, 0.587]
(0.587, 0.590]
(0.590, 0.593]
(0.593, 0.595]
(0.595, 0.598]
(0.598, 0.601]
(0.601, 0.604]
(0.604, 0.607]
(0.607, 0.610]
(0.610, 0.612]
(0.612, 0.615]
(0.615, 0.618]
(0.618, 0.621]
(0.621, 0.624]
(0.624, 0.626]
(0.626, 0.629]
(0.629, 0.632]
(0.632, 0.635]
(0.635, 0.638]
(0.638, 0.641]
(0.641, 0.643]
(0.643, 0.646]
(0.646, 0.649]
(0.649, 0.652]
(0.652, 0.655]
(0.655, 0.658]
(0.658, 0.660]
(0.660, 0.663]
(0.663, 0.666]
(0.666, 0.669]
Closeness Degree

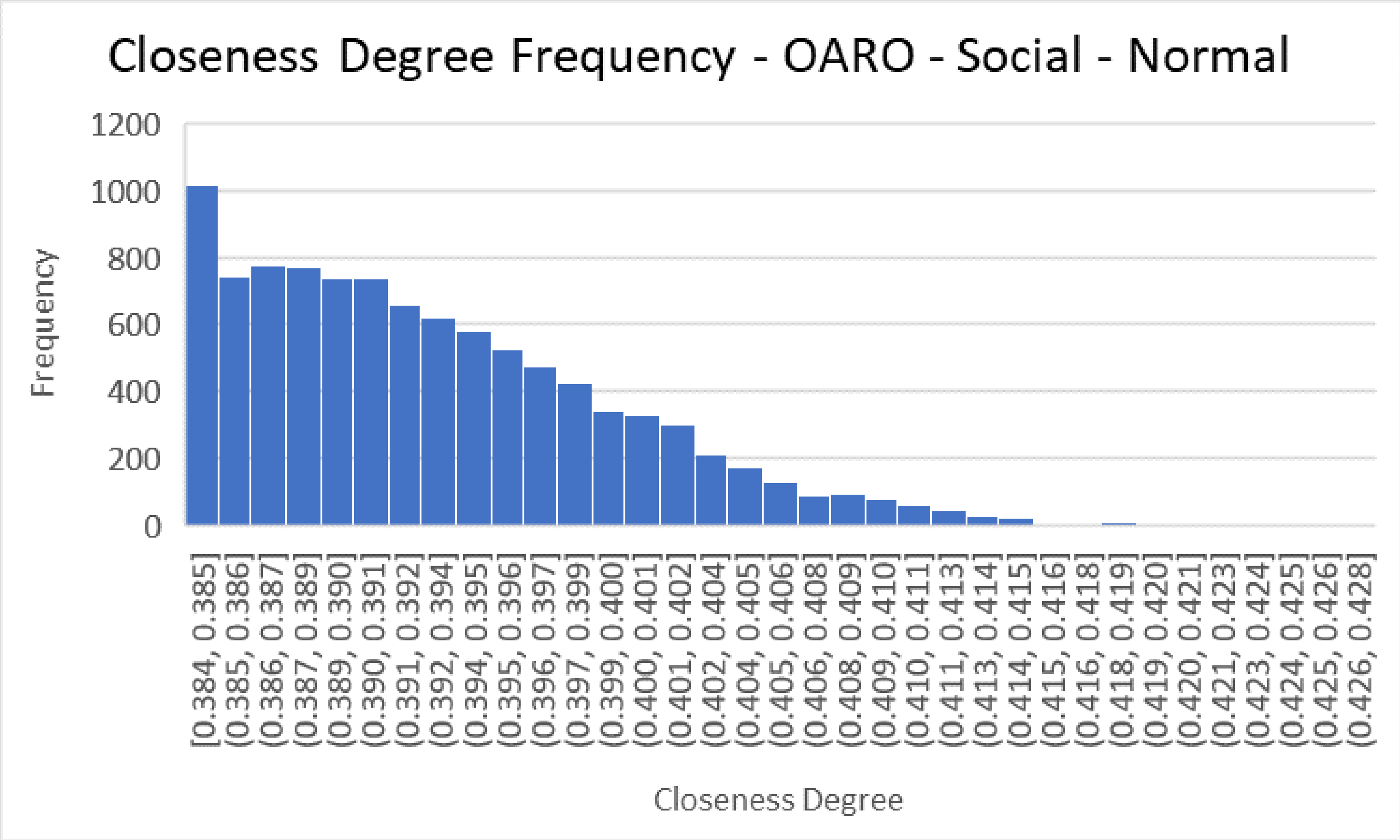
Closeness Degree Frequency - OARO - Social - Normal
1200
1000
800
600
400
200
0
Frequency
[0.384, 0.385]
(0.385, 0.386]
(0.386, 0.387]
(0.387, 0.389]
(0.389, 0.390]
(0.390, 0.391]
(0.391, 0.392]
(0.392, 0.394]
(0.394, 0.395]
(0.395, 0.396]
(0.396, 0.397]
(0.397, 0.399]
(0.399, 0.400]
(0.400, 0.401]
(0.401, 0.402]
(0.402, 0.404]
(0.404, 0.405]
(0.405, 0.406]
(0.406, 0.408]
(0.408, 0.409]
(0.409, 0.410]
(0.410, 0.411]
(0.411, 0.413]
(0.413, 0.414]
(0.414, 0.415]
(0.415, 0.416]
(0.416, 0.418]
(0.418, 0.419]
(0.419, 0.420]
(0.420, 0.421]
(0.421, 0.423]
(0.423, 0.424]
(0.424, 0.425]
(0.425, 0.426]
(0.426, 0.428]
Closeness Degree

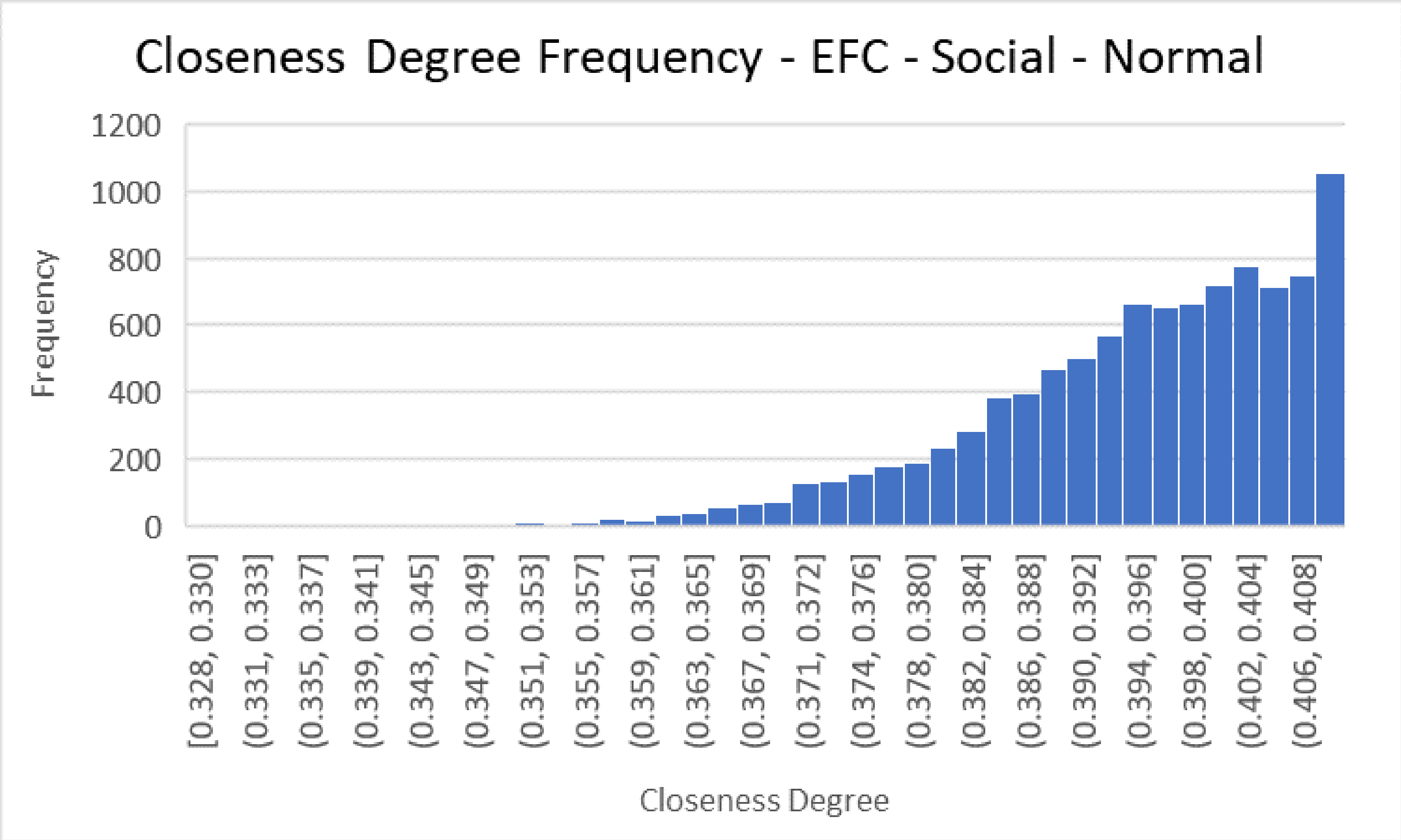

Closeness Degree Frequency - EFC - Social - Normal
Frequency
1200
1000
800
600
400
200
0
[0.328, 0.330]
(0.331, 0.333]
(0.335, 0.337]
(0.339, 0.341]
(0.343, 0.345]
(0.347, 0.349]
(0.351, 0.353]
(0.355, 0.357]
(0.359, 0.361]
(0.363, 0.365]
(0.367, 0.369]
(0.371, 0.372]
(0.374, 0.376]
(0.378, 0.380]
(0.382, 0.384]
(0.386, 0.388]
(0.390, 0.392]
(0.394, 0.396]
(0.398, 0.400]
(0.402, 0.404]
(0.406, 0.408]
Closeness Degree

8.2.5.2 Uniform Input Distribution

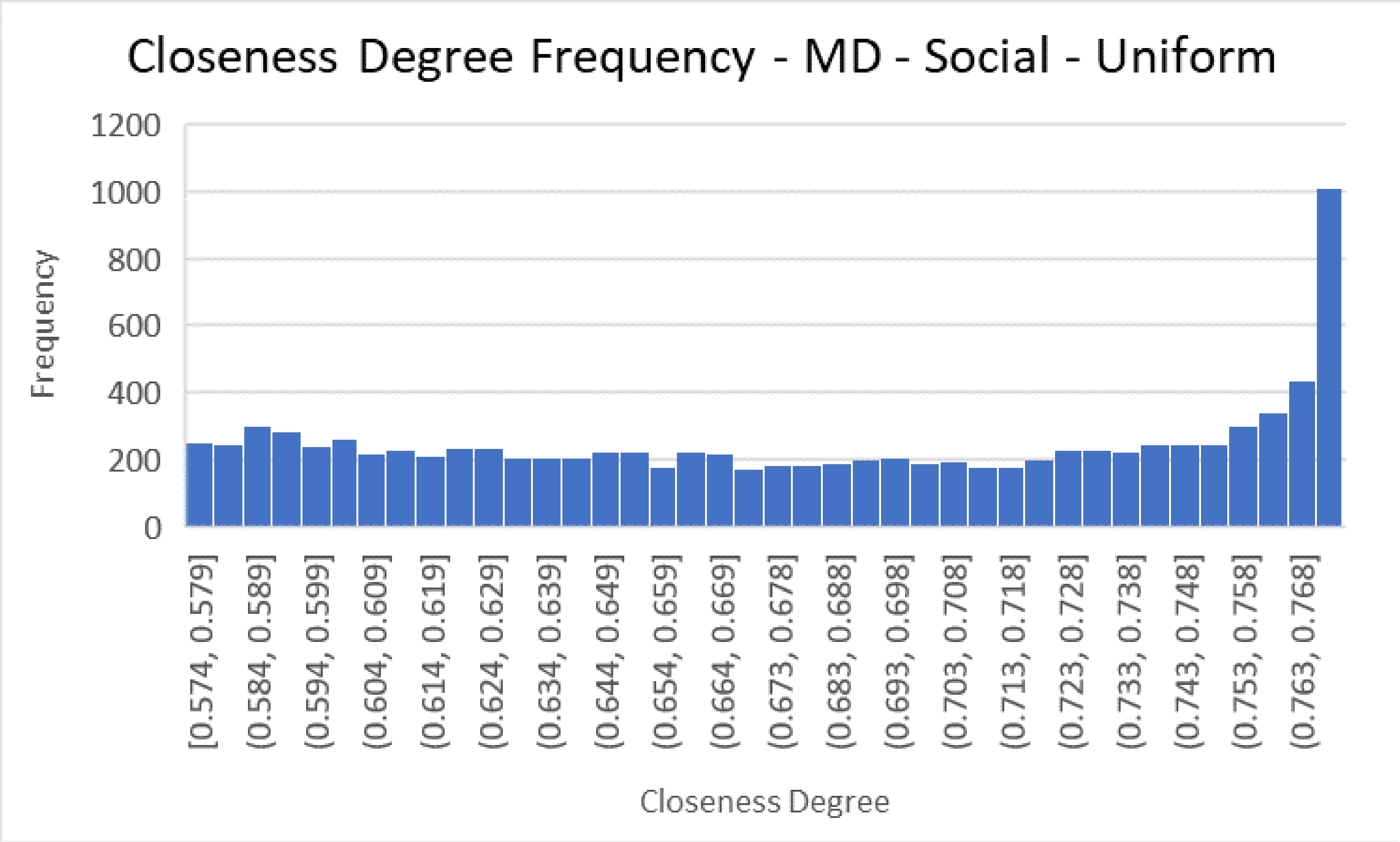

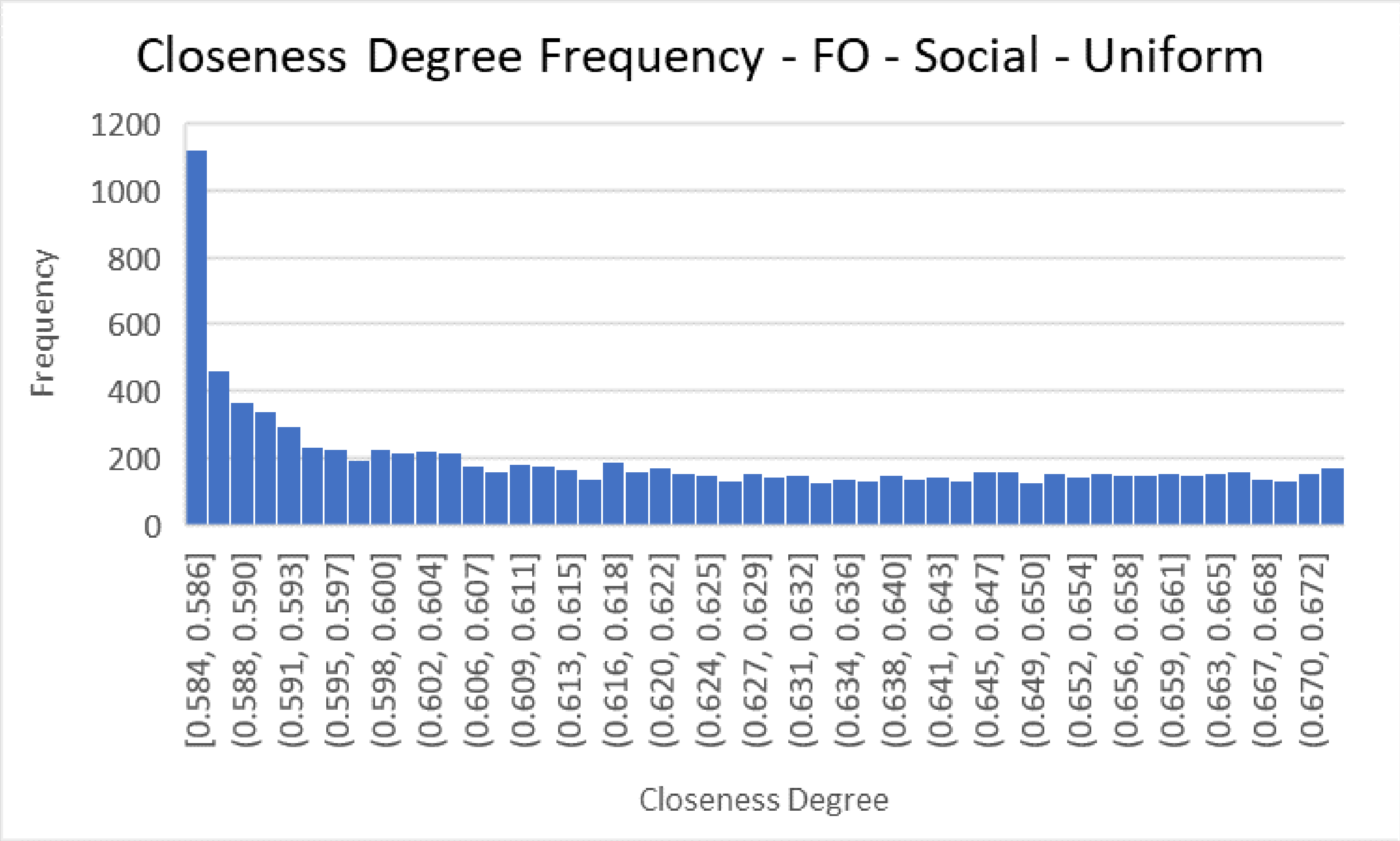

Closeness Degree Frequency - FO - Social - Uniform
Frequency
1200
1000
800
600
400
200
0
[0.584, 0.586]
(0.588, 0.590]
(0.591, 0.593]
(0.595, 0.597]
(0.598, 0.600]
(0.602, 0.604]
(0.606, 0.607]
(0.609, 0.611]
(0.613, 0.615]
(0.616, 0.618]
(0.620, 0.622]
(0.624, 0.625]
(0.627, 0.629]
(0.631, 0.632]
(0.634, 0.636]
(0.638, 0.640]
(0.641, 0.643]
(0.645, 0.647]
(0.649, 0.650]
(0.652, 0.654]
(0.656, 0.658]
(0.659, 0.661]
(0.663, 0.665]
(0.667, 0.668]
(0.670, 0.672]
Closeness Degree

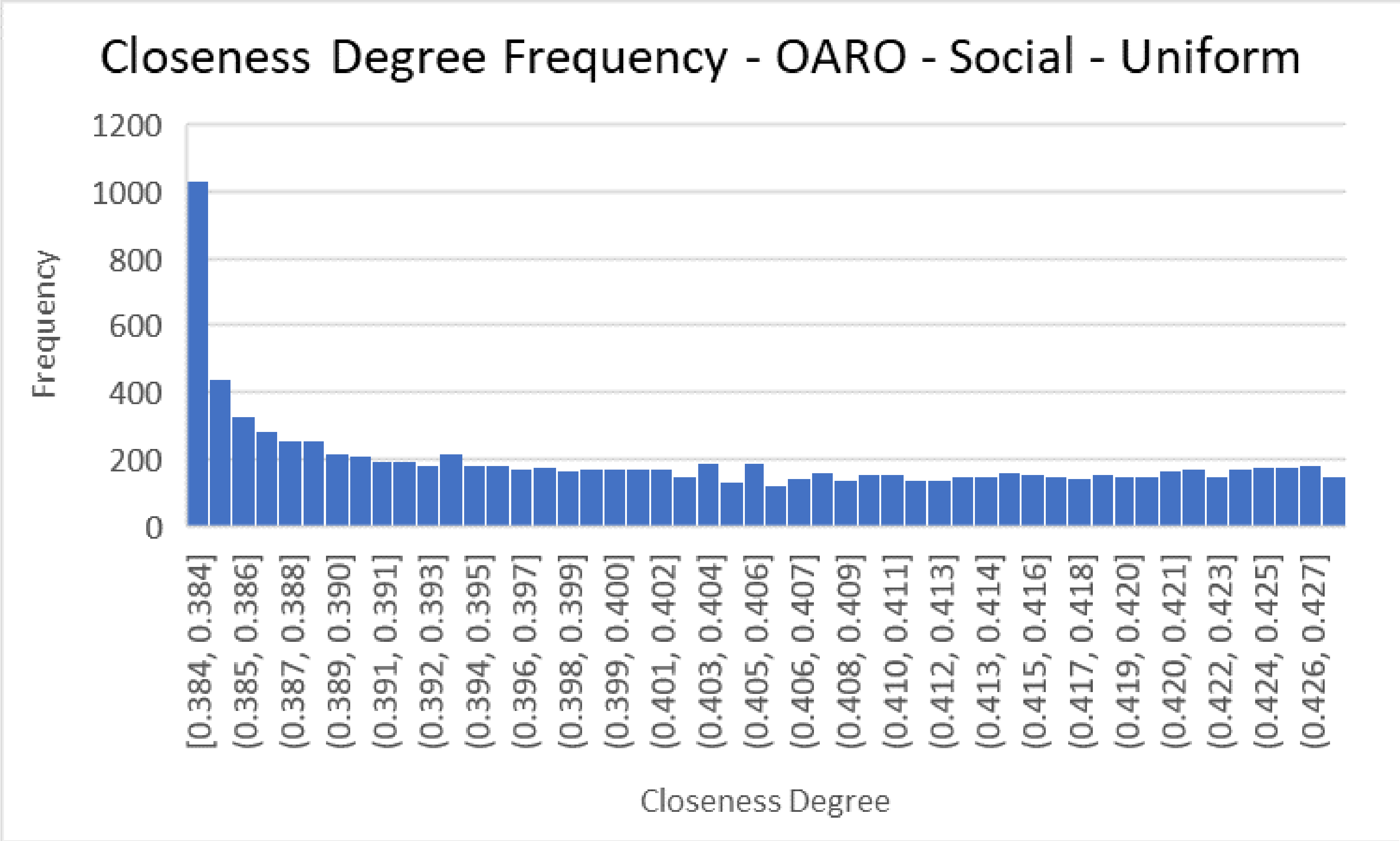

Closeness Degree Frequency - OARO - Social - Uniform
Frequency
0
200
400
600
800
1000
1200
[0.384, 0.384]
(0.385, 0.386]
(0.387, 0.388]
(0.389, 0.390]
(0.391, 0.391]
(0.392, 0.393]
(0.394, 0.395]
(0.396, 0.397]
(0.398, 0.399]
(0.399, 0.400]
(0.401, 0.402]
(0.403, 0.404]
(0.405, 0.406]
(0.406, 0.407]
(0.408, 0.409]
(0.410, 0.411]
(0.412, 0.413]
(0.413, 0.414]
(0.415, 0.416]
(0.417, 0.418]
(0.419, 0.420]
(0.420, 0.421]
(0.422, 0.423]
(0.424, 0.425]
(0.426, 0.427]
Closeness Degree

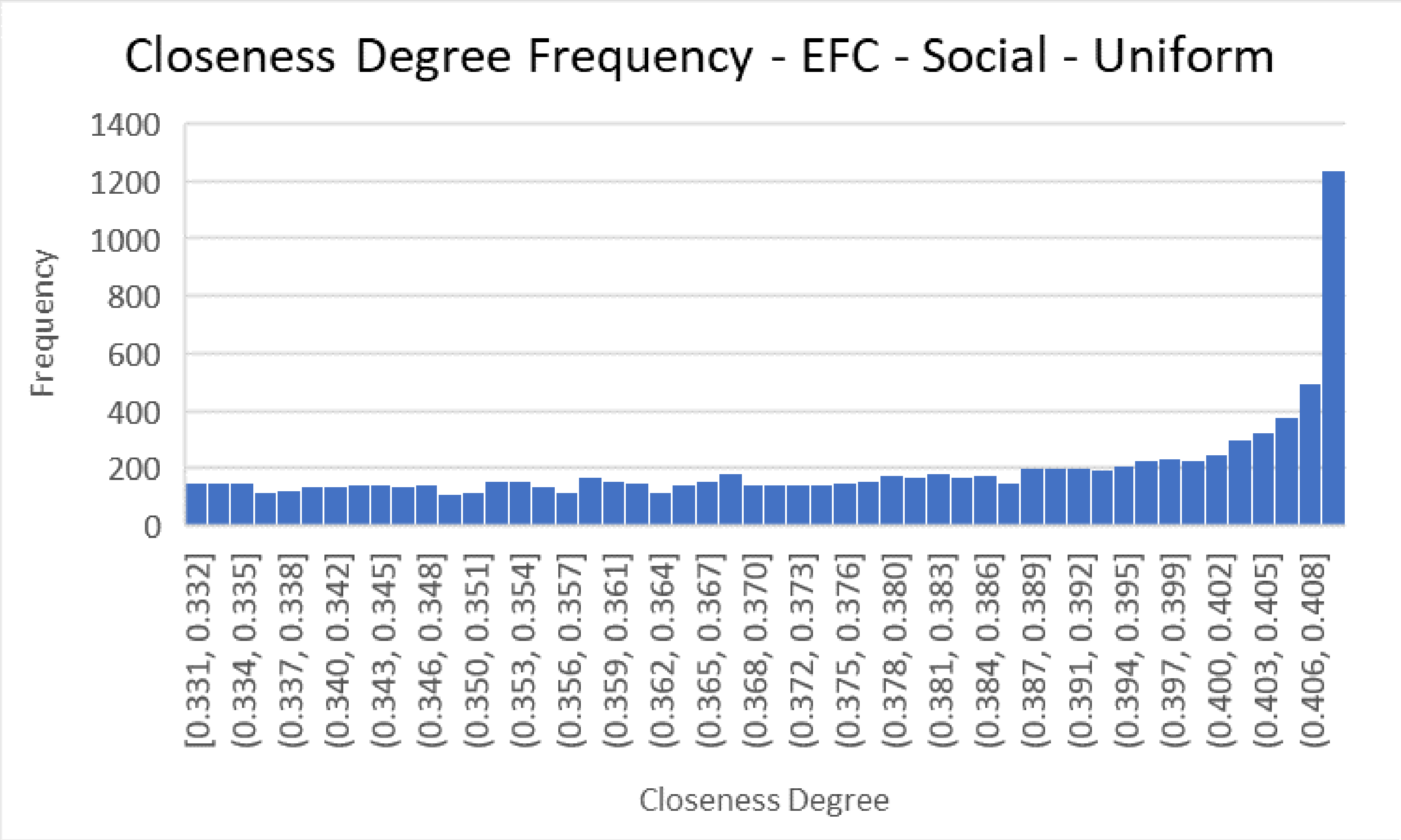
Closeness Degree Frequency - EFC - Social - Uniform
Frequency
1400
1200
1000
800
600
400
200
0
[0.331, 0.332]
(0.334, 0.335]
(0.337, 0.338]
(0.340, 0.342]
(0.343, 0.345]
(0.346, 0.348]
(0.350, 0.351]
(0.353, 0.354]
(0.356, 0.357]
(0.359, 0.361]
(0.362, 0.364]
(0.365, 0.367]
(0.368, 0.370]
(0.372, 0.373]
(0.375, 0.376]
(0.378, 0.380]
(0.381, 0.383]
(0.384, 0.386]
(0.387, 0.389]
(0.391, 0.392]
(0.394, 0.395]
(0.397, 0.399]
(0.400, 0.402]
(0.403, 0.405]
(0.406, 0.408]
Closeness Degree